UNIVERSITEIT VAN PRETORIA
UNIVERSITY OF PRETORIA
YUNIBESITHI YA PRETORIA

IMPACT OF COAL QUALITY ON EQUIPMENT LIFETIME AT COAL-FIRED POWER STATIONS

by

Bernard Cornelius van der Westhuizen

Submitted in partial fulfilment of the requirements for the degree
Master of Engineering (Mechanical Engineering)

in the

Department of Mechanical and Aeronautical Engineering

Faculty of Engineering, Built Environment and Information Technology

UNIVERSITY OF PRETORIA

December 2019

UNIVERSITY OF PRETORIA

DECLARATION OF ORIGINALITY

This document must be signed and submitted with every essay, report, project, assignment, dissertation and / or thesis.

Full names of student: Bernard Cornelius van der Westhuizen

Student number:17336300

Declaration

1. I understand what plagiarism is and am aware of the University's policy in this regard.

2. I declare that this, thesis is my own original work. Where other people's work has been used (either from a printed source, Internet or any other source), this has been properly acknowledged and referenced in accordance with departmental requirements.

3. I have not used work previously produced by another student or any other person to hand in as my own.

4. I have not allowed, and will not allow anyone, to copy my work with the intention of passing it off as his or her own work.

SIGNATURE OF STUDENT:.....  .....

SUMMARY

IMPACT OF COAL QUALITY ON EQUIPMENT LIFETIME AT COAL-FIRED POWER STATIONS

by

BERNARD CORNELIUS VAN DER WESTHUIZEN

Supervisor: Prof. Johan Wannenburg

Department: Mechanical and Aeronautical Engineering

University: University of Pretoria

Degree: Master of Engineering (Mechanical Engineering)

Keywords: Coal, Damage Mechanisms, Equipment Life

ABSTRACT

With the export of coal being more lucrative than selling coal to South African power producers, power station operators might consider accepting lower-quality coal. While the impact lower quality coal has on cycle efficiency is understood, the influence it has on equipment reliability and lifetime is often not understood. This study focusses on addressing the question of how different characteristics of coal influences different damage mechanisms of common power station equipment. The results are translated into a reference framework that can be used when coal quality variation is expected.

The influence of coal calorific value and ash content has on air-heater element erosion was evaluated. This was accomplished by establishing a correlation between calorific value and ash content of coal from a specific colliery; this was

then used to calculate the mass of fly ash and flue gas produced when burning enough coal to satisfy the boiler load. An erosion model was then used along with historical coal quality and air heater erosion history to develop and fit a model for full boiler load. The model was verified against data not used during the development of the model, and a seemingly good prediction was made when compared to the measured result. The calorific value of the coal in the model was varied for a hypothetical situation; this indicated that as calorific value decreases the erosion of air heater elements increases.

The influence abrasiveness index has on mill liners was also investigated as part of this study. Historical liner ultrasonic thickness and coal abrasiveness index results were used to fit a mathematical formula. The results indicate that for the ball mills at the power station used in the case study, the abrasiveness index did not have a significant influence on the wear rate of mill liners. The relationship was established to be directly proportional to increased abrasiveness index resulting in an increased wear rate.

The final two case studies that form part of this overall study were focussed on boiler temperature variations as a result of variation in coal calorific value and establishing the impact coal “hang-ups” have on the lifetime of a drum reclaimer.

The first of these two case studies was completed by creating a mathematical thermo-hydraulic model of a hypothetical boiler and calculating the effect calorific value would have on the boiler temperature distribution. The results were then compared to temperature-related damage mechanisms; the comparison indicated that a variation in calorific value, whether up or down from the designed value would be negative for overall boiler health.

The final case study was not completed due to the unavailability of related equipment. A full description of the envisaged study is provided.

LIST OF ABBREVIATIONS

AI	Abrasiveness Index
CV	Calorific Value
HGI	Hardgrove Grindability Index
NDT	Non-Destructive Testing
NDE	Non-Destructive Examination
MJ	Mega Joule
kg	Kilogram
V.M	Volatile Matter
ω_{H_2O}	Moisture content of coal
$A.C$	Coal Ash content
εr	Erosion rate (kg/kg)
$\dot{\varepsilon}$	Erosion rate (kg metal loss/ hour)
x	Silica mass fraction of ash
T_d	Flue gas dew point temperature
σ_a	Stress amplitude
σ'_f	Fatigue strength coefficient
b	Fatigue strength exponent
$2N_f$	Reversals to failure
b	Fatigue strength exponent
E	Modulus of elasticity
ε'_f	Fatigue-ductility coefficient
c	Fatigue-ductility exponent
q''	Heat flux (W/m^2)

k	Thermal conductivity of the material (W/m.K)
$\frac{dT}{dx}$	Temperature gradient (K/m)
h_c	Convection coefficient (W/m^2.K)
T_s	Surface temperature (K)
G	Mass flux of flue gas (kg/m^{2}s)
cp	Specific heat (J/kg.K)
μ	Dynamic viscosity (kg/m.s)
Fr	Correction factor for geometry and emissivity
BBSA	Black body surface area
$\dot{m}_{coal}$	Mass flow of coal (kg/s)
$\dot{m}_{air}$	Combustion airflow
$\dot{m}_{flue\ gas}$	Flue gas mass flow
ω	Unit load (MW or MJ/s)
η	Cycle efficiency
$W.R$	Average wear rate mm/1000hours)

TABLE OF CONTENTS

1 INTRODUCTION

1.1 BACKGROUND

Coal constitutes approximately 72% of South Africa's primary energy supply and is used in electricity generation, petroleum production and metal production [1]. This important resource is found in deposits that are called seams; these seams were formed by the accumulation of vegetation that has undergone a chemical and physical transformation through a geochemical process known as coalification as seen in Figure 1 [2].

Coal is classified into four main categories, namely Lignite (lowest rank), Sub-bituminous, Bituminous and Anthracite (highest rank). The depth of the coal determines the rank with the amount of fixed carbon increasing and moisture decreasing with higher ranking.

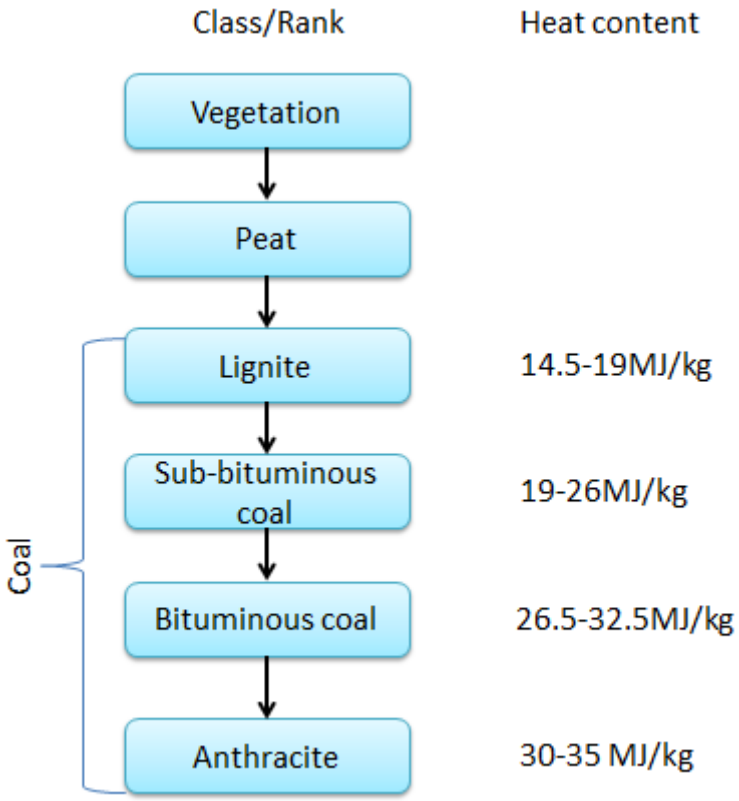

Figure 1 Coalification oversimplified (Heat content from [3])

To ensure that these coal-fired power stations continue to provide electricity, an important part of the process is moving and handling coal from the stockyard to the steam generator. Moving and handling coal is a complex process that has many stages and equipment that makes this possible. Figure 2 shows the basic process starting at the stockpile and ending at the steam generator.

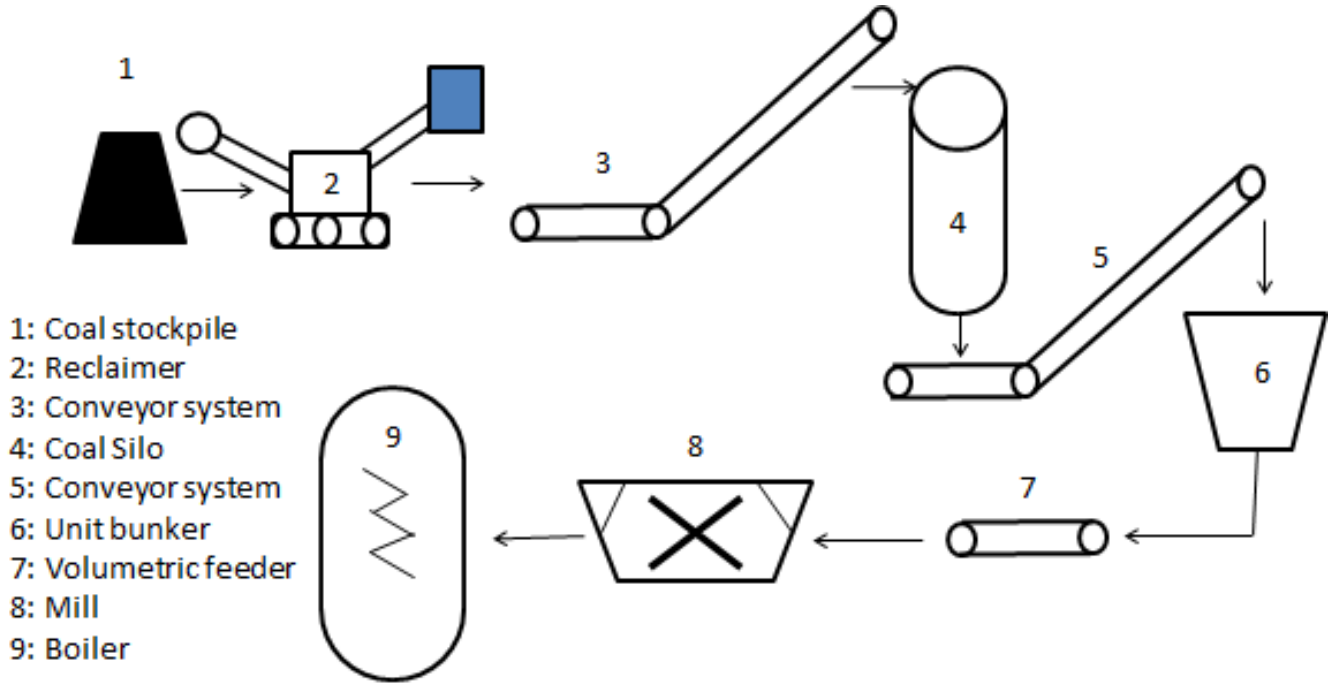

Figure 2 Basic coal handling process

Throughout South Africa, coal-fired power stations make use of a wide variety of coal with varying properties. The older power stations commonly referred to as return to service stations make use of higher-grade coal (23 MJ/kg) whereas some power stations make use of coal that has a significantly lower calorific value (16 MJ/kg) [1]. The variation in coal characteristics is not only limited to calorific value and chemical composition but also applies to the physical properties of the coal such as wettability, porosity, density, and abrasion index.

The export of coal is mostly more lucrative for mining companies than selling coal to the power generation industry in South Africa. This could result in the coal quality supplied to power stations deteriorating [4] & [5]. The question then arises what the impact of deteriorating coal quality will be on equipment lifetime and reliability.

It is known that increased ash content of coal being burnt leads to a proportional increase in slag formation throughout the boiler [6]. Slag build-up causes corrosion of boiler tubes and excessive soot blower usage that, in turn, causes soot blower erosion [7]. In a 2007 study on a 350MW boiler in China, the maintenance cost associated with soot and slag formation was determined to be $190000 (US Dollars) for the relatively small boiler. The total capital cost to the Chinese economy due to power plant fouling was calculated as $4.68 billion (US Dollars) [8].

An increase in ash content also results in higher rates of fly-ash erosion in downstream induced draught fans [9]. The partial load losses caused by draught group problems at South African power stations account for 29 % of all partial load losses [10]. Although the reasons for ID fans/ draught group load losses are numerous, the contribution of wear is believed to be significant.

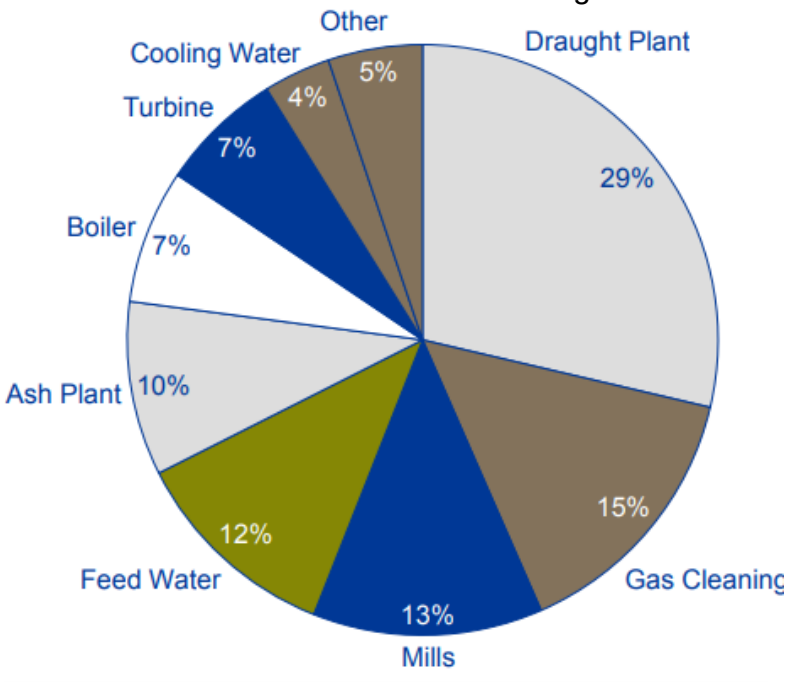

Figure 3 Partial load losses at South African power stations for the 2020 financial year [10]

It is also known that sulphur content of coal influences the concentration of sulfur-trioxide in the flue gas produced. The sulfur-trioxide concentration in the flue gas influences the sulphuric acid dew point [11]. The impact from dew point corrosion is thought to be in terms of air heater cold end corrosion failure and efficiency reduction due to material loss.

To understand the impact coal quality has on the life span of power station equipment, a consolidated view is required of the research done to date on this topic. Further research is also required to quantify the impact the various coal characteristics, not covered by past research studies, have on equipment lifetime.

1.2 PROBLEM STATEMENT

The present study aims to investigate the impact of varying and deteriorating coal quality on the life-time and reliability of equipment in coal power stations. Since it is argued that there is a need for a consolidated view of the problem, a holistic approach is adopted, considering the impact of variation of various coal characteristics, including thermal and mechanical characteristics on various critical equipment in a coal power station production chain, in terms of various degradation mechanisms.

The limited duration of the study only allowed for indicative combinations of the above to be addressed in detail at the hand of case studies. The main objective of the study is, therefore, to lay the foundation for a comprehensive, consolidated view of the problem, to be completed through further studies, following the same approach.

1.3 DOCUMENT STRUCTURE

The document is structured as demonstrated in Figure 1.

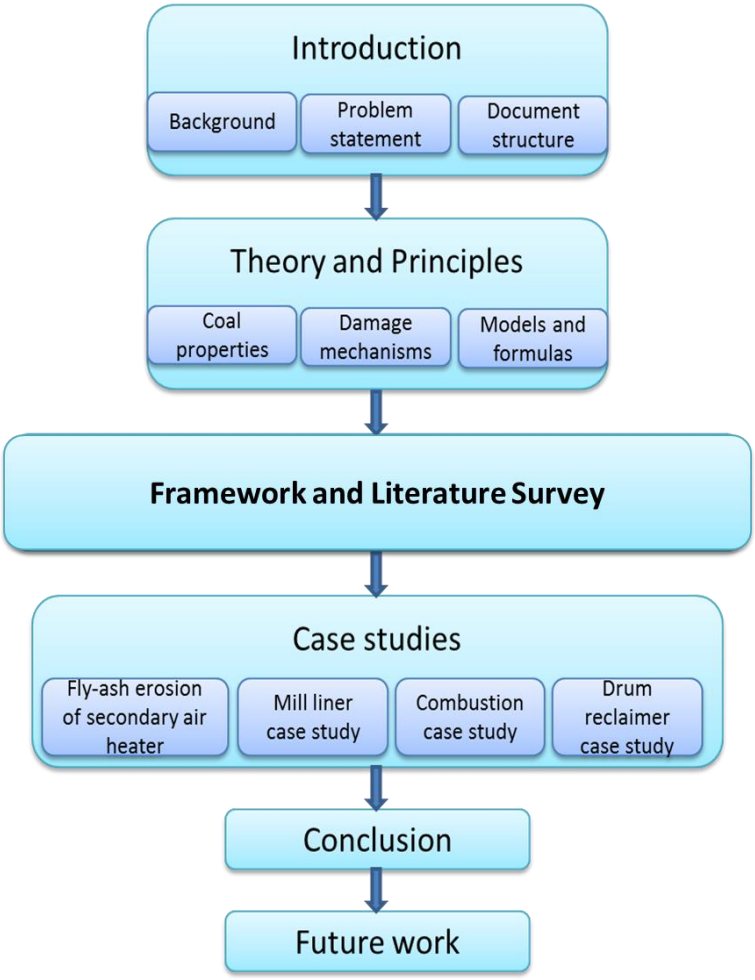

Figure 4 Document structure

2 THEORY AND PRINCIPLES

2.1 GENERAL

The theory surveyed and described is applicable to the research conducted in this study. The theory is divided into coal characteristics, failure mechanisms and the mathematical and physics-based theory that the models used in this study are based on.

The identification of the coal characteristics and failure mechanisms is essential; it provides the ability to link them in a cause and effect type of relationship. The mathematical and physics-based theory provides the framework in which the relationship between coal properties and damage mechanisms can be quantified.

2.2 COAL MECHANICAL PROPERTIES

2.2.1 Mechanical strength

Mechanical strength refers to the ability of coal to withstand external force and is related to the physical properties of coal such as its shatter index, grindability index, and abrasion index [3].

2.2.1.1 Drop Shatter Test

The drop shatter test consists of dropping pre-determined size coal lump onto a steel plate from a specified height and sorting all the pieces that shattered into size groupings. The weight of each group is recorded and the percentage ratio of the weight in each group indicates the coal's friability.

The test is performed according to the national SANS 401:2010 standard which is based on the ASTM D440 - 07 standard.

2.2.1.2 Hardgrove Grindability Index (HGI)

The Hardgrove Grindability Index gives a measure of coals resistance to crushing and is conducted in the following way:

1. A 50-gram sample of prepared coal that is uniform in size is placed inside a grinding unit
2. The unit undergoes a standard number of revolutions under a specified pressure
3. Steel balls within the unit crush the coal sample
4. The coal fines are sorted and the quantity of coal less than a specified size is recorded and converted into a Hardgrove Grindability Index (HGI) value

The test is done in accordance with the ASTM D 409 and ISO 5074:2015(en) standards.

Figure 5 Hardgrove grindability testing machine

2.2.1.3 Abrasion index

The YGP abrasion test was first proposed by Yancey, Geer, and Price in 1951 it involves spinning a device with four blades of carbon steel in a 2 kg sample of coal with a starting maximum particle size of 6.7mm. The four blades are spun inside the sample at a constant speed for 12000 revolutions. The blades are then cleaned and weighed [12] [13]. The abrasion index is calculated as follows:

$$AI = \frac{(m_1 - m_2) \times 10^3}{m_3}$$

Equation 1 YGP test formula

Where:

AI= The abrasion index

m_1= The initial mass in grams of the four blades.

m_2= The final mass of the four blades in grams

m_3= The mass in kilograms of the test portion

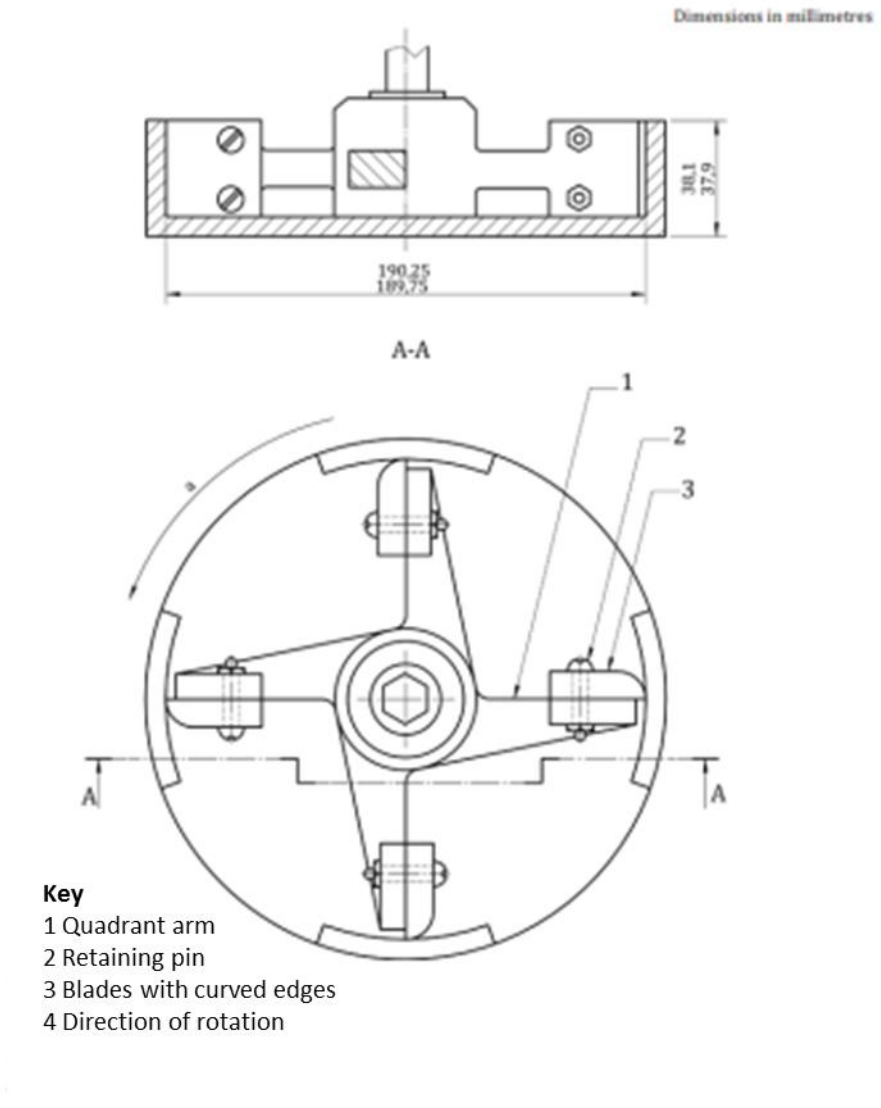

Figure 6 mill mortar specifications (BS 12900:2018)

2.3 COAL CHEMICAL PROPERTIES

The coal chemical qualities refer to the chemical composition of coal, as well as the internal energy of the coal known as the calorific value of the coal.

2.3.1 Proximate analysis of coal

Proximate analysis is the most common and simplest chemical analysis to perform. The proximate analysis provides an indication of the heating value of the coal which is used for commercial decision making when buying coal. [14]

The proximate analysis of coal describes the constitution of coal in terms of 4 classes namely [15]:

1. Fixed Carbon
2. Moisture
3. Volatile matter
4. Ash

2.3.1.1 Volatile matter

Volatile matter is a mixture of gasses that have condensed into oils or tars; volatile presence generally increases as coal rank decreases. Coal with high volatile matter composition generally ignite easier and is more reactive during combustion [16].

The volatile matter percentage of coal is determined in a laboratory in accordance with the ISO 562:2010 standard.

The principle of the experiment is to expose a small sample of coal to a high temperature (900°C) for 7 minutes in the absence of oxygen and measuring the mass loss experienced. The volatile matter mass is then equal to the total mass loss during the experiment minus the mass loss due to moisture.

The procedure for this experiment is as follows [17]:

Preparation

- The coal is ground to a particle size that will fit through a sieve with 212 µm apertures.
- A portion of the same test sample is taken for parallel moisture testing.

Procedure

- Heat the furnace to 900 °C ± 5 °C
- Place empty crucibles into the oven
- After 7 minutes remove crucibles from oven and allow crucibles to cool down
- Measure and note the weight of each empty crucible to the nearest 0.1mg

- After empty crucible weights have been noted, fill 1g± 0.1mg of coal sample into each crucible and note the weights
- Place charged crucible into the furnace at 900 °C ± 5 °C for 7min ± 5 sec
- Remove charged crucible from furnace and allow crucibles to cool down
- Measure and note the weight of each charged crucible to the nearest 0.1mg

Expression of results

$$V.M = \frac{100(m_2 - m_3)}{m_2 - m_1} - \omega_{H_2O}$$

Equation 2 Volatile matter test formula

Where

$V.M$= Mass fraction of volatile matter

m_1=Mass of empty crucible and lid (g)

m_2=Mass of the crucible and lid and test portion before heating (g)

m_3=Mass of the crucible and lid and contents after heating (g)

ω_{H_2O}= Mass fraction of moisture as determined in accordance with the method specified in ISO 11722 or SANS 5924

2.3.1.2 Moisture content

Moisture content refers to moisture on the surface as well as inherent moisture inside the coal.

The moisture tests are done in accordance with a standard such as ISO 11722 or SANS 5924 the latter in the case of this study.

Preparation

The same ground coal sample used during volatile matter testing is used. The coal particles should be able to pass through a sieve with 212 µm apertures.

Procedure

- Heat the furnace to 105 °C to 110 °C
- Fill 1g± 0.1mg of coal sample into each crucible and note the initial weights
- Place charged crucible into the furnace at 105 °C to 110 °C and keep the sample in the oven until the mass remains constant, 1 hour is normally sufficient
- Remove charged crucible from furnace and allow crucibles to cool down
- Measure and note the weight of each charged crucible to the nearest 0.1mg

Expression of results

$$\omega_{H_2O} = \frac{(m_2 - m_3)}{m_2 - m_1} \times 100$$

Equation 3 Moisture content test formula

m_1=Mass of empty crucible and lid (g)

m_2=Mass of the crucible and lid and test portion before heating (g)

m_3=Mass of the crucible and lid and contents after heating (g)

2.3.1.3 Ash content

The ash content of the coal is the remaining mineral matter after combustion has taken place. The ash content of the coal is determined by laboratory testing in accordance with standards such as SANS131:2011 and ISO 1171:2010.

Preparation

The coal particles should be able to pass through a sieve with 212 µm apertures.

Procedure

- Weigh the clean dry dish to the nearest 0.1 mg; if silica or porcelain dish is used it should be heated and cooled according to SANS 131 before weight measurement
- Spread approximately 1 g of the test sample evenly across the dish and way the dish and sample
- Place dish in the furnace and raise the temperature evenly to 500°C over a period of 60 minutes and keep at this temperature for 30 minutes.
- Continue heating to 810 °C ± 10 °C and keep at this temperature for 60 minutes
- When the incineration period is complete allow to cool with a lid in place or in an environment flushed with gasses to prevent moisture accumulation.
- Weigh the dish and ash

Expression of results

$$A.C = \frac{m_3 - m_1}{m_2 - m_1} \times 100$$

Equation 4 Ash content test formula

Where:

A.C = Ash mass fraction

m_1=Mass of the empty dish (g)

m_2=Mass of the dish and test portion

m_3=Mass of the dish and ash (g)

before heating (g)

2.3.1.4 Fixed carbon

The fixed carbon is determined by deduction of the ash content, volatiles and moisture from 100% [18]. This is described in SANS 17246:2011 by the following equation

$$FC = 100\% - \left(\omega_{H_2O} + V + A.C\right)$$

Where:

FC= Mass fraction fixed carbon (%) ω_{H_2O}= Mass fraction moisture (%)

$V.M$= Mass fraction volatile matter (%) $A.C$= Mass fraction ash (%)

2.4 DAMAGE MECHANISMS

2.4.1 Creep

Creep is a damage mechanism defined as time-dependent plastic deformation under a constant load at elevated temperature. Creep as a damage mechanism is generally only present in metals operating above 426 ^{o}C and is particularly applicable to power plant components as well as jet engines [19]& [20].

Creep consists of three stages namely the primary, secondary and tertiary creep stage. The primary creep stage is characterised by a relatively high gradient that decreases on a strain vs time graph. The secondary creep stage which is also known as steady-state creep is characterised by a constant creep rate (steady gradient on the strain vs time graph). During the tertiary or unstable creep stage, the creep rate accelerates until failure occurs.

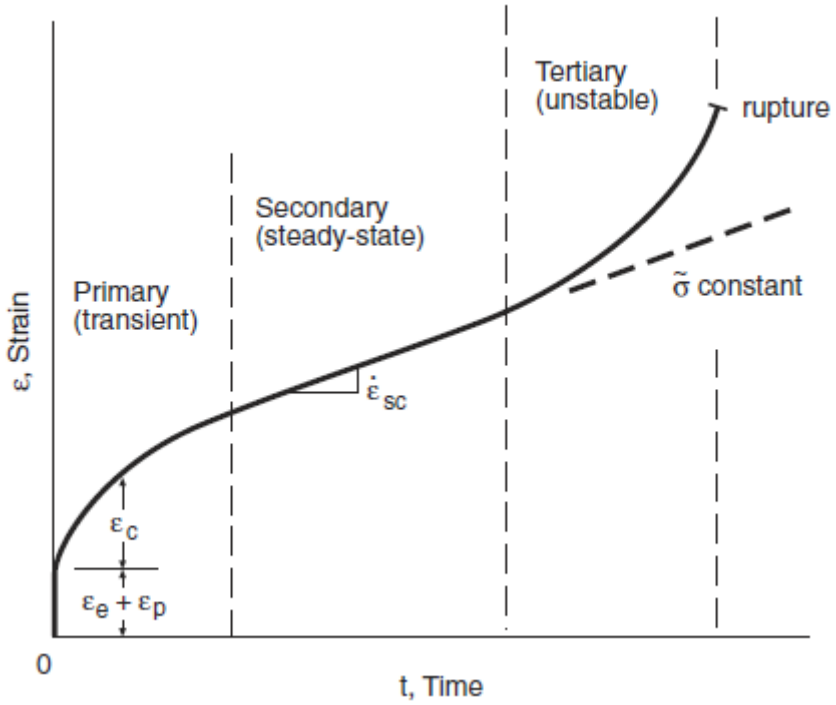

Figure 7 stages of creep [19]

Creep is influenced by temperature with higher temperatures resulting in lower creep strength over time. The creep strength is defined as the rupture strength of a material at a specific exposure time and temperature.

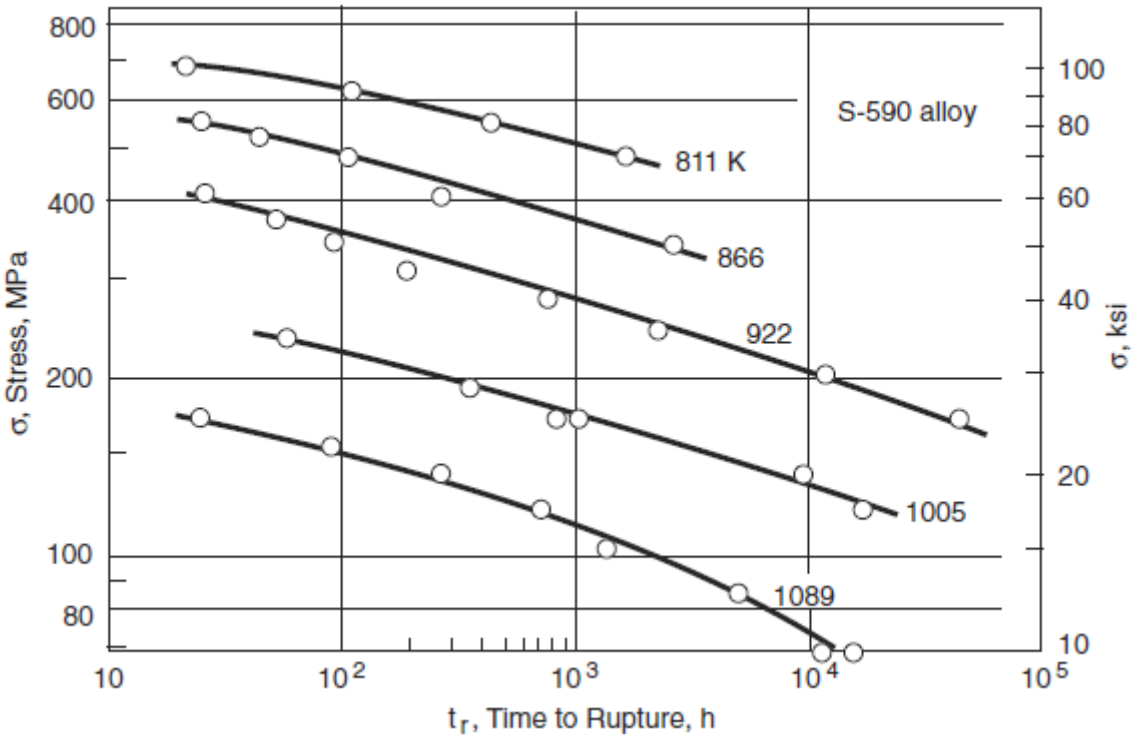

Figure 8 Time to rupture at different temperatures and stress magnitudes for S-590 heat resistant alloy [19]

2.4.2 Fly Ash erosion

Erosion is the process whereby material is removed by abrasive particles moving across the surface of an object. The erosive particles that cause wear in the gas path in the boiler are ash particles transported by the flue gasses produced by the combustion of coal [21]. Fly ash erosion causes damage to the heat collection components in the flue gas flow path such as the heat collection plates of air heaters and boiler tubes with fly ash erosion being the primary cause for approximately 35% of all boiler tube failures [22]& [21].

The amount of damage caused by erosion is generally a function of the mass of the particles impacting the surface, the velocity of the particles, the angle of impingement and the sharpness of the particles. The effect of the impingement angle is determined by the material being impacted with brittle material showing the most material loss with a normal impaction (90^o angle between material and particle direction) and soft metals showing the highest erosion with an impingement angle between 20^o and 30^o [20].

For the South African ash experienced at power stations, . Mbabazi et al. (2004) conducted a study to determine a usable formula for estimating the erosion the air heater elements would experience due to fly ash. The experiment consisted of ash being fed into a gas stream where it was blown onto a plate. The plate's angle

could be changed to allow the researchers to establish the influence of the impingement angle. The particle velocity was also varied to establish the influence particle velocity had on erosion.

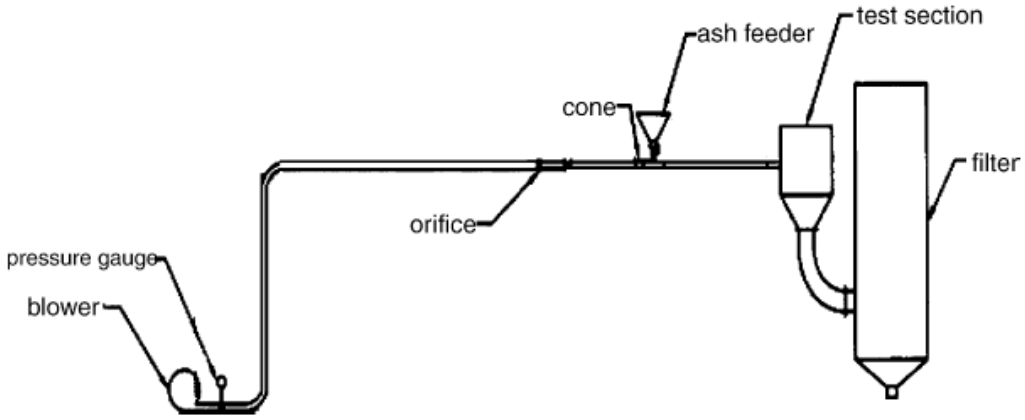

Figure 9 Erosion test experimental setup [23]

The study by Mbabazi et al. (2004) resulted in the following formula for fly ash erosion of flat plates.

$$\varepsilon r = \frac{k x^{4.95} \rho_m {\rho_p}^{1/2} V^3 sin^3 \beta}{{\sigma_y}^{3/2}}$$

Equation 5 Erosion rate formula

With

εr= Erosion rate (kg metal loss/ kg ash in stream)

k= Overall erosion constant (determined to be 0.47 by [23])

x= mass fraction of silica contained in ash

ρ_m=Pack metal density (kg/m^3)

ρ_p= Ash density (kg/m^3)

β= Ash impingement angle

2.4.3 Abrasive wear

Abrasive wear is the removal of material from a surface by a harder material impinging or moving across the surface under load [24]. Two-body abrasion is caused when two surfaces move across each other whilst maintaining contact such as between a grinding wheel and a workpiece. Three-body abrasion is when loose abrasive particles are trapped between two surfaces, these particles cause metal-loss on both surfaces [20]. The abrasive wear experienced on power station components is generally due to three-body abrasion.

There are no agreed models for abrasive wear with most models being based on the Archard equation. These models are not developed to the point where they can be used to calculate wear solutions [20].

$$W = K \times s \times P$$

Equation 6 The Archard equation [25]

Where:

W= Volume of material loss	K= Coefficient of wear that is determined experimentally
s= Sliding distance	P= Applied load

Abrasion is generally characterised into four categories namely low-stress abrasion, high-stress abrasion, gouging abrasion and polishing.

Low-stress abrasion is caused by sliding of abrasive over the surface of the material being worn whereas high-stress abrasion is typified by the abrasive medium being imposed on the surface with enough force for the abrasive medium to be crushed. During gouging abrasion, macroscopic plastic deformation occurs within a single contact. Polishing is produced by very fine abrasives where the abrasive particles remove oxide layers and the polishing fluid corrodes the surface. [20]

2.4.4 Dew point corrosion

In coal-fired power stations, dew point corrosion occurs when the flue gas is cooled to the point of partial condensation. The sulphur trioxide in the flue gas interacts with the water present in the flue gas to form sulphuric acid. When the sulphuric acid droplets form they deposit on the ducting and air heater surfaces causing deterioration of the surfaces. [26]

The dew point is calculated by the following formula [11] :

$$T_d = {}^{1000}/_{\{2.276 - 0.0294ln(P_{H2O}) - 0.0858ln(P_{SO3}) + 0.0062ln(P_{H2O})(P_{SO3})\} - 273}$$

Where

T_d= Dew point (^oC)

P_{H2O}= Partial pressure of moisture (mmHg)

P_{SO3}= Partial pressure of sulphur trioxide (mmHg)

2.4.5 Fatigue

Components of machinery and infrastructure that are exposed to cyclic stresses develop microscopic physical damage even when the magnitude of maximum stress during these cycles is well below the material's ultimate strength; this phenomenon is referred to as material fatigue [19]& [27].

The study of fatigue originated as early as the 1820s when mine hoist ropes were tested under cyclic conditions. The modern stress-based approach to fatigue is largely attributed to the work of August Wohler who tested various materials under cyclic conditions and found that not only is fatigue related to cyclic loading but is also influenced by the mean stress of the cycles [19]. The S-N or Wohler curve is an empirically determined curve where the failure life in cycles vs the nominal stress range. From this curve material constants that describe the fatigue strength are derived, these derived constants are used in design to determine the fatigue life of components.

2.4.5.1 Miner's rule

Miner's rule is a relatively simple cumulative damage model for the assessment of fatigue damage caused by variable amplitude loading. The rule gives the resultant damage as a fraction that is determined by dividing the number of cycles (N_1) divided with the number of cycles it would take to cause fatigue failure at the said stress amplitude (N_{f1}) normally obtained from an S-N curve.

The fraction of life used from all the different stress amplitude cycles is added together to determine a total fraction of life used. The Palmgren-Miner rule simply states that that fatigue failure will occur when all the life fractions sum to unity [19].

$$\frac{N_1}{N_{f1}} + \frac{N_2}{N_{f2}} + \frac{N_3}{N_{f3}} + \cdots = \frac{N_j}{N_{fj}} = 1$$

Equation 7 Palmgren-Miner Rule

2.4.5.2 Irregular stress cycle counting

For highly irregular load variations it is often very difficult to identify cycles that can be used in the Palmgren-Miner rule. Although many methods of cycle counting exist consensus is that the Rain flow cycle counting algorithm developed by Professor T. Endo and his colleagues in Japan during 1968 is the best approach [19].

The rules for the Rain flow method are laid out in ASTM E 1049-85 [28] as follows:

"Let X denote the range under consideration; Y the previous range adjacent to X; and S the starting point in the history.

1. Read the next peak or valley. If out of data, go to step 6.
2. If there are less than three points, go to step 1. Form ranges X and Y using the three most recent peaks and valleys that have not been discarded.

3. Compare absolute ranges of X and Y.
    a. If X<Y, go to step 1.
    b. If Y≤X, go to step 4
4. If range Y contains starting point S, go to step 5; otherwise, count range Y as one cycle; discard the peak and valley of Y, and go to step 2.
5. Count range Y as one-half cycle; discard the first point (peak or valley) in range Y; move the starting point to the second point in the range Y, and go to step 2.
6. Count each range that has not previously been counted as a one-half cycle."

An example given in ASTM E 1049-85 (2005) is given in **Figure 10**

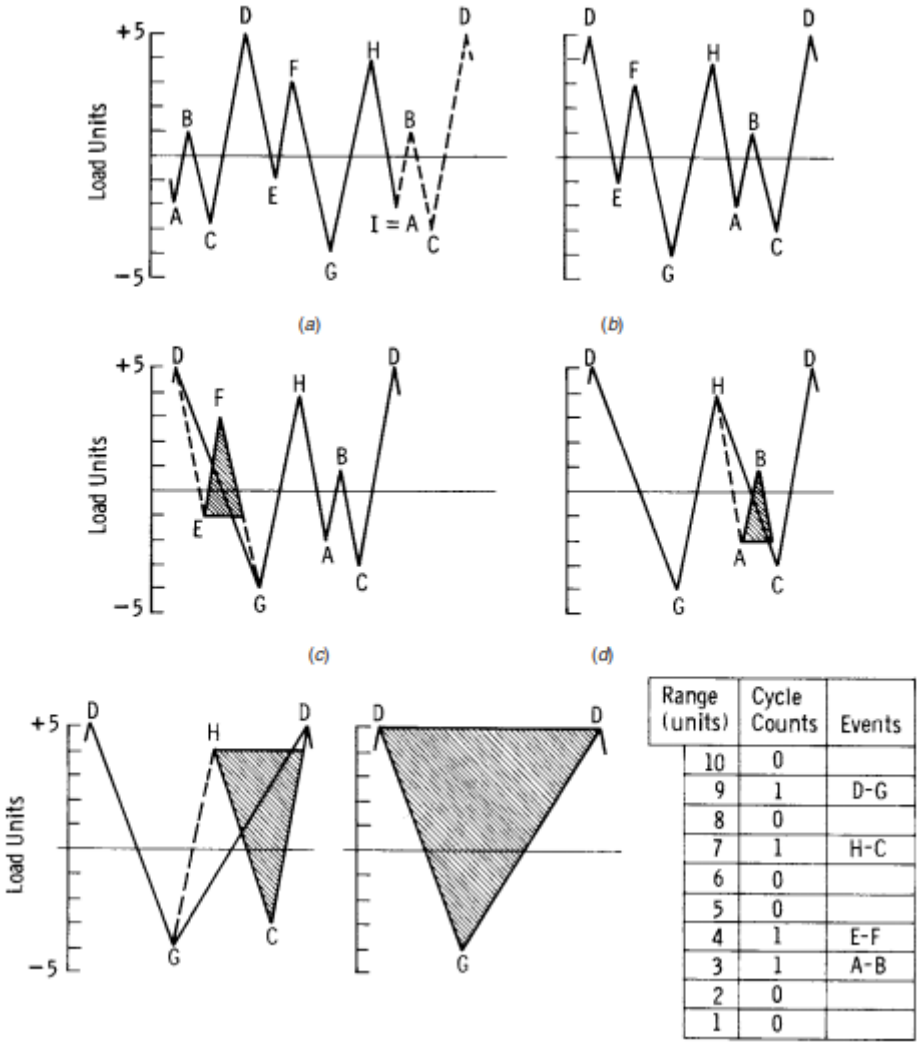

Range (units)	Cycle Counts	Events
10	0	
9	1	D-G
8	0	
7	1	H-C
6	0	
5	0	
4	1	E-F
3	1	A-B
2	0	
1	0	

Figure 10 Rain flow counting example ASTM E 1049-85 (2005)

2.4.5.3 Stress-life equations

The expected life in cycles for completely reversed loading is given by the following equations:

$$\sigma_a = \sigma'_f \left(2N_f\right)^b$$

Equation 8

Where

σ_a= Stress amplitude

σ'_f = Fatigue strength coefficient

$2N_f$ = Reversals to failure (one cycle has two reversals)

b = Fatigue strength exponent

2.4.5.4 Mean stress effect on stress-life calculations

The S-N curve is only valid for completely reversed loading cases where the mean stress is non-zero and cannot be evaluated by using the stress amplitude of the S-N curve or the accompanying equations. To evaluate the expected life of components operating where non-zero mean stress is present an equivalent stress amplitude (σ_{ar}) that represents an equivalent completely reversed cycle needs to be estimated and used in **Equation 9** [19]. Many approaches in determining σ_{ar} including the Morrow approach and the Smith, Watson and Topper approach as shown in **Equation 10** and **Equation 11**.

$$\sigma_{ar} = \sigma'_f \left(2N_f\right)^b$$

Equation 9

$$\frac{\sigma_a}{\sigma_{ar}} + \frac{\sigma_m}{\sigma'_f} = 1$$

Equation 10 Morrow's modification of the Goodman line

$$\sigma_{ar} = \sqrt{\sigma_{max}\sigma_a} \ \ (\sigma_{max} > 0)$$

Equation 11 SWT parameter approach

2.4.5.5 Strain-based approach to fatigue calculations

Strain-based fatigue calculations consider the plastic deformation in localised regions such as at concentration geometries for example at edges of beams, holes in plates and sudden cross-sectional area changes. This approach is suitable to establish life estimates in ductile materials where local yielding is involved but is also applicable to calculations for scenarios where little plasticity and long lives are being analysed. The strain-based approach is, therefore, a comprehensive approach that can be used in the place of the stress-based approach [19].

2.4.5.6 Strain-life equations

Strain vs life plot is a strain amplitude vs cycles to failure graph. This type of graph is used to make life estimations in the strain-based approach in the same way that the S-N curve is used in the stress-based approach [19]. It is important to note that

the strain amplitude can be divided into two parts plastic strain and elastic strain denoted as ε_{ea} and ε_{pa}respectively in the equation :

$$\varepsilon_a = \varepsilon_{ea} + \varepsilon_{pa}$$

Equation 12 Strain Amplitude components

The elastic and plastic components can then be expanded to yield the stain life equation for completely reversed loads [19]& [29]:

$$\varepsilon_a = \frac{\sigma'_f}{E}\left(2N_f\right)^b + \varepsilon'_f\left(2N_f\right)^c$$

Equation 13 Strain-life curve equation for completely reversed loading

Where:

ε_a= Strain amplitude

σ'_f = Fatigue strength coefficient

E = Modulus of elasticity

$2N_f$ = Reversals to failure (one cycle has two reversals)

b = Fatigue strength exponent

ε'_f = Fatigue-ductility coefficient

c = Fatigue-ductility exponent

2.5 MATHEMATICAL OPTIMISATION

During the research, significant data was analysed making use of the “solver” functionality in the Microsoft Excel software application as well as the Bisection method. The solver has three optimisation options namely Simplex, General Reduced Gradient (GRG) method, and Evolutionary.

2.5.1 Bisection method

The bisection method is a numerical method to estimate roots for a continuous formula within an upper and lower bound [a,b]. The method does not deliver the answer to the equation but rather an approximation, the approximation is subject to an error allowance ε.

The method is based on repetitively using the midpoint between the upper and lower bounds as a candidate solution to find the root of the function. The one requirement of this function is that f(a) and f(b) have different signs (indicating that at least one root exists between a and b). [30]

Algorithm (assuming f(a)<0 and f(b)>0)

1. Calculate the first midpoint between the upper and lower limits
$$c = \frac{a+b}{2}$$
2. Check if f(c) is a suitable solution:

If $|f(c)| < \varepsilon$, accept c as the root
If $|f(c)| > \varepsilon$, continue to step 3

3. Determine new upper and lower bounds:
   If $f(c) > 0$, Upper bound b takes the value of c and return to step 1
   If $f(c) < 0$, Lower bound a takes the value of c and return to step 1

2.5.2 Excel simplex solver

The simplex algorithm makes use of the simplex method developed by George Dantzig in the 1940s. This solver option is used for linear problems with multiple variables. [31].

The simplex algorithm consists of seven steps [32] :

1. Re-write function in standard form

The problem must be a maximisation problem, this means that if minimisation is required it can be re-written in negative form and maximised. All constraints must be less than or equal to inequality. All variables need to be non-negative. These conditions must be met by using basic algebra and substitution.

2. Introducing slack variables

Slack variables are additional variables that are introduced into the linear constraints of a linear program to transform them from inequality constraints to equality constraints. The slack variables always have a coefficient of 1.

3. Setting up the tableau

A simplex tableau is used to do row operations as well as check for optimality the tableau consists of the coefficient corresponding to the linear constraint variables and the coefficients of the objective function. The bottom row of the tableau contains the objective function coefficients and the rows above the constraint function coefficients.

4. Checking for optimality

.The bottom row represents the coefficients for the objective function, once all these values are non-negative the optimum solution has been reached. Negative values indicate that the variable has not reached t its optimum value. If the tableau is not optimal the pivot variable is determined.

5. Determining the pivot variable

To identify the pivot variable first the pivot column needs to be identified, the pivot column is the column that has the smallest negative number in the last row of the tableau. The pivot variable in the pivot column is determined by calculating the indicator value, the indicator value is the row beta value divided by the variable. The smallest indicator value provides the pivot variable as in Figure 11.

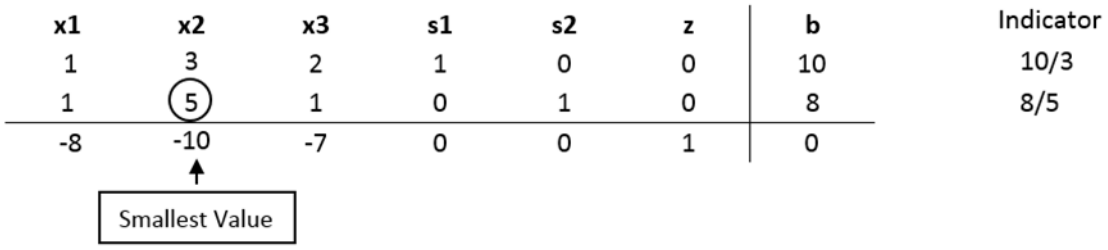

Figure 11 Example of determining pivot variable from the tableau [32]

6. Setting up new tableau

The new tableau is set up by optimising the slack variable identified in the step above to be equal to 1 through algebraic manipulation. Row operations are then done to ensure that the other rows have a zero value for that variable in this case the tableau in Figure 11 becomes.

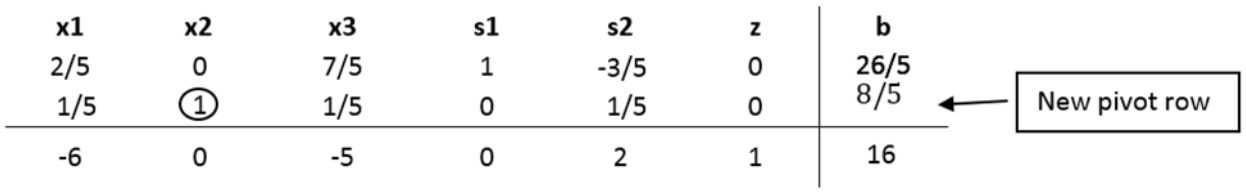

Figure 12 New tableau example [32]

7. Identify optimal values

First, a check is done for optimality as in step 4 if the optimality check fails steps 5-6 are carried out again before checking for optimality again. Once the optimality test is positive the optimum values are calculated by first identifying basic and non-basic and non-basic variables. A basic variable can be classified to have a single 1 value in its column and the rest be all zeros. If a variable does not meet this criterion, it is considered non-basic. If a variable is non-basic it means the optimal solution of that variable is zero. If the variable is basic it is equal to the beta value of the row that it is represented in.

2.5.3 Excel GRG solver

The excel GRG solver is based on the Generalised Reduced Gradient Algorithm. This solver option is proposed for smooth non-linear problems. The GRG solver is dependent on starting condition as it will converge to a local minimum and might not give an optimum solution a graphical explanation is given in. A function known as multi-start is possible in excel that runs the algorithm with multiple starting values increase the chance that the global minimum is found. [33] & [34]

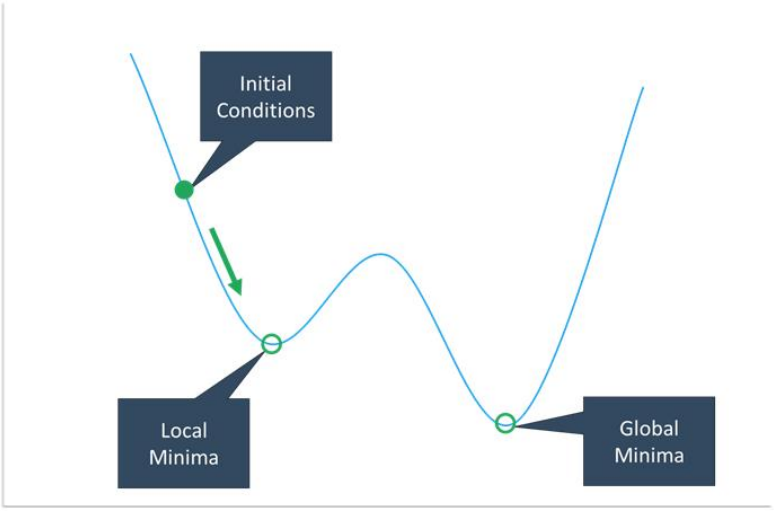

Figure 13 Smooth non-linear function

2.5.4 Excel evolutionary solver

For non-smooth nonlinear functions, the GRG2 algorithm may skip over the non-smooth region or never even reach the point where a peak is formed. This is however dependent on starting value. For non-smooth, non-linear and non-continuous functions the general approach is to make use of evolutionary algorithms that are non-deterministic. The evolutionary algorithm incorporated into excel solver makes use of 5 strategies namely [34]:

1. Randomness

Random samples in the search space of the variables are analysed, this leads to the possibility that the same models might result in different answers on different runs. The search space needs to be properly defined as a too large search space that might result in long calculation times.

2. Population

In non-deterministic algorithms, a population of candidate solutions are kept. Although only one is deemed the best solution the other candidate solutions in other areas are points in the search space where better solutions might later be found.

3. Mutation

Mutation refers to the random change of some variables in candidate solutions to form new candidate solutions. These solutions might be better or worse than the parent candidate solution.

4. Crossover

Crossover is a strategy where the decision variables of parent candidate solutions are used in other parent candidate solutions to form new candidate solutions.

5. Selection

Selection refers to the selection of more fit candidate solutions over less fit candidate solutions. Once the selection is completed the algorithm provides the best candidate solution.

The drawback of this algorithm is that it does not find an optimum solution but only the best candidate solution as it is non-deterministic. The solution can also be improved by running the algorithm a couple of times and changing the variable upper and lower bounds.

2.6 HEAT TRANSFER

2.6.1 Conductive heat transfer

Conductive heat transfer occurs when energy is transferred between molecules of higher energy to molecules with lower energy within a substance. There is no bulk or macroscopic motion of a fluid involved in conductive heat transfer. For thermal conduction to occur a temperature gradient needs to exist across the substance [35]

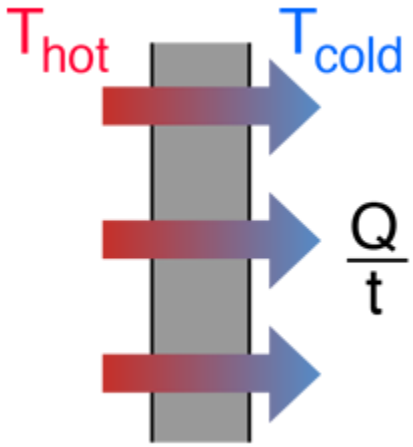

Figure 14 Conductive heat transfer [36]

The heat rate equation is known as Fourier's law and is as follows:

$$q'' = -k\frac{dT}{dx}$$

Equation 14 Fourier's law

Where:

q''=Heat flux (W/m^2)

k= Thermal conductivity of the material (W/m.K)

$\frac{dT}{dx}$= Temperature gradient (K/m)

The heat flux can be multiplied with the area of heat transfer to calculate the heat transfer.

2.6.2 Convective heat transfer

Convection consists of two methods of energy transfer firstly through the random molecular motion (diffusion) such as with conduction but also through bulk and macroscopic motion of the fluid. The movement of the fluid over a bounding surface creates a boundary layer. The heat transfer in the boundary layer is mainly due to diffusion; the impact macroscopic movement of the fluid has on heat transfer is reliant on boundary layer growth due to the macroscopic movement. The fluid in the boundary layer is effectively replaced by fluid outside the boundary layer ensuring the hotter fluid is in contact with the surface. [35]

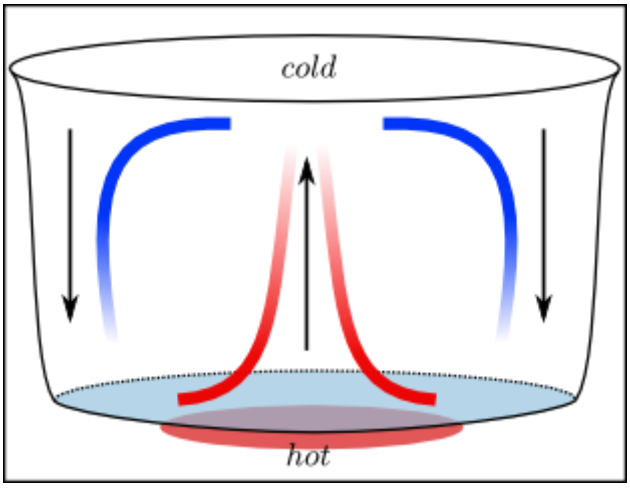

Figure 15 Example of convection [37]

Convective heat transferred is described by Newton's law of cooling and the heat flux is given by the following formula:

$$q'' = h_c(T_s - T_\infty)$$

Equation 15 Newton's law of cooling

q''=Heat flux (W/m^2) h_c = Convection coefficient (W/m^2.K)

T_s= Surface temperature (K) T_∞= Fluid temperature (K)

2.6.2.1 Convective heat transfer coefficient

The convective heat transfer coefficient for a bundle of tubes in crossflow conditions can be calculated as follows [38]

$$h_c = K.D^{-0.4}G^{0.6}cp^{0.33}\mu^{-0.27}k^{0.67}$$

Equation 16

Where:

h_c = Convection coefficient (W/m^2.K)

K= Constant (0.287 for in-line tubes and 0.32 for staggered tube)

D= Outside diameter of tube (m)

G = Mass flux of flue gas (kg/m^{2}s)

cp= Specific heat of flue gas (J/kg.K)

μ= Dynamic viscosity of flue gas (kg/m.s)

k = Thermal conductivity of flue gas (W/m.K)

All properties are taken for average film temperature.

The convective heat transfer coefficient on the inside of the tubes is calculated as follows [38]:

$$h_c = 0.161{D_h}^{-0.2}G^{0.8}\mu^{0.2}c_p$$

Equation 17

Where:

D_h= Hydraulic diameter (m)

G = Mass flux of flue gas (kg/m^{2}s)

μ= Dynamic viscosity of fluid (kg/m.s)

c_p= Specific heat (kJ/kgK)

2.6.3 Radiative heat transfer

Thermal radiation is emitted by all matter that is at non-zero temperatures and the energy emitted is transported by electromagnetic waves. [35]

The radiative energy absorbed by a boiler furnace is given by the following formula [38]:

$$E = \frac{20{,}53 \times Fr \times BBSA}{m_f}\left[\left(\frac{Te}{100}\right)^4 - \left(\frac{Tw}{100}\right)^4\right]$$

Equation 18

Where:

$20{,}53$= Stefan-Boltzmann constant

Fr= Correction factor for geometry and emissivity

Te=Absolute exit gas temperature (°K)

Tw=Absolute temperature of furnace walls (°K)

.

3 FRAMEWORK AND CASE STUDIES FROM THE LITERATURE

3.1 FRAMEWORK

A framework was developed to obtain a holistic view of the influence of coal quality characteristics on power station equipment. The framework lists the different equipment in rows and the coal characteristics in columns. Where an influence is expected, the intersection cell names the expected damage mechanism by which the coal characteristic would influence the life of the equipment. The framework is depicted in Figure 16 .

	Coal Characteristics							
Power Station Equipment		Calorific Value	Ash Content	AI	HGI	Sulphur content	Moisture content	Ash hardness
	Coal reclaimer			Wear			Hang-ups Fatigue Corrosion	
	Coal handling			Chute wear				
	Milling plant			Wear (liners) PF erosion	Wear (liner)			
	Boiler	Erosion Creep Heat damage	Slagging Erosion			Fire side corrosion		
	Air heaters	Erosion	Erosion			Dew point corrosion	Dew point corrosion	Erosion
	Draft group	Erosion	Erosion					
	Ash systems	Wear	Wear					Wear

Figure 16 Expected damage mechanisms

3.2 CASE STUDIES FROM THE LITERATURE

The impact coal quality has on various damage mechanisms has been researched for various power plant components.

3.2.1 Boiler slag formation and erosion

Slag formation is caused by ash fusion temperatures being exceeded in a boiler, the molten mineral matter then makes contact with colder tube surfaces in the boiler. The molten mineral matter solidifies on the colder tube surfaces causing what is known as slag formation. Slag and soot build-up causes various problems in terms of soot blower erosion when soot is removed and thermal conductivity problems.

The American Society for Testing and Materials (ASTM) standard D1857 provides a guideline to test the fusion properties of the ash generated by burning coal as fuel. The test reports four temperatures namely the initial deformation temperature, softening temperature, hemispherical temperature, and the liquid temperature. The standard approach when designing boilers is to have the flue gas at approximately 60-90 ^{o}C cooler than the softening temperature [39].

The test indicates the temperatures where softening and melting would occur for a given ash sample the question still exists what influence ash mineral composition would have on slagging and fouling. In a study completed by Abbott and Austin, the adhesion strength of slag was determined for different metal substrate temperatures, impact angles, and ash chemical compositions. The study was completed for a certain synthetic ash mixture the adhesion strength of the various mineral components that make up ash was also tested. The results indicate that pyrite disproportionally increases slagging adhesion strength and is therefore suspected to be a main driver in accelerated slag formation [40]. This is a starting point for slag formation prediction based on coal quality; the authors note that the test was done in a laboratory environment at temperatures generally higher than that of furnaces.

Various slagging indices for coal quality exists. Two of the prominent indices are the base to acid (B/A) ratio and the silica ratio [41] & [42] these are shown in Table 1.

Table 1 Slagging indices

Ratio	Formula	Low slagging	Medium slagging	High slagging
B/A and Sulphur	$\frac{(Fe_2O_3 + MgO + K_2O + Na_2O)}{(SiO_2 + Al_2O_3 + TiO_2)} \times \%S$	<0.6	0.6-2.0	>2 (>2.6 severe)
Silica ratio	$\frac{100 * SiO_2}{(SiO_2 + Fe_2O_3 + CaO + MgO)}$	72-80	65-72	50-65

3.2.2 Boiler corrosion

The effect that coal chemical composition has on fireside corrosion was established employing Adaptive Neural Network formulation in a 2016 study. The result of this study indicates that fireside corrosion increases proportionally with coal sulphur content; the study also indicates a proportional increase in fireside corrosion when compared to the weight percentage of potassium oxide in the resultant fly ash [43].

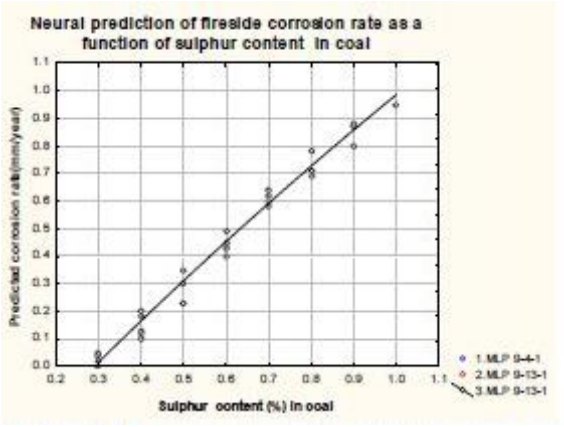

Figure 17 Fireside corrosion vs coal sulphur content [43]

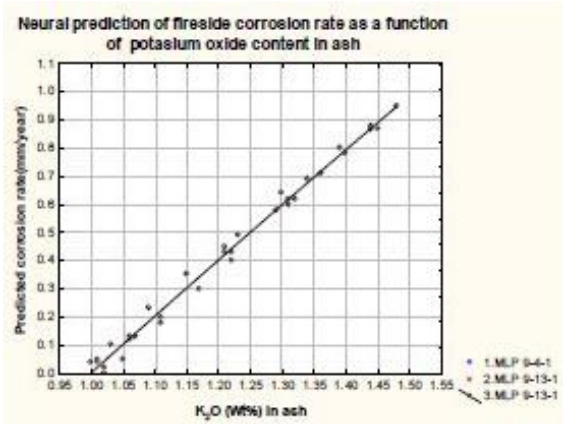

Figure 18 Fireside corrosion vs potassium oxide content [43]

3.2.3 Erosion of pneumatic conveying system

Pulverised coal causes erosion during pneumatic conveying between the mill and the boiler burners. The erosion of the pipework is non-uniform due to a phenomenon known as “coal roping”, this roping refers to areas in the pipework where the concentration of pulverised fuel is higher than normal forming a dense rope-like structure. Roping generally occurs where a direction change in the flow path is experienced and extends to a certain distance after the directional change as seen in Figure 19 [44] & [45].

The particle size, particle feed concentration, and density influences the roping behaviour [46]. To estimate the effect pulverised coal fineness and density would have on roping a CFD model can be created for the system [47]

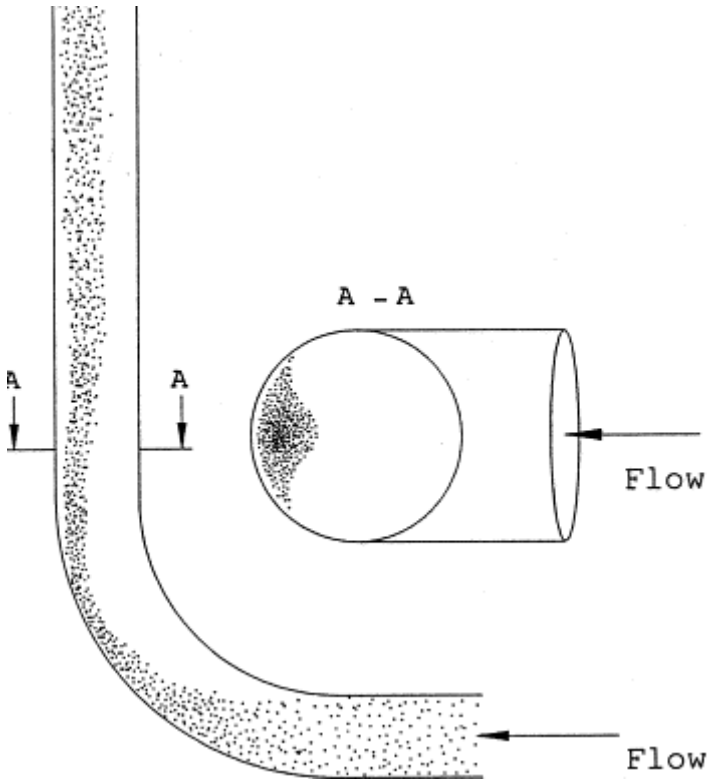

Figure 19 Example of coal roping [44]

The YGP abrasion index is generally the expression used to indicate the abrasiveness of coal. An explanation of this metric can be found in section 2.2.1.3 Abrasion index. The YGP index does relate to the mineral matter in coal but does not have a direct correlation to ash content [48].

A better indication than ash content for erosion of pipework is the quartz and pyrite content even this causes significant scattering making an accurate prediction impossible. Wellsa et al. conducted a study of the correlation between abrasive wear of PF pipework and mineral particles in the pulverised coal that is larger than 25 μm and harder than steel. The results can be seen in Figure 20, and Figure 21 shows that this gives a significantly improved correlation.

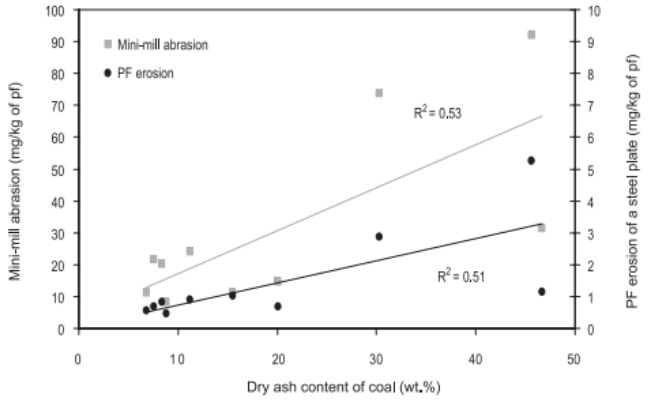

Figure 20 Correlation between ash content and erosion [48]

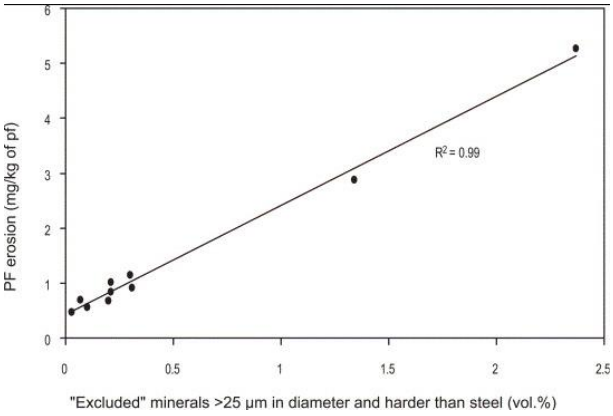

Figure 21 Correlation between mineral inclusions > 25µm that is harder than steel and erosion [48]

To effectively calculate the erosion impact of coal on PF pipework, a CFD study has to be conducted. The results from the CFD study needs to be used to identify the areas where the highest density of coal particles due to roping occurs. The results of this can then be used to calculate the erosion potential taking into account the abrasiveness index or the mineral matter larger than 25µm and harder than the steel of the pipe.

3.3 CLOSURE

This study aims to address the suspected damage mechanisms that relate to coal quality identified in Figure 16. Some of the interaction between coal quality and the damage mechanisms has already been addressed by literature.

A selection of damage mechanisms not found to be addressed in the literature, was identified for investigation through case studies performed, as part of the present study. These are reflected in Figure 22.

Coal Characteristics								
Power Station Equipment		Calorific Value	Ash Content	AI	HGI	Sulphur content	Moisture content	Ash hardness
	Coal reclaimer			Wear			Hang-ups Fatigue Corrosion	
	Coal handling			Chute wear				
	Milling plant			Wear (liners) PF erosion	Wear (liner)			
	Boiler	Erosion Creep Heat damage	Slagging Erosion			Fire side corrosion		
	Air heaters	Erosion	Erosion			Dew point corrosion	Dew point corrosion	Erosion
	Draft group	Erosion	Erosion					
	Ash systems	Wear	Wear					Wear

Figure 22 Damage mechanisms addressed by case studies

4 FLY ASH EROSION OF SECONDARY AIR HEATERS CASE STUDY

Air pre-heaters heats cold incoming air by exchanging heat between the outgoing flue gasses and the incoming air. There are two types of air heaters in a conventional power station, namely primary and secondary air heaters. The primary air heaters are tube and bundle type heat exchangers that heat the portion of the air that is fed to the milling plant for pneumatic conveying of pulverised coal to the burners. The secondary air heaters are generally of the rotating Ljungström type that exchanges heat by rotating sections of regenerative heat-absorbing material known as air heater packs through the hot flue gas and cold incoming air streams. This causes increased temperature of the secondary or combustion air that is directly supplied to the coal burners.

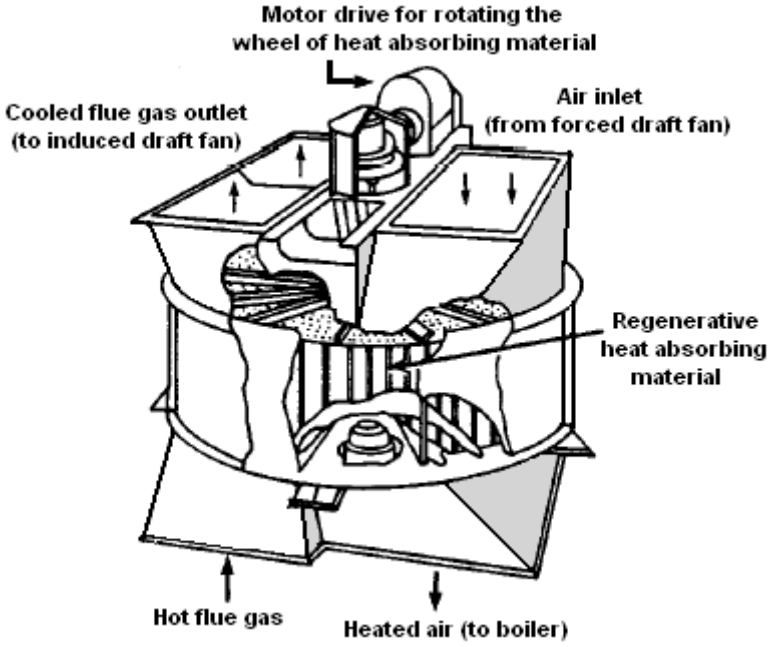

Figure 23 Secondary air heater [49]

Erosion is the process whereby material is removed from a surface by the impact of particles in a fluid stream passing over the surface. In coal-fired power stations fly ash erosion is a damage mechanism present in the boiler and downstream equipment such as air pre-heaters and ducting. Secondary air heater failure occurs when the plates between the air heater packs become eroded to such an extent that holes start forming and the heater packs collapse. Erosion also impacts the heat transfer capability of the secondary air heaters as they are of the regenerative type, which implies that thermal energy is stored in a volume of conductive material. As the volume decreases the amount of thermal energy storage capability decreases.

The secondary air pre-heaters that are the focus of this case study shows significant material loss due to erosion as can be seen in Figure 24 and Figure 25. The current strategy is to replace the air heater packs every 6 years.

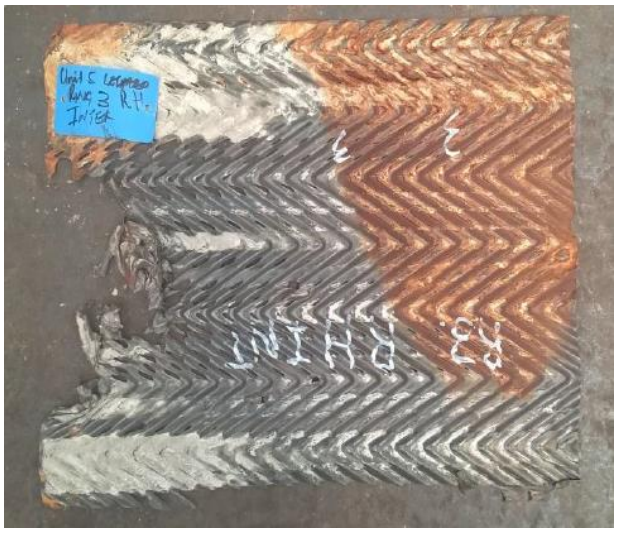

Figure 24 erosion damage on 3rd ring top pack

Figure 25 erosion damage on 5th ring bottom pack

The ash content of the coal burnt at the power station this case study is based on varies quite significantly (between 36% and 45% by weight). It was expected that this variability would cause more aggressive or less aggressive erosion of the air heater depending on the ash content in the wear period as the volume of grinding media (ash in this case) influences the wear.

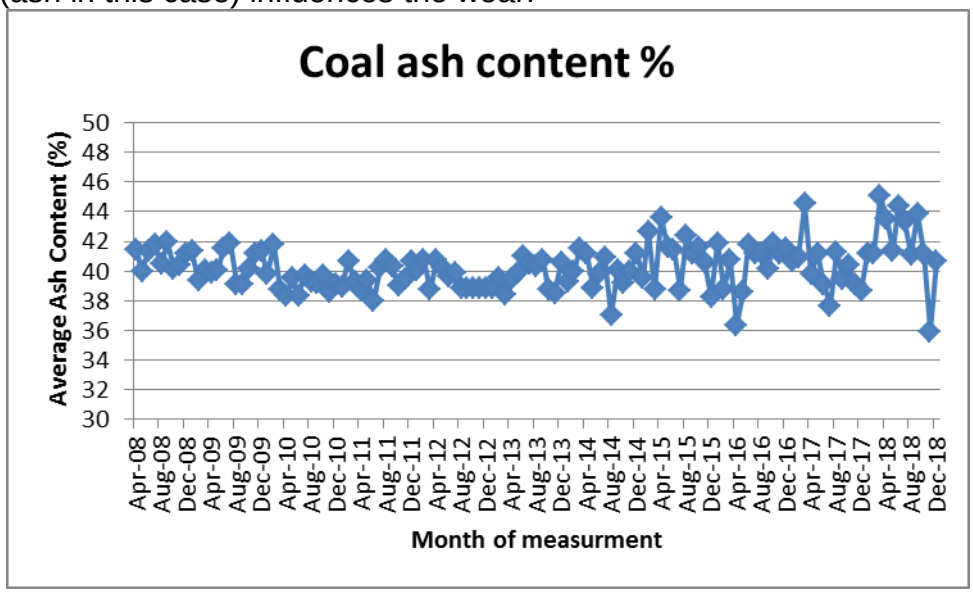

Figure 26 Coal ash content history

The calorific value of the coal also varies significantly and varies between approximately 14 MJ/kg to 17 MJ/kg. The variation was thought to impact the flue

gas velocity due to differing combustion air requirements as well as coal mass flow requirements based on calorific value

The study aims to evaluate the erosion rate based on a single coal parameter to enable the plant engineer to estimate replacement requirements based on the quality of the feedstock.

4.1 METHOD

Without significant wear data that are obtained over periods with different burnt coal characteristics, the study is based on combustion calculations and the effect it has on grinding media (ash) production and flue gas velocity.

The first step was to identify the relationships between the different characteristics of coal. The aim was to identify a characteristic that provides an indication of the others. For this case study calorific value was chosen as it is widely reported at the power station and most stringently controlled by the power station. Part of the relationship identification step included combustion calculations of different coal samples received by the power station to identify the relationship between coal calorific value and flue gas production as well as ash production.

The second step was to reduce the ash and flue gas production relationships to percentage values with 100% set at the values obtained at coal with a calorific value of 17 MJ/kg. This was done to provide a clear percentage driven change indication.

The final step consisted of modifying a proven erosion model for ash particle impingement to indicate the erosion rate as a function of coal calorific value. The erosion rate, which is given in kg material loss/kg ash was modified by multiplying it with the ash production rate to give a time-based erosion rate.

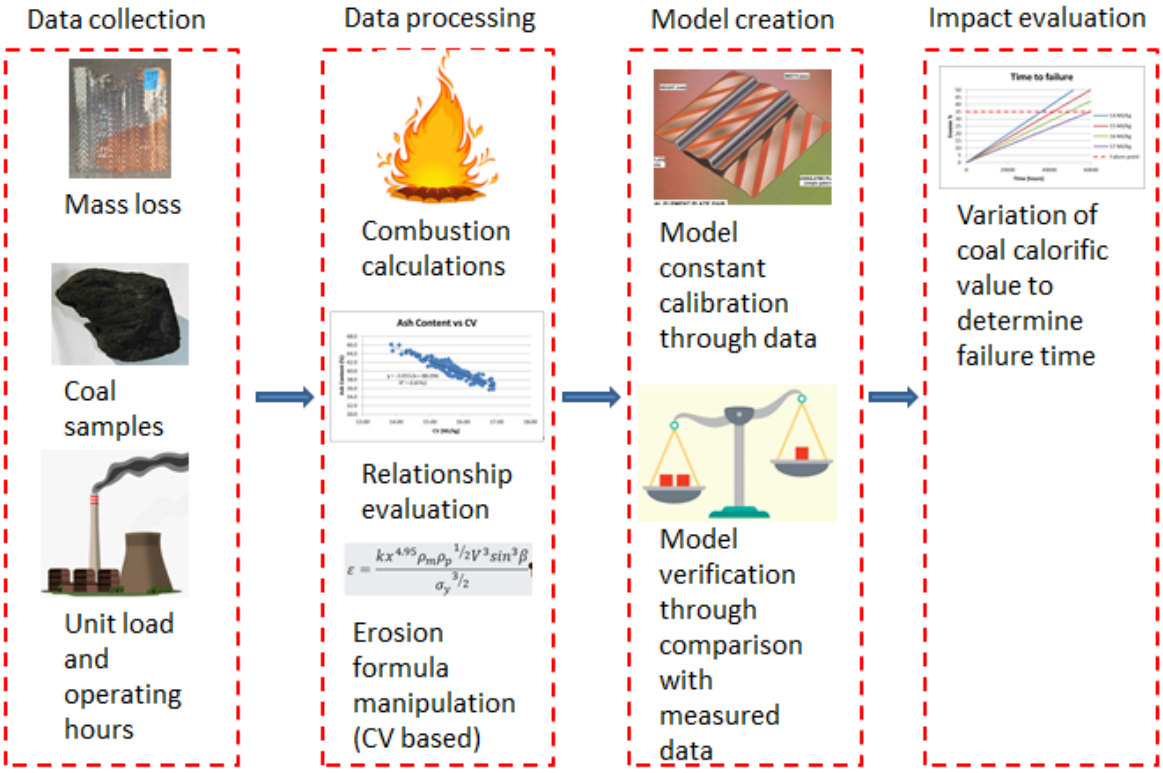

Figure 27 Air heater case study method

4.2 RELATIONSHIP IDENTIFICATION

The known relationship between coal usage and calorific value is that coal usage will increase as the calorific value of the coal decreases, and the boiler load stays constant. The unknown relationships that were analysed for the coal at the specific power station are as follows:

- Ash content of coal vs calorific value
- Required combustion air per kilogram coal vs calorific value
- Fly ash produced for a steady boiler load of 618 MW vs calorific value
- Flue gas mass flow produced for a steady boiler load of 618MW vs calorific value

4.2.1 Ash content vs calorific value

The first relationship that was evaluated was the relationship between calorific value and ash content of coal; the general assumption was that the relationship would be inversely proportional. This was done by making use of 173 coal samples supplied by the mine to the power station.

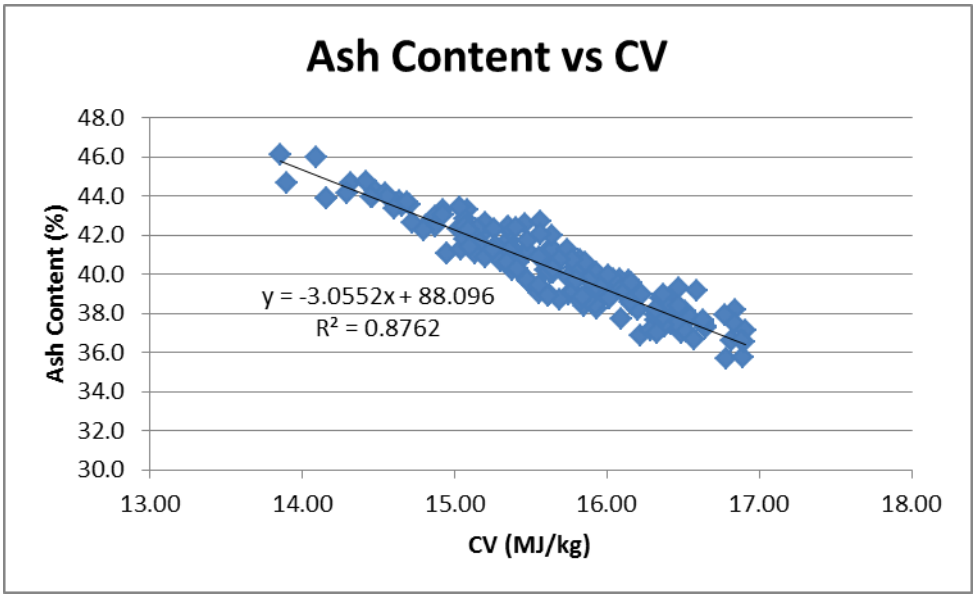

Figure 28 Ash content vs calorific value

The results of the proximate analysis samples were plotted and a linear regression line fitted by making use of the method of least squares regression. By evaluating the fitness of the regression line, a favourable coefficient of determination of 0.8762 was obtained, indicating that the linear relationship between ash content and calorific value of coal is a reasonable assumption.

4.2.2 Required combustion air per kilogram vs calorific value

After establishing that a reasonable correlation exists between ash content and calorific value, it was decided to evaluate the required combustion air including excess air in relation to calorific value. The reason this was expected to have a strong correlation, is that the calorific value of coal is influenced by the ratio of combustible elements inside coal to overall coal weight.

The first step in determining the required combustion air is by evaluating the combustion chemical reactions. For coal, the combustible elements are hydrogen, carbon and sulphur. The following is an example of a calculation for a single coal sample:

Coal Characteristics		
Element	Molecular	Mass fraction (%)
N2	28	1.86984
O2	32	4.019943
C	12	38.00374
Ash		42.25
S	32	0.7
H2	2	2.676481
H2O	18	10.48

Figure 29 Example of coal ultimate analysis

Combustion Calculations				
C (12)	+	O2 (32)	=	CO2(44)
0.380037365	+	1.013432973	=	1.39347
H2 (2)	+	1/2 O2 (32)	=	H2O (18)
0.026764805	+	0.21411844	=	0.240883
S (32)	+	O2 (32)	=	SO2 (64)
0.007	+	0.007	=	0.014

Figure 30 Mass-based oxygen required calculation

After the stoichiometric air requirement is calculated the fraction of oxygen already present in the coal sample is subtracted from the requirement. This gives the amount of additional oxygen required for stoichiometric combustion. Assuming air is 23% oxygen, the additional oxygen requirement is divided by 0,23 to calculate the equivalent amount of air needed for stoichiometric combustion. Industrial coal combustion is done with the presence of excess oxygen to ensure complete combustion is achieved. This is typically 20% and is added to the required amount of air as can be seen in Table 2:

Table 2 Combustion requirements

Combustion requirements	
Oxygen required per kg of coal (kg/kg)	1.234551413
Oxygen already present in 1 kg of coal (kg)	0.04019943
Additional oxygen needed (kg/kg)	1.194351983
Stoichiometric volume of air needed per kg of coal (23% of air is oxygen)	5.19283471
% excess air	20
Combustion air required per kg coal (kg)	6.231401652

This was done for the 173 coal samples already mentioned to give the following correlation with calorific value.

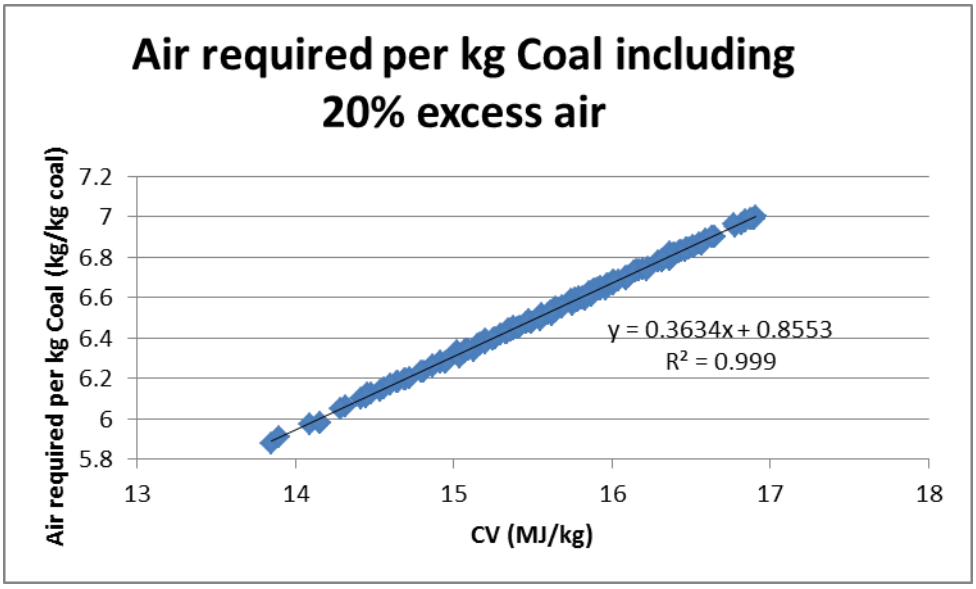

Figure 31 Air required vs calorific value

From the results, it can be seen that the air required for complete combustion is directly proportional to the calorific value of coal. This is thought to be because a higher calorific value coincides with a larger proportion of combustible elements in coal and the ratio between the combustible elements stays relatively constant for coal from a single origin.

4.2.3 Flue gas produced vs calorific value

The effect calorific value will have on flue gas production taking into account the trends already identified is unknown. This is because air required for combustion per kilogram coal increases with CV, and the mass flow of coal required decreases with increasing calorific value.

To calculate the flue gas produced the results from the combustion calculations for each sample are used along with the following formulas:

$$\dot{m}_{coal} = \frac{\frac{\omega}{CV}}{\eta}$$

Equation 19

Where

$\dot{m}_{coal}$= Mass flow of coal (kg/s) ω= Unit load (MW or MJ/s)

CV= Calorific value (MJ/kg) η= Cycle efficiency

The following assumptions are made from the specific power plants operating manual:

ω= 618 MW (full load) η= 35%

The total airflow is equal to the combustion air requires per kilogram coal multiplied by the coal mass flow.

$$\dot{m}_{air} = \dot{m}_{coal} \times \left(\frac{kg\ Air}{kg\ Coal}\right)$$

Equation 20

With the mass flow of coal available the flue gas can be calculated from the coal data and the combustion calculations. The mass of flue gas produced is equal to the sum of the coal burnt and the mass of the combustion air minus the ash produced.

$$\dot{\boldsymbol{m}}_{\boldsymbol{flue\ gas}} = \dot{\boldsymbol{m}}_{\boldsymbol{coal}} \times (\mathbf{1} - \boldsymbol{Ash\ content}) + \dot{\boldsymbol{m}}_{\boldsymbol{air}}$$

Equation 21

Where

$\dot{m}_{flue\ gas}$= Flue gas mass flow $\dot{m}_{coal}$= Coal mass flow

$Ash\ content$= Ash content as of coal as a fraction $\dot{m}_{air}$= Combustion airflow

For the coal sample in Figure 29, the following is the calculations for flue gas produced by a 618 MW power generating unit:

Flue gas produced	
CV (MJ/kg)	14.8
Unit load (MW) (MJ/s)	618
Cycle efficiency (%)	35
Mass of coal per second (kg/s)	119.305019
Mass of air required per second (kg/s)	743.437494
Mass of flue gas produced per second (kg/s)	812.336143

Figure 32 Flue gas produced for 14.8 MJ/kg coal

The same data set of coal was used to calculate the amount of flue gas produced per second for each coal sample. This was plotted on a chart and a regression line was fitted to determine if a trend exists.

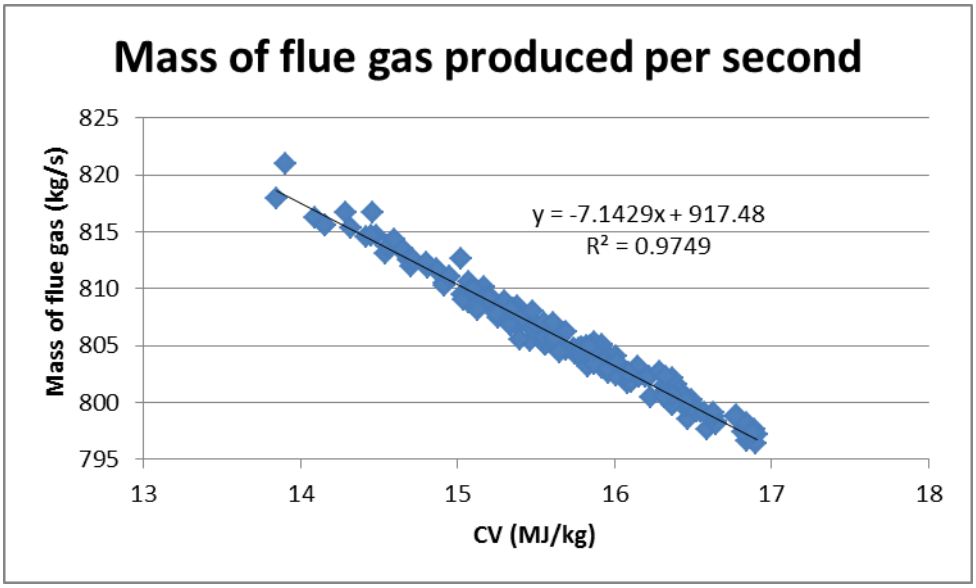

Figure 33 Mass of flue gas produced per second vs Calorific value

The coefficient of determination is favourable thus indicating that the regression line's formula can be used for general trend calculations that rely on the relationship between the mass of flue gas produced and the calorific value of coal burned.

4.2.4 Fly-Ash produced vs calorific value

The two types of ash produced by a utility boiler are fly ash and coarse ash. Fly ash travels through the boiler and moves through components such as the air heaters, the coarse falls down the furnace into a submerged scraper conveyor and does not cause erosion of components in the flue gas path. The ratio between the fly- and coarse ash is generally 80:20 at the power station this study is based on.

To calculate the fly ash produced the coal mass flow is multiplied by the ash content fraction, this gives the total ash produced per second (course + fly ash). This value is then multiplied by 0.8 to calculate the mass of fly ash produced.

$$\dot{m}_{fly\ ash} = 0.8 \times \dot{m}_{coal} \times Ash\ content$$

Equation 22

For the coal sample used as an illustration of combustion calculations in section 4.2.2 the following is the amount of fly ash produced per second.

Fly ash production	
Mass of ash produced per second (kg/s)	50.40637
Mass of Bottom ash produced per second (kg/s)	10.08127
Mass of fly ash produced per second (kg/s)	40.3251

Figure 34 Fly ash production

When this calculation is done for the 173 coal samples used in this study, the following graph is produced. The data was used to generate a regression line and the coefficient of determination is calculated to indicate the correlation.

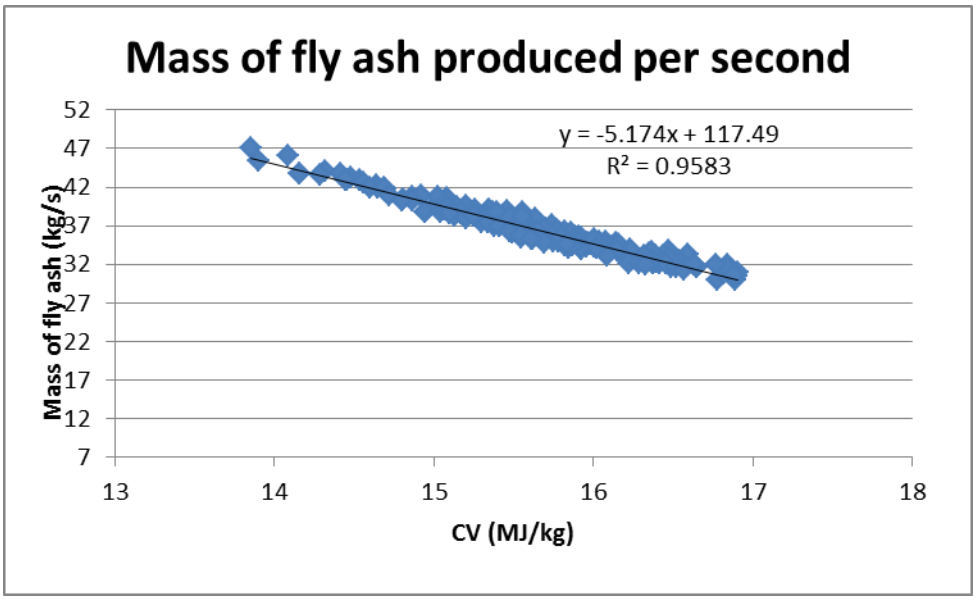

Figure 35 Fly ash production

While some deviation from the trend line can be seen, the coefficient of determination indicates a good fit and a definite trend is evident. The formula from the regression line can, therefore, be used for general calculation involving the fly ash production as a product of coal calorific value in this specific power station.

4.3 RATIO BASED ASH AND FLUE GAS PRODUCTION INCREASE WITH DECREASING COAL CALORIFIC VALUE

With the range of coal calorific value being analysed a base ash and flue gas production rate was taken at coal with a calorific value of 17 MJ/kg. The formulas of the trend lines in Figure 33 and Figure 35 was modified by dividing them by the value obtained when 17 MJ/kg is used to determine the amount of flue gas/ fly ash produced. This results in the following formulas:

For fly ash production

$$Fly\ ash\ gas\ production = -0.1752 \times CV + 3.9785 \quad (14 \leq CV \leq 17)$$

Equation 23

For flue gas

$$Flue\ gas\ production = -0.009 \times CV + 1.1525\ (14 \leq CV \leq 17)$$

Equation 24

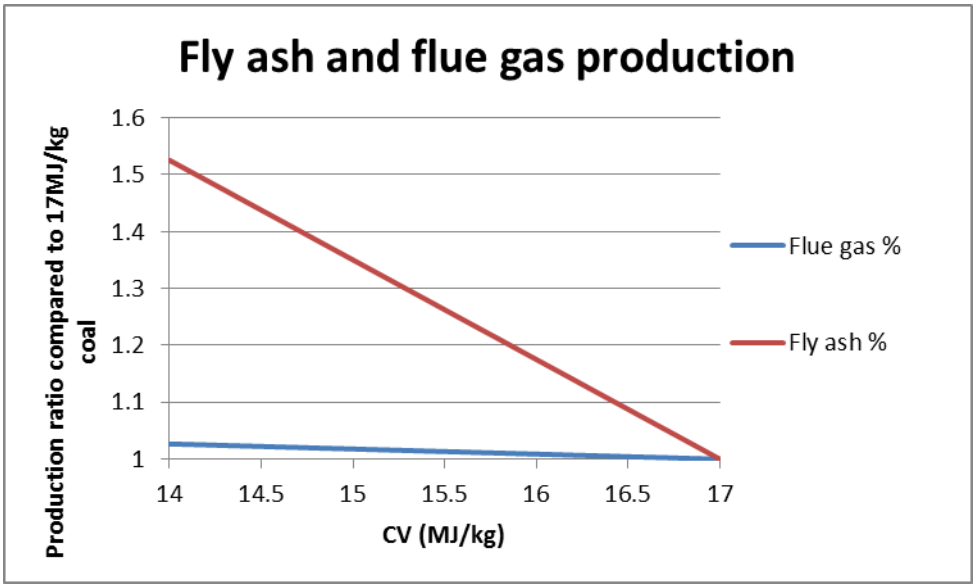

Figure 36 Flue gas and ash production as a dimensionless increase with the calorific value

4.4 FLY ASH EROSION

The base formula used for erosion, in this case study as described by [23] is as follows:

$$\varepsilon = \frac{kx^{4.95}\rho_m {\rho_p}^{1/2} V^3 sin^3\beta}{{\sigma_y}^{3/2}}$$

Equation 25

With

ε= Erosion rate (kg metal loss/ kg ash in stream)

k= Overall erosion constant (determined to be 0.47 by [23])

x= mass fraction of silica contained in Ash

ρ_m=Pack metal density (kg/m^3)

ρ_p= Ash density (kg/m^3)

β= Ash impingement angle

For the formula to be used to indicate the effect coal quality variation has on erosion, it needs to be modified by making certain assumptions.

4.4.1 Assumptions

1st assumption: the ash physical properties stay constant independent of other coal characteristics for the same mine

This assumption includes both the density as well as the silica content; this assumption must be made as mineral matter tests are not conducted on any incoming coal samples. The result of this is that a relationship between silica content/ash density and calorific value cannot be established for use in this case study

2nd assumption: The air heater pack material's characteristics stay constant

This assumption is true for pack material as the material does not change as it is eroded. This assumption is specifically made for density and yield stress.

3rd assumption: Ash impingement angle stays constant at all air velocities generally expected at full boiler load for coal with calorific values of between 14 and 17 MJ/kg

Without conducting a full Finite Element Analysis (FEA), it is not possible to determine the angle at which the ash particles impact the surface of the air heater pack material at different flue gas velocities.

4th assumption: Flue gas temperature, density, and pressure stays constant at the air heater for flue gas production at different coal qualities within the 14 to 17 MJ/kg band

This assumption implies that the velocity of the flue gas is directly proportional to the amount of flue gas produced.

4.5 TIME-BASED EROSION MODEL

With ash and metal qualities, as well as impingement angle, staying constant, the base erosion model is a function of only ash velocity.

$$\varepsilon = kV^3$$

Equation 26

Ash velocity is assumed to increase directly with flue gas mass flow increase, and flue gas mass flow is a function of the calorific value of the coal burnt. The formula can be re-written as:

$$\varepsilon = k(-0.009 \times CV + 1.1525)^3$$

Equation 27

The erosion rate is a function of ash mass in the flue gas passed over the pack material and has a unit of kg metal loss/kg ash in the air stream. To convert this to a time-based erosion rate the formula is multiplied by the ash production mass flow in kg/second to effectively produce an erosion rate measured in kg metal loss/second.

$$\dot{\varepsilon} = \dot{m}_{ash}\varepsilon$$

Equation 28

With ash production a function of calorific value the formula is transformed to

$$\dot{\varepsilon} = (-0.1752 \times CV + 3.9785 \quad)k(-0.009 \times CV + 1.1525)^3$$

Equation 29

To gauge the percentage change of erosion rate the value of the constant k is set at 1 to give an indication of change from a base CV of 17 MJ/kg. This results in Figure 37

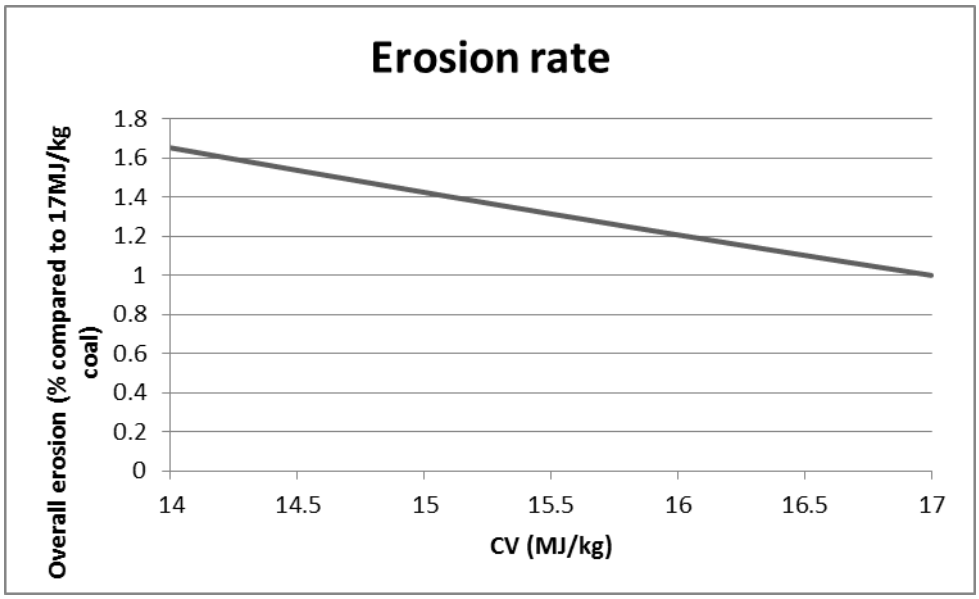

Figure 37 Fractional change of erosion rate as a function of coal calorific value

To estimate the erosion that has taken place over a period the operating hours need to be taken into account. This changes the erosion rate formula to provide total erosion for the operating hours effectively.

$$Erosion = \dot{\varepsilon}t$$

Equation 30

Where

$Erosion$= Erosion (kg metal loss) $\dot{\varepsilon}$= Erosion rate (kg metal loss/ hour)

t= Time (hours)

4.6 APPLICATION OF THE METHOD TO PREDICT EROSION MASS LOSS

To accurately verify the usability of this method, one would need mass loss results for multiple units subjected to different qualities of coal and different hours of use. The units also need to run at the same load factor, preferably full load, to eliminate the load-dependent variation of flue gas production.

Unfortunately, only two sets of erosion mass loss results that overlapped were available, meaning that the data for input into the model does not differ significantly enough to test the method fully. The average load over the period indicates that the units were generally subjected to the same load factors.

Unit	Date from	Date to	Boiler hours	Average ash Content (%)	Average CV (MJ/kg)	Average Boiler load MW
2	2013/05/01	2016/04/30	21972	40.21474	15.62821	546.335535
5	2013/08/01	2016/12/31	26465	40.33959	15.63531	546.567447

Table 3 Mass loss report parameters

4.6.1 Mass loss measurements

The mass loss measurement was done by cutting out sample plates from air heater pack elements after newly installed air heaters have been in service for approximately three years. The elements from which the plates were cut contain a pair of plate namely a corrugated plate and an undulated plate as seen in Figure 38.

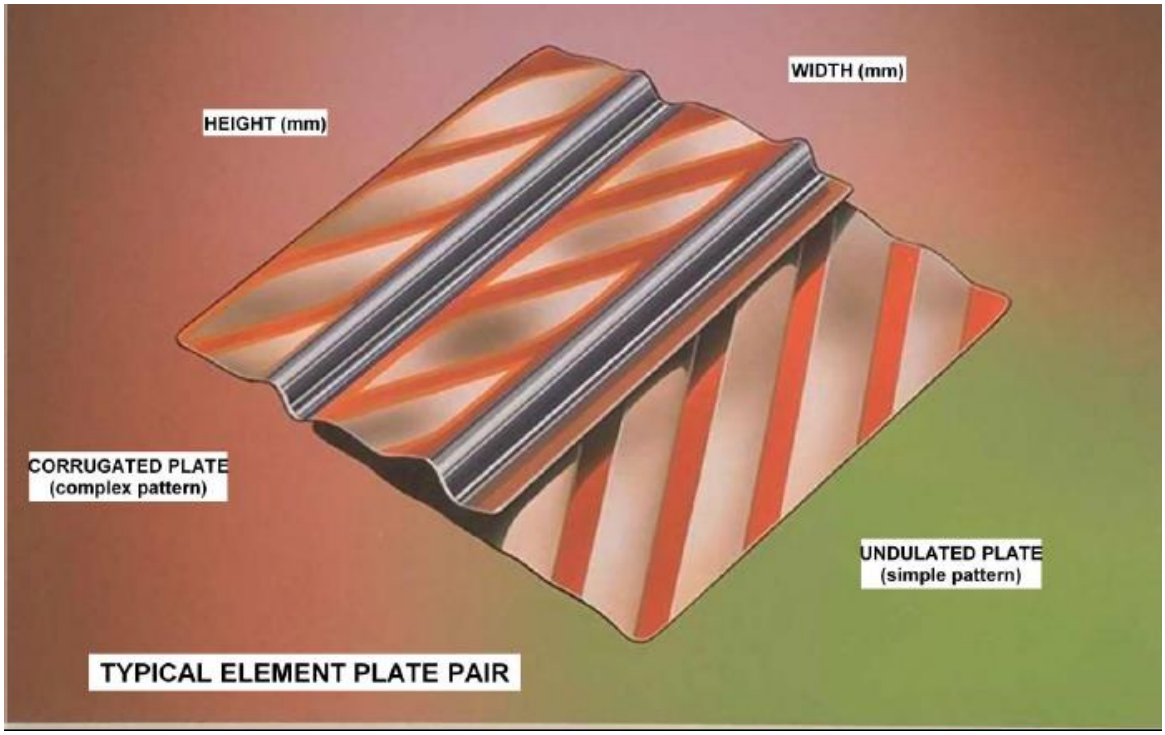

Figure 38 Typical air heater plate pair [50]

The rotating air heater is split into five rings with ring 1 being the innermost ring and ring 5 being the outer most ring. Each ring has 48 “packs” with each pack containing a hot/upper element, intermediate/middle element and cold/lower element. This results in a total of 240 packs with three elements per pack or 720 elements per air heater.

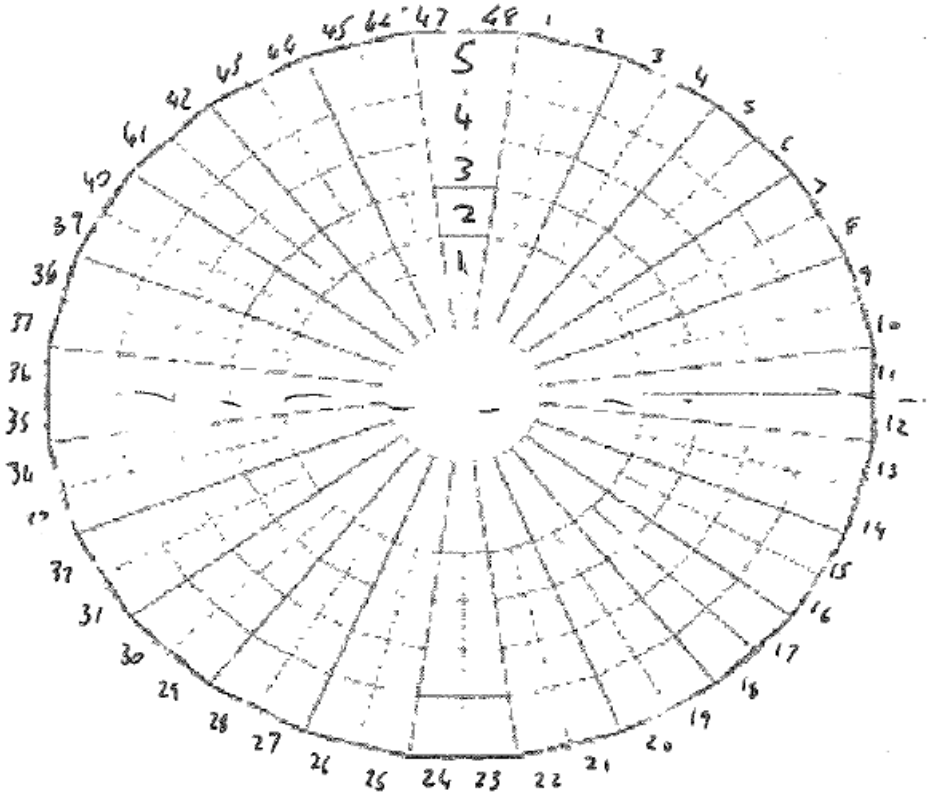

Figure 39 Air heater rings

The samples were cut out from rings 3 and 5 on both units 2 and 5, the samples consisted of hot, inter, and cold elements with both the corrugated and undulated plates being sampled.

These samples were then weighed and compared to the original weight to establish mass lost to erosion.

Table 4 Mass loss test results (Left-hand air heater)

Unit	Start date	End date	Ring	Layer	Type	Original mass	Measured mass	Mass loss	%mass loss
2	2013/05/01	2016/04/30	3	HE	Und	1.47	1.3	0.17	11.56463
2	2013/05/01	2016/04/30	3	HE	Corig	2.59	1.9	0.69	26.64093
2	2013/05/01	2016/04/30	3	INT	Und	1.31	1.2	0.11	8.396947
2	2013/05/01	2016/04/30	3	INT	Corig	2.32	1.7	0.62	26.72414
2	2013/05/01	2016/04/30	3	CE	Und	1.54	1.5	0.04	2.597403
2	2013/05/01	2016/04/30	3	CE	Corig	2.71	2.5	0.21	7.749077
2	2013/05/01	2016/04/30	5	HE	Und	2.2	1.8	0.4	18.18182
2	2013/05/01	2016/04/30	5	HE	Corig	3.89	2.75	1.14	29.30591
2	2013/05/01	2016/04/30	5	INT	Und	1.99	1.8	0.19	9.547739
2	2013/05/01	2016/04/30	5	INT	Corig	3.81	2.5	1.31	34.3832
2	2013/05/01	2016/04/30	5	CE	Und	1.93	1.9	0.03	1.554404
2	2013/05/01	2016/04/30	5	CE	Corig	3.42	2.65	0.77	22.51462
5	2013/08/01	2016/12/31	3	HE	Und	1.5	1.25	0.25	16.66667
5	2013/08/01	2016/12/31	3	HE	Corig	2.65	2	0.65	24.5283
5	2013/08/01	2016/12/31	3	INT	Und	1.59	1.3	0.29	18.23899
5	2013/08/01	2016/12/31	3	INT	Corig	2.81	2.05	0.76	27.04626
5	2013/08/01	2016/12/31	3	CE	Und	1.37	1.2	0.17	12.40876
5	2013/08/01	2016/12/31	3	CE	Corig	2.43	1.75	0.68	27.98354
5	2013/08/01	2016/12/31	5	HE	Und	2.2	1.8	0.4	18.18182
5	2013/08/01	2016/12/31	5	HE	Corig	3.89	2.9	0.99	25.44987
5	2013/08/01	2016/12/31	5	INT	Und	2.32	1.85	0.47	20.25862
5	2013/08/01	2016/12/31	5	INT	Corig	4.1	2.95	1.15	28.04878
5	2013/08/01	2016/12/31	5	CE	Und	2.16	2.1	0.06	2.777778
5	2013/08/01	2016/12/31	5	CE	Corig	3.81	3.05	0.76	19.94751

From the above results, a weighted average was calculated, and the following was the average wear rate per air heater for each unit:

Table 5 Average air heater mass loss

Unit	Start date	End date	%mass loss
2	2013/05/01	2016/04/30	16.60%
5	2013/08/01	2016/12/31	20.12%

4.6.2 Evaluation of method

An average coal calorific value for the time between new and mass loss measurement cannot be used, the produced formula for determining wear rate as a function of calorific value is non-linear. The erosion can, therefore, be written as the sum of the erosion in each period in the total time. For this study, the smallest period for which coal quality and unit running hours are reported is monthly. The erosion rate for each month is there for added up to give total erosion.

$$E = \sum \dot{\varepsilon} t$$

It is typically accepted that structural failure and unacceptable performance occurs at 35% [50]. This means that the model needs to provide a percentage based output of erosion with the original mass as base mass. This is accomplished by dividing the above formula by original air heater weight. The air heaters are identical for the station used in this case study it can, therefore, form part of the constant in the erosion rate calculation. The data used to determine the constant should then be in percentage base to accurately get a constant.

$$E = \sum(-0.1752 \times CV + 3.9785 \quad)k(-0.009 \times CV + \ 1.1525)^3 t$$

Equation 31

To test this, unit 2 percentage mass loss from loss Table was used to determine the constant by making use of a numeric method. The value of the constant was determined to be 0.000587.

Table 6 U2 data for constant estimation

Date	Average CV (MJ/kg)	U2 hours	U2 erosion %
May-13	15.79400511	0	0
Jun-13	15.74411724	414.16	0.306572187
Jul-13	15.7014966	595.87	0.444283529
Aug-13	15.77128826	744	0.548181751
Sep-13	15.613224	720	0.544880806
Oct-13	16.04731078	744	0.52249749
Nov-13	15.95826096	720	0.513625661
Dec-13	15.33544829	742.87	0.588538471
Jan-14	15.62415793	637.81	0.481796734
Feb-14	15.25069907	672	0.539726995
Mar-14	15.33961289	744	0.589035477
Apr-14	15.70784787	720	0.53625789
May-14	15.85322162	740.67	0.53810293
Jun-14	15.93851245	720	0.515400666
Jul-14	15.71952656	744	0.553036208
Aug-14	15.86895639	686.83	0.497632962
Sep-14	16.18398586	590.9	0.404977283
Oct-14	15.56002317	744	0.568070902
Nov-14	15.41229451	505.02	0.395122492
Dec-14	15.21939481	339.3	0.27388574
Jan-15	15.72959639	742.97	0.55132655
Feb-15	15.83041269	672	0.49013682
Mar-15	16.0141974	740.27	0.522925914
Apr-15	15.13803002	720	0.588776175
May-15	15.12237935	714.7	0.585893942
Jun-15	15.41941617	664.37	0.519190445
Jul-15	15.35656929	744	0.587414845
Aug-15	15.40507776	624	0.488788069
Sep-15	15.35839168	720	0.568297496
Oct-15	15.12117662	744	0.61002957
Nov-15	15.14374394	400.65	0.327332424
Dec-15	15.45836373	744	0.57771307
Jan-16	15.75619349	699.41	0.516657333
Feb-16	16.01356812	430.15	0.303891172
		Total erosion %	16.6
		k	0.000587434

Using the constant obtained and the data from unit 5, the erosion for unit 5 was estimated and compared to the measured percentage:

Table 7 Unit 5 erosion percentage estimation

Date	Average CV (MJ/kg)	u 5 hours	U5 erosion %
Aug-13	15.7712883	306.68	0.225962876
Sep-13	15.613224	720	0.544880806
Oct-13	16.0473108	744	0.52249749
Nov-13	15.958261	720	0.513625661
Dec-13	15.3354483	625.81	0.495797731
Jan-14	15.6241579	744	0.562011838
Feb-14	15.2506991	614.91	0.493874295
Mar-14	15.3396129	744	0.589035477
Apr-14	15.7078479	720	0.53625789
May-14	15.8532216	685.48	0.498006935
Jun-14	15.9385124	720	0.515400666
Jul-14	15.7195266	744	0.553036208
Aug-14	15.8689564	738.83	0.535308827
Sep-14	16.1839859	720	0.493456835
Oct-14	15.5600232	744	0.568070902
Nov-14	15.4122945	665.81	0.520922947
Dec-14	15.2193948	671	0.541636698
Jan-15	15.7295964	710.7	0.527380351
Feb-15	15.8304127	384.17	0.280202176
Mar-15	16.0141974	690.05	0.487450561
Apr-15	15.13803	720	0.588776175
May-15	15.1223794	744	0.60991338
Jun-15	15.4194162	683.11	0.53383534
Jul-15	15.3565693	711.15	0.561478585
Aug-15	15.4050778	744	0.582785775
Sep-15	15.3583917	720	0.568297496
Oct-15	15.1211766	701.1	0.574854478
Nov-15	15.1437439	720	0.58824247
Dec-15	15.4583637	744	0.57771307
Jan-16	15.7561935	932.64	0.68894539
Feb-16	16.0135681	696	0.491708138
Mar-16	16.2797963	744	0.501127649
Apr-16	15.8251776	603.43	0.44052054
May-16	16.0573795	523.18	0.366765362
Jun-16	15.5066557	720	0.554638909
Jul-16	15.7246339	707.95	0.525782936
Aug-16	15.6921646	744	0.555607203
Sep-16	15.3881876	691.64	0.543268685
Oct-16	15.5003581	673.08	0.519035455
Nov-16	16.2248052	98.07	0.066719331
Dec-16	15.5777565	0	0
		Total erosion calculated %	20.44483353

The erosion percentage was estimated as 20.44% and measured 20.12%. This is only a single point verification, even though it seems that the formula is accurate, it cannot be used as verification.

4.6.3 Time to failure for different coal qualities represented by corresponding calorific value

Accepting the constant determined in 4.6.2 and the formula the constant is used in the following graph was produced for this specific air heater and boiler design using coal from this specific mine.

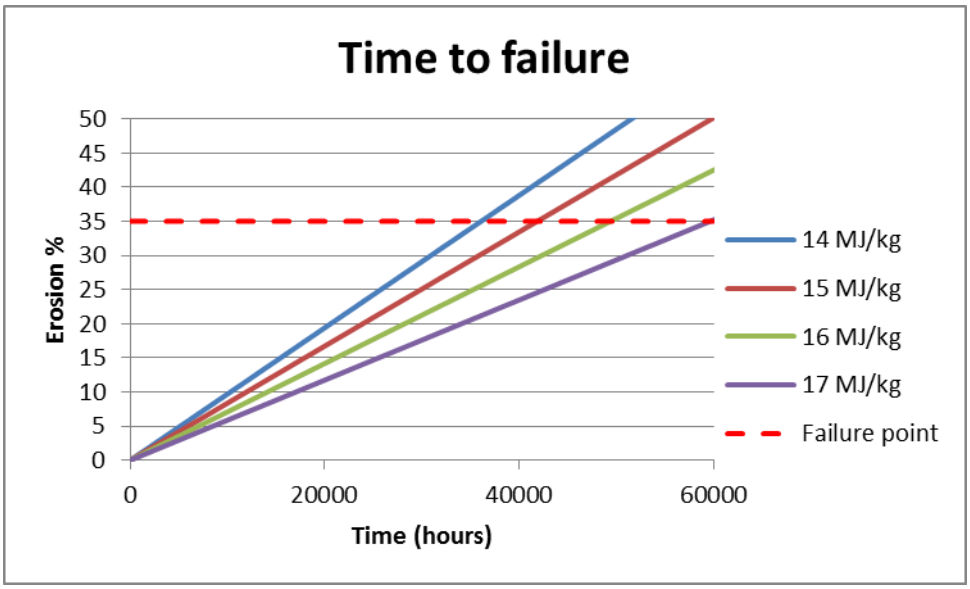

Figure 40 Time to failure for different coal qualities

Accepting the general assumption that pack failure in terms of structural rigidity and performance occurs at 35 % mass loss [50] the results indicate a significant increase in erosion with lower grade coal. This is due to higher flue gas velocities as well as higher ash mass flow produced due to more coal being required.

4.7 DISCUSSION

This case study showed a strong correlation between coal quality and erosion drivers such as ash production and flue gas velocity. The method followed also indicated that a strong correlation between calorific value and coal physical attributes such as ash content and volatiles concentration exists. Calorific value was as a result used as a single characteristic that implied the other characteristics of coal. This is particularly useful as calorific value is one of the most reportedcoal characteristics and also the most diligently tested.

It should be noted that this method can only be used where the coal is from a single origin and a correlation between calorific value and other characteristics are proven. The use of calorific value as an independent variable in stations with a variable feedstock supply could lead to incorrect prediction. This is due to calorific value being a product od the chemical composition of coal.

Other equipment which may be subjected to the same type of mechanism would be economiser tubes. The orientation of the economiser tubes put them directly in the flue gas flow path, using the same method it would be possible to establish the impact of coal quality on economiser tube fly-ash erosion.

4.7.1 Load impact on erosion

The impact of load variation was not taken into account in this case study as the assumption is that the units are run at full load. This assumption is justified as the station observed provides the lowest cost of energy in the power producers fleet and is, therefore, ran at capacity as often as possible. The average load of the two units observed is also almost identical, as seen in validating the assumption.

Table 8 Load conditions during observations

Unit	Date from	Date to	Boiler hours	Average ash Content (%)	Average CV (MJ/kg)	Ash content (kg/MJ)	Weighted load MWh	Average Unit load (weighted per hour) MW
2	2013/05/01	2016/04/30	21972	40.21473707	15.62821	0.025732	12004084.38	546.3355351
5	2013/08/01	2016/12/31	26465	40.33958896	15.63531	0.0258	14464907.49	546.5674471

It is possible that in future, a change in the operating philosophy of the power station may become necessary. A possible scenario would be that a large influx of renewable energy suppliers causes an oversupply of energy during daylight hours resulting in the coal baseload stations having to ramp down the load to stabilise the grid. This would result in the assumption, as mentioned earlier, to become null and void, and the formula for erosion should then be re-examined. It would not be possible to just scale down the erosion rate in accordance with the mass of flue gas and fly ash produced. The reason for this is that even if the cycle efficiency is assumed the temperature at which the flue gas enters the air heaters change depending on load conditions due to different rates of heat exchange occurring.

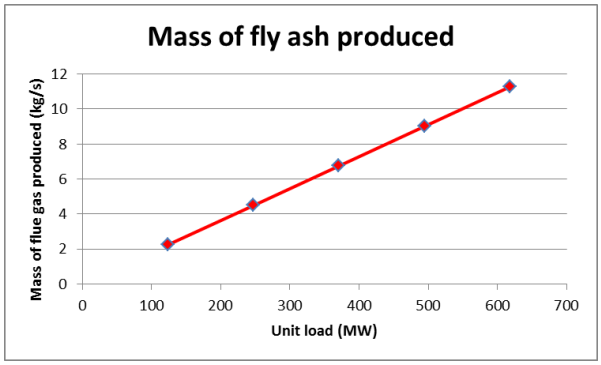

Figure 41 Fly ash production vs unit load

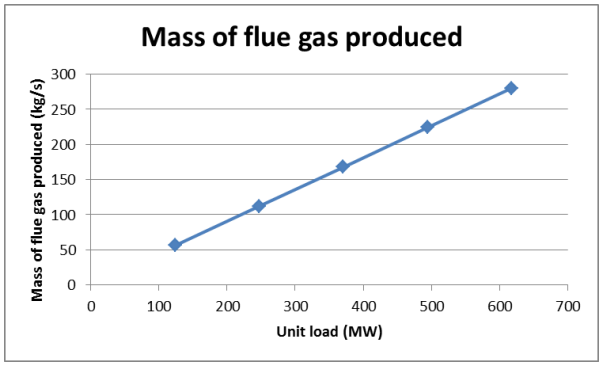

Figure 42 Flue gas production vs unit load

4.7.2 Erosion on different levels of air heater packs

As mentioned earlier in this report the air heater packs are made up out of 3 layers namely the Hot End (HE) or upper layer, Intermediate layer (INT) and the Cold end (CE) or lower layer. The data indicates that the erosion rate decreases from the hot end to the cold end, as seen in Figure 43 and Figure 44. This is thought to be due to the increasing density of flue gas due to the flue gas cooling down as it moves through the air heaters. The volume flow, therefore, decreases for the same mass flow and the velocity is directly proportional to volume flow. The formula has a velocity component that is elevated to the power of 3.

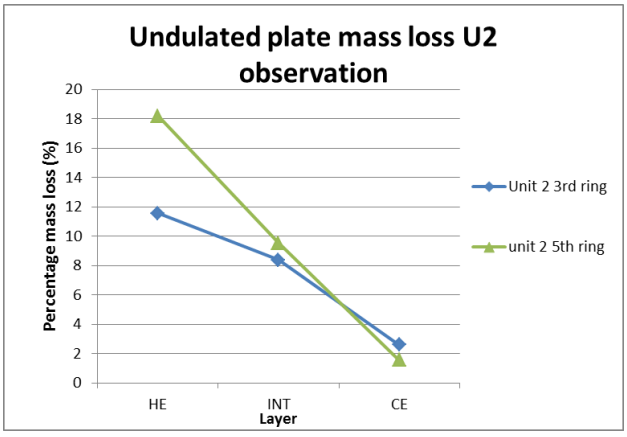

Figure 43 Unit 2 undulated plate mass loss

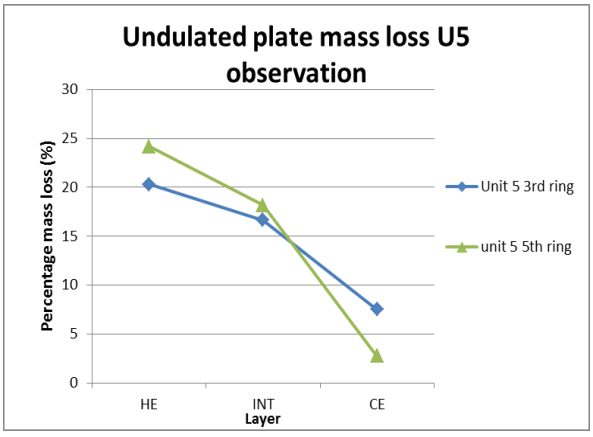

Figure 44 Unit 5 undulated plate mass loss

4.7.3 Usability in practice

One of the outcomes from this case study was a formula that can be used to estimate air heater pack erosion percentage. This formula can be used when making decisions about replacement times and can bring about better planning in

spares management. This formula is however specific to this power station as the coal delivered from the mine binds it. The reason this is true is that it is assumed that the ratio between the different combustibles in coal is nearly constant for an individual seam and this formula was not tested with coal from another source.

As mentioned in 4.7.1, the fitted constant and formula are only valid for the current load conditions where the power station is being run as a baseload station at full load constantly. The verification of the constant was done with data from only one additional unit and although it is favourable caution should be applied when using this formula to estimate erosion rates in future. The velocity exponent used to derive this formula (3) as determined by Sheer et al. is for a flat plate. Further tests are therefore required to determine the suitability of this exponent as well as the constant k.

5 MILL LINER CASE STUDY

In coal-fired power stations, a mill is used to grind the coal into a fine dust that is called pulverised fuel. The liners that are investigated in this study is of the ball and tube type as seen in Figure 45. In this type of mill coal is fed into the mill and the rotating drum caused the balls inside to roll over and fall on top of the coal inside in ordere to crush it. The fine pulverised fuel is then pneumatically conveyed into the classifier which rejects particles that are too coarse back to the mill. The fine particles that pass through the classifier are fed to the boiler burners.

Figure 45 Lethabo Power Station ball mills being installed

The primary function of mill liners is to act as a sacrificial surface to protect the mill shell from the aggressive abrasion environment inside the mill. The secondary function is to transfer mechanical energy from the rotating shell to the grinding media and coal.

The mill studied in this case study has three different types of liners, namely the End Liners, Inner End Liners and the Lifting liners. The liners have profiles and minimum thicknesses for replacement, as shown in Figure 46, Figure 47 and Figure 48:

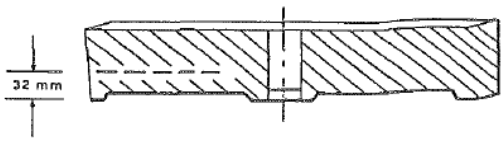

Figure 46 Trunnion end liner (Outer)

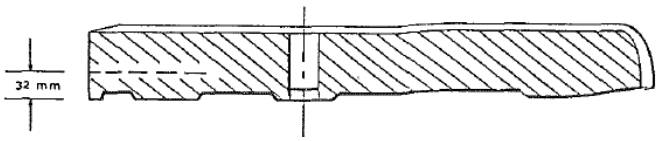

Figure 47 Trunnion end liner (Inner)

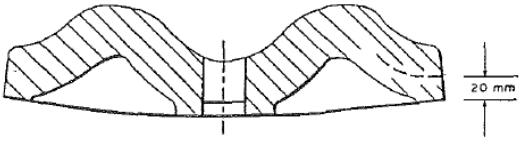

Figure 48 Lifting liner

Replacement of the mill liners can only be done during a unit shut down due to the long duration needed for the liner replacement to be completed. Accurate estimation of wear rates is therefore of utmost importance as it enables the plant engineer to plan replacements, spare holding, operating philosophy and the quantification of shell damage risk.

Wear rate testing of mill liners in a laboratory setup has however proven to be notoriously inaccurate and misleading as the tests fail to accurately reproduce the wear modes found in production mills [51]. The difficulty with plant-based testing is the invariability of feedstock (coal in this case) quality and the period needed for meaningful results. For this study, we have ten years' history of coal quality, mill running hours and NDT results for 36 mills. The aim is to utilise this information to create an accurate model of the influence coal abrasiveness has on the wear rate of mill liners.

5.1 EXPERIMENTAL PROCEDURE

The first step in the process is to collect data for mill usage, coal characteristics, grinding media top-up, liner replacement dates and results from inspections. The data is then matched to periods between inspections or between new installation and inspection.

Once isolated relationships and correlations were determined, based on this a basic formula for wear prediction was formulated and initial constants and exponents estimated.

Once the initial values of some of the constants and exponents have been estimated an iterative process was undertaken to fit the formula to the data in order to get a maximum coefficient of determination between the predicted values and the measured results. After an optimum solution was found for the formula's coefficients and constants, it was applied for various coal qualities to estimate the influence coal quality would have on mill liner lifespans.

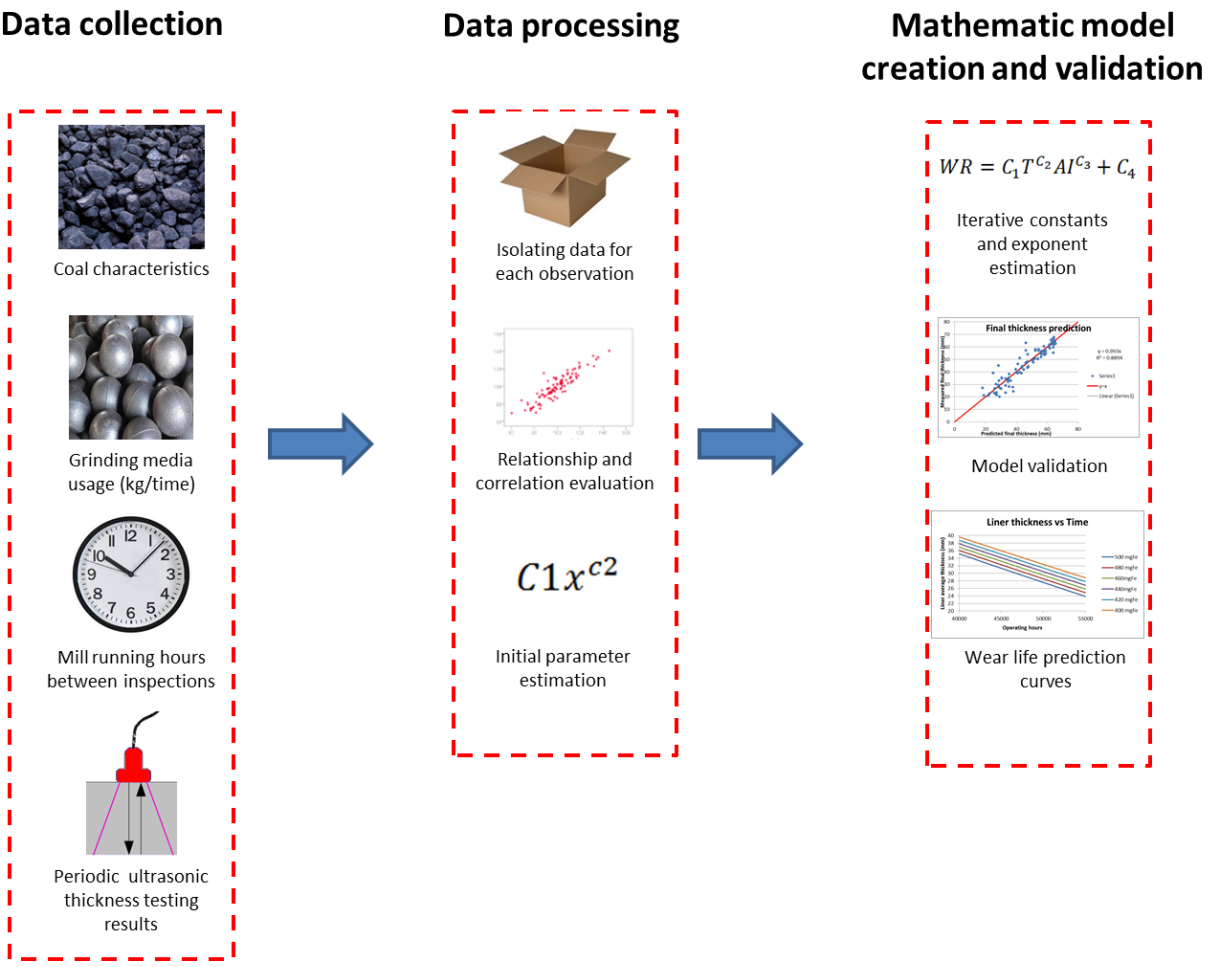

Figure 49 Model creation process

5.2 DATA COLLECTION

5.2.1 Mill liner ultrasonic thickness testing

The mill liner ultrasonic thickness tests are performed by making use of a template to ensure the measurements are taken at the same positions on the liners at each inspection. The inspections are done on a single liner on both the drive end (DE) and the non-drive end (NDE) of the mill. Once the results of the inspection are available, the non-destructive testing (NDT) technician notes the results on a control sheet that has numbers that correspond to the template inspection positions. The results from inspections between 2008 and 2017 were used for this study by compiling all the data from the control sheets into a spreadsheet and calculating average thicknesses from the template for wear calculation. It is important to note that results from inspection point 1 are not used for calculation as it has been noted that material loss at that location is far less than at the other locations.

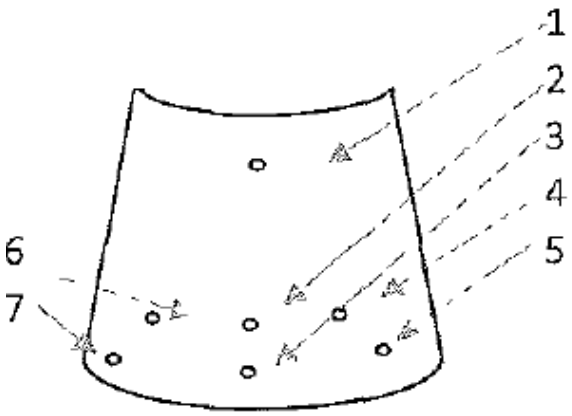

Figure 50 End liner outer NDT template

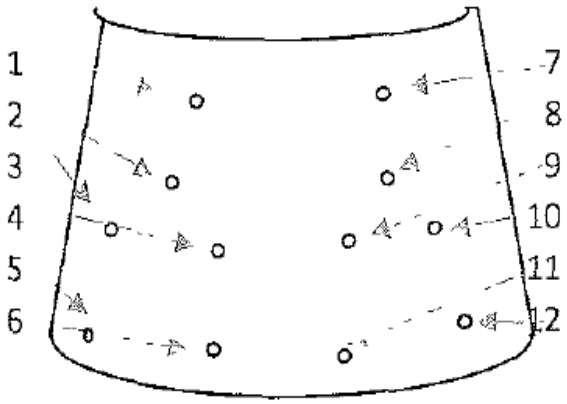

Figure 51 End liner inner NDT template

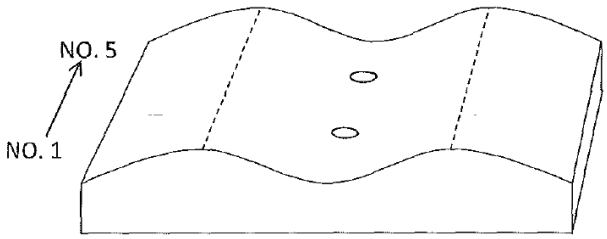

Figure 52 Lifting liners NDT map (tests are done in centre and both side crowns)

5.2.2 Coal characteristics

The coal quality data was extracted from the monthly quality reports supplied by the coal supplying mine. The report contains data for a wide variety of mechanical and chemical qualities of the coal supplied. For this case study, the following was extracted from the monthly reports:

- Abrasiveness Index (mgFe)
- Hardgrove Grindability Index (dimensionless)
- Calorific Value (MJ/kg)

The data extracted is represented in the graphs below:

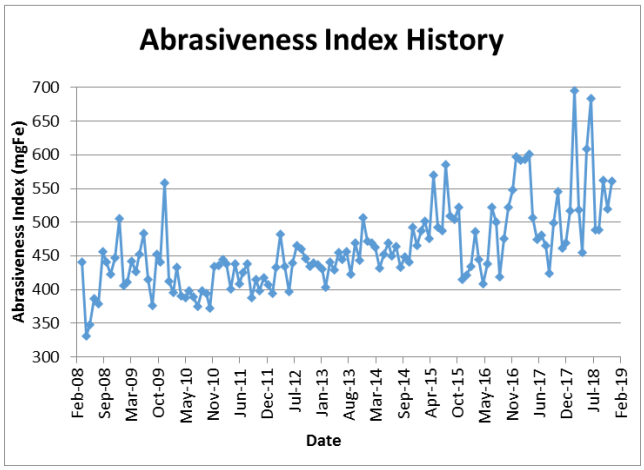

Figure 53 Abrasiveness Index historical data

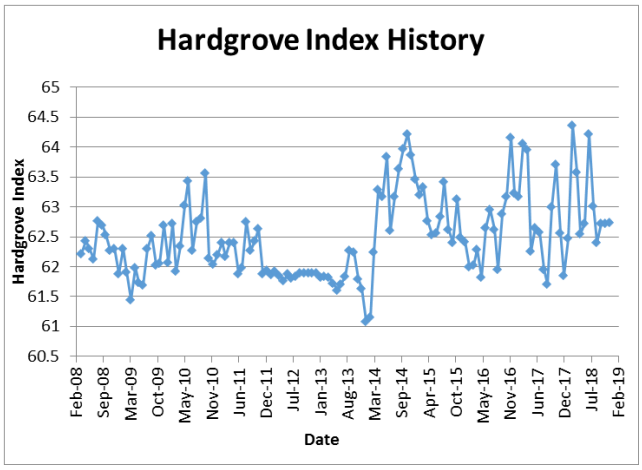

Figure 54 Hardgrove Index historical data

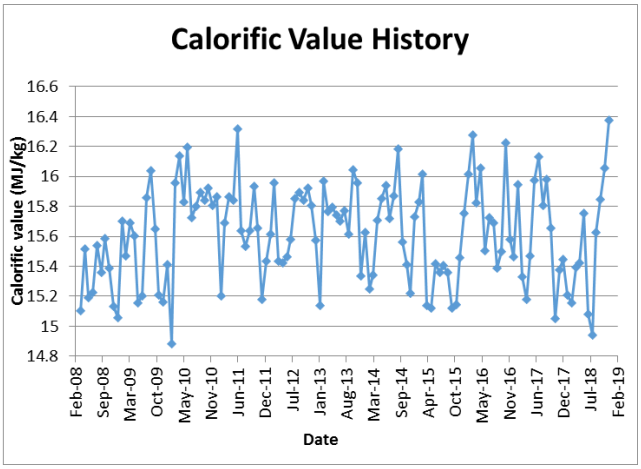

Figure 55 Calorific value historical data

From the data collected, it can be easily seen that extensive variability exists in the Abrasiveness Index of the coal received by the power station. The Hardgrove

Grindability Index and calorific value seem to have much less variability if a percentage deviation is considered.

5.3 DATA PROCESSING

After all the data has been recorded on an electronic spreadsheet, it was used to calculate meaningful indicators. These indicators include measured liner wear rate as a function of milling hours expressed as $WR = {}^{mm}/_{1000\ hours}$, grinding media usage expressed as $GMW = {}^{ton}/_{1000\ hours}$ and inter test period averages for abrasiveness index, grindability index, and calorific value.

The average inter-inspection Abrasiveness Index varies considerably with a minimum of 406 mgFe and a maximum of 504 mgFe, which is a considerable increase of 24% as seen in Figure 56. The average inter-inspection Calorific Value and Grindability Index value differs by only 2.6% and 2.6% respectively when the maximum of each is compared to the minimum. It is therefore assumed that the data will not provide significant insight into the effect grindability and calorific value has on mill liner wear and because the variation is minimal its effect will be incorporated in a constant in the mathematical model rather than adding a term for either grindability or calorific value.

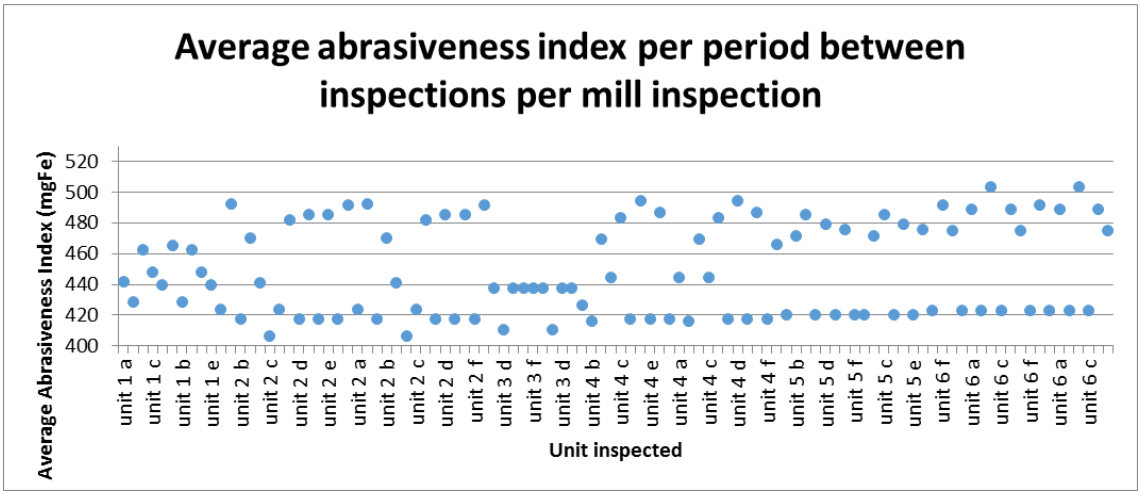

Figure 56 Inter-period AI for inspection results available

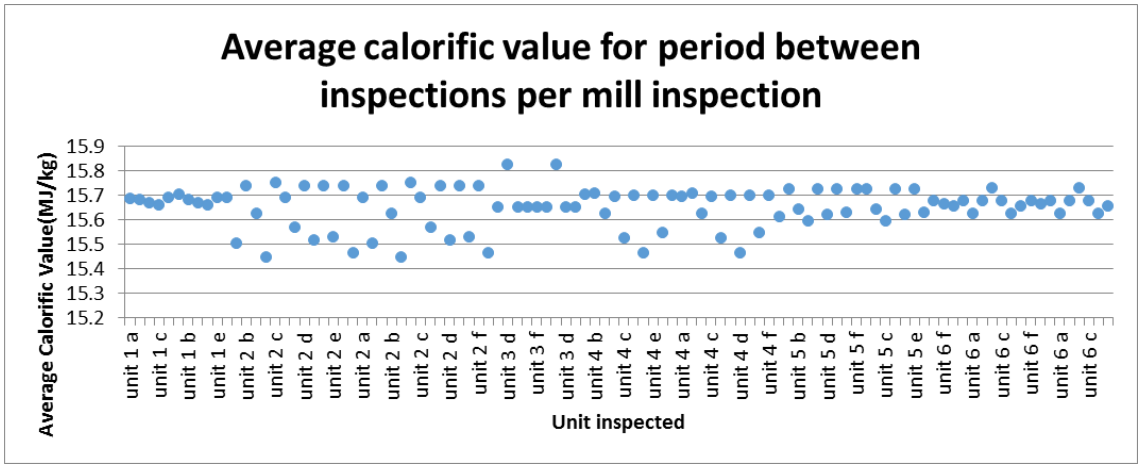

Figure 57 Inter-period CV for inspection results available

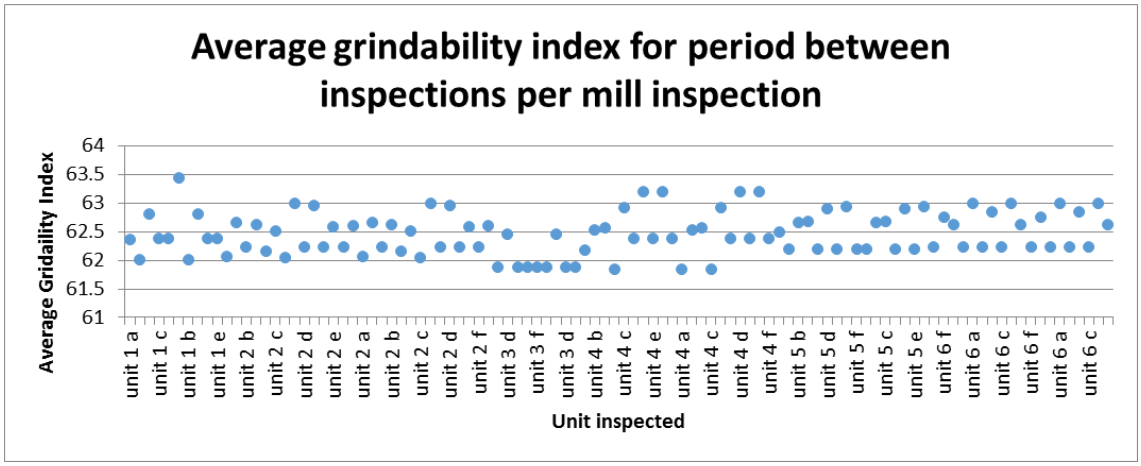

Figure 58 Inter-period GI for inspection results available

5.3.1 Relationship and correlation evaluation

As a result of the assumption made that not enough variability exists in terms of calorific value or grindability index for the data observed, only abrasiveness index was used to establish relationships and correlation.

The average wear rate for the period between inspections was plotted against the average abrasiveness between the specific inspections. The method of least squares linear regression line was calculated, and the corresponding coefficient of determination was calculated as 0.39. This indicates a weak correlation or more specifically that the variation of abrasiveness index does not properly explain the variation of wear rate and that other factors play a role.

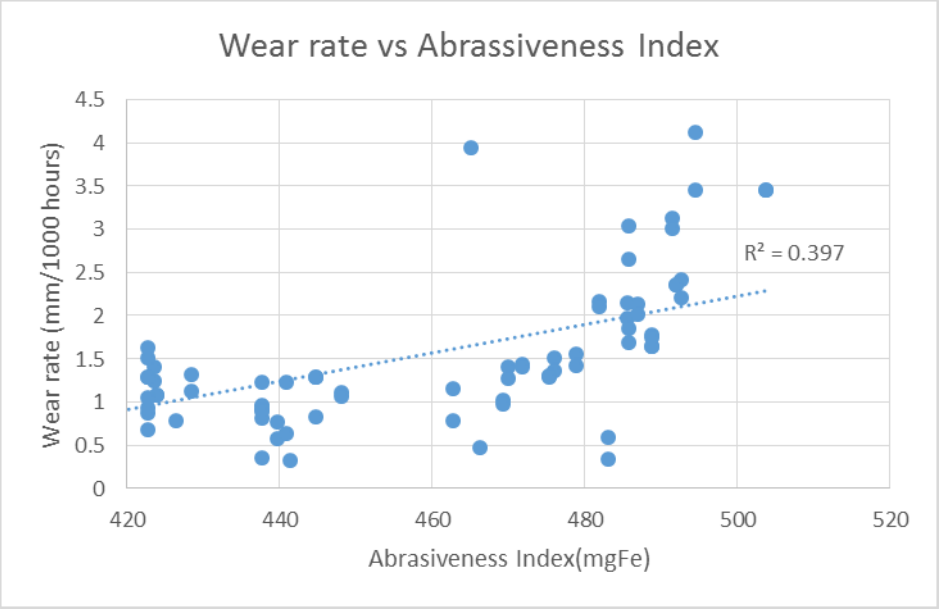

Figure 59 Wear rate vs Abrasiveness Index

When the starting thickness of mill liner is considered as in Figure 60, it is observed that a large variation of liner wear rate occurs at the new liner thickness of 81mm. Even though the coefficient of determination between the linear regression line and the data is low, it seems that an increased wear rate is observed with thicker liners, this indicates that a time/usage related process is affecting the wear resistance of the liners. It is suspected that this process is work hardening, as a result of the unavailability of old liners due to the recycling of old liners it was not possible to confirm this.

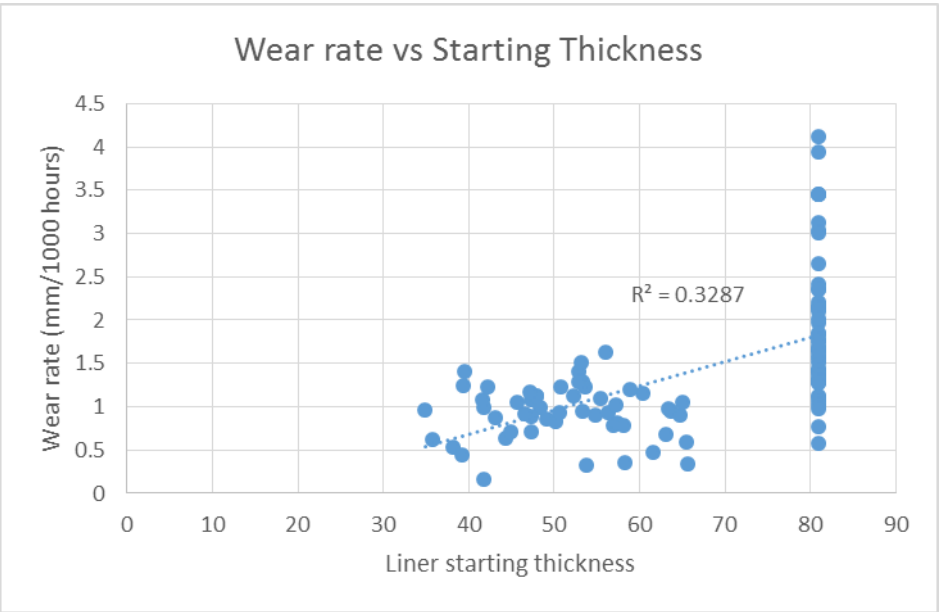

Figure 60 Wear rate vs Liner Thickness

5.3.2 Initial parameter estimation of the mathematical model

As a result of the suspicion that the liner wear might be affected by a time/usage related process such as work hardening, it was decided to evaluate the possibility that the following formula might describe the average wear rate for new liners.

$$W.R = C_1 t^{c2} AI$$

Equation 32 Initial form of the equation for liner average wear rate from start

Where

$W.R$ =Average wear rate from new (mm/1000hours)

AI =Abrasiveness Index (mgFe)

t =Time (hours)

C_1 =Constant to compensate for unknowns

C_2 =Unknown exponent of time

This gives the possibility of a term $\frac{W.R}{AI}$ that is used to isolate the influence of time on wear rate; this is under the assumption that the Abrasiveness Index has a linear effect on wear rate. It is important to have a strong initial guess of the constants that will be used in the mathematical model as the Generalized Reduced Gradient (GRG) method that will be used to optimise the formula is prone to finding the local minimum/maximum rather than the global best solution.

To test this $\frac{W.R}{AI}$ was plotted against time for new liners with a starting thickness of 81mm to ensure that the starting condition of the liner are uniform. A regression curve was fitted using the method of least squares regression for a power function, and the coefficient of determination was determined for the regression curve. The coefficient of determination of the regression curve to the data is 0.7524 as seen in Figure 61. As a result of the higher coefficient of determination, the formula for wear rate proposed can be fitted with the regression curve formula constant and exponent. The initial parameters for the mathematical curve explaining the average wear rate are, therefore:

$$W.R = 1.3355 t^{-0.622} AI$$

Equation 33

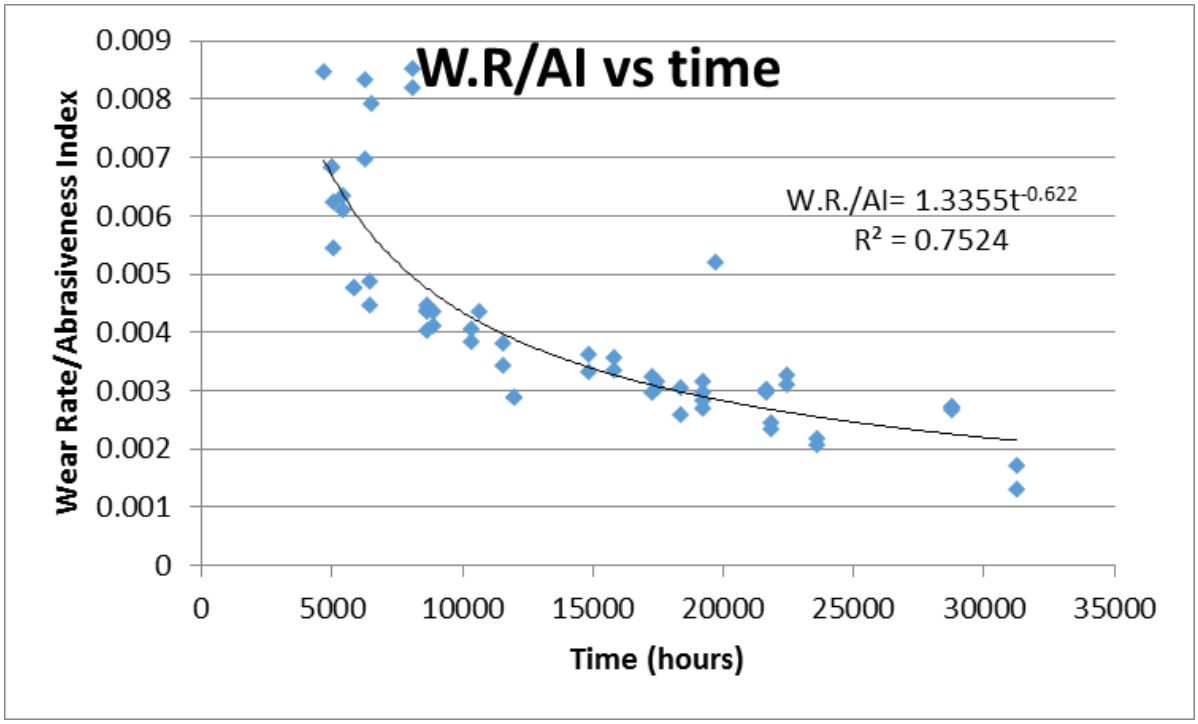

Figure 61 W.R vs Time

5.4 CREATION OF A MATHEMATICAL MODEL

The first step in the mathematical model was to estimate a formula for the average wear rate for liners from brand new condition (81mm). The formula suggested is as follows:

$$W.R = C_1 t^{C_2} AI^{C_3} + C_4$$

Equation 34 Mathematical model equation for average wear rate from start

Where

$W.R$ =Average wear rate from new (mm/1000hours)

AI =Abrasiveness Index (mgFe)

t =Time from new (hours)

C_1 =Constant to compensate for unknowns

C_2 =Unknown exponent of time

C_3 =Exponent of Abrasiveness

C_4 =Constant

Initial values comprise of those determined in 5.3.2 and setting the remaining constants equal to either 0 or 1 giving the initial values as C1=1.3355, C2=-0.622, C3=1, and C4 =0.

5.4.1 Estimation of equivalent time to starting thickness as the first step

The mathematical equation given by Equation 34 provides a curve for average wear rate from new condition (81mm), thus to be able to use this curve a total time from new needs to be used as input for t. The curve is also abrasiveness index dependent meaning that historical time cannot be used to make a prediction as the average abrasive index might differ from new condition to last inspection thickness and last inspection thickness to current condition.

It is, therefore, necessary to estimate an equivalent initial time which will be added to the time difference between the last inspection and the time for which the prediction is made to get to a final time for which the average wear rate is determined.

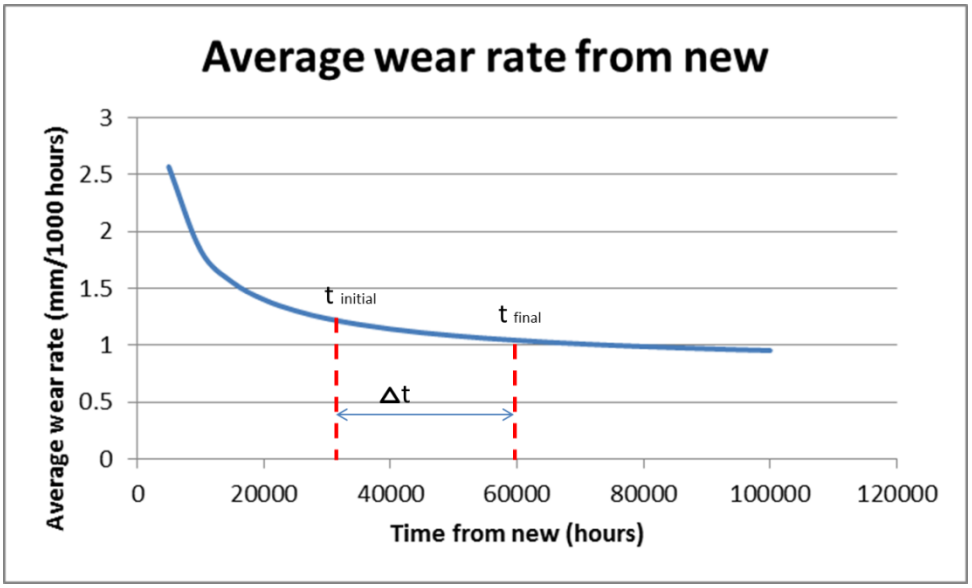

Figure 62 Equivalent initial time

To get the equivalent initial time the bisection method was used to get the intersecting point of the following function where the left side is the total wear divided by the equivalent initial time to get the wear rate in mm/1000 hours and the right side Equation 34.

$$\frac{1000 \times (81 - T_{initial})}{t} = C_1 t^{C_2} AI^{C_3} + C_4$$

Equation 35 Formula for bisection time estimation

Where

$T_{initial}$ =Liner thickness at last inspection

The Bisection method was applied for a minimum time of 0 hours and a maximum of 150000 hours, if the liner thickness was 81 mm time was set to 0 automatically. The sensitivity decided on was 10 hours.

5.4.2 Estimating the final thickness for a given time

The final thickness estimation is the purpose of this case study and it can be done by multiplying the average wear rate by the total time (initial equivalent time and time from the last inspection) dividing it by 1000 and subtracting that from the thickness of a new liner. The reason for dividing by 1000 is to harmonise the units within the formula.

$$T_{thickness} = 81 - (W.R)\left(\frac{t_{eq} + \Delta t}{1000}\right)$$

$$T_{thickness} = 81 - \left(C_1\left(t_{eq} + \Delta t\right)^{C_2} AI^{C_3} + C_4\right)\left(\frac{t_{eq} + \Delta t}{1000}\right)$$

Equation 36 Final thickness formula for the mathematical model

Where

$T_{thickness}$ =Thickness at last inspection t_{eq} = Equivalent initial time (mm)

Δt =Time from the last inspection

5.4.3 Optimising constants and exponents of model

The first step in optimising the mathematical model is to calculate the coefficient of determination between the predicted final thickness and measured final thickness. It is important to note the coefficient of determination was calculated for the actual values of the mathematical model and not a regression line.

The second step is to optimise the constants from their initial guess values to values that result in the highest coefficient of determination. This is done using the Generalized Reduced Gradient (GRG) method iteratively. This means that the iterative process includes estimating an initial equivalent time and coefficient of determination for each prediction every time the method is iterated. This was very memory intensive to compute and gave the following results:

5.4.3.1 Mill outer end liner

The first attempt was made by keeping the assumption that the relationship between coal abrasiveness and liner wear is linear, thus keeping C3=1. This resulted in the following formula for average wear rate and coefficient of determination:

$$W.R = 2.11672\left(t_{eq} + \Delta t\right)^{-0.74825} AI + 0.76343$$
$$R^2 = 0.87$$

It was then decided to check if ignoring the assumption would increase the coefficient of determination significantly. This yielded the following formula for wear rate and coefficient of determination:

$$W.R = 1.01243\left(t_{eq} + \Delta t\right)^{-1.4353} AI^{2.1114} + 0.97562$$
$$R^2 = 0.89$$

This indicates that the non-linear assumption provides a 2% better fit of the data, to decide if this is justified a visual representation of the model fit was created for each case and can be seen in Figure 63 and Figure 64:

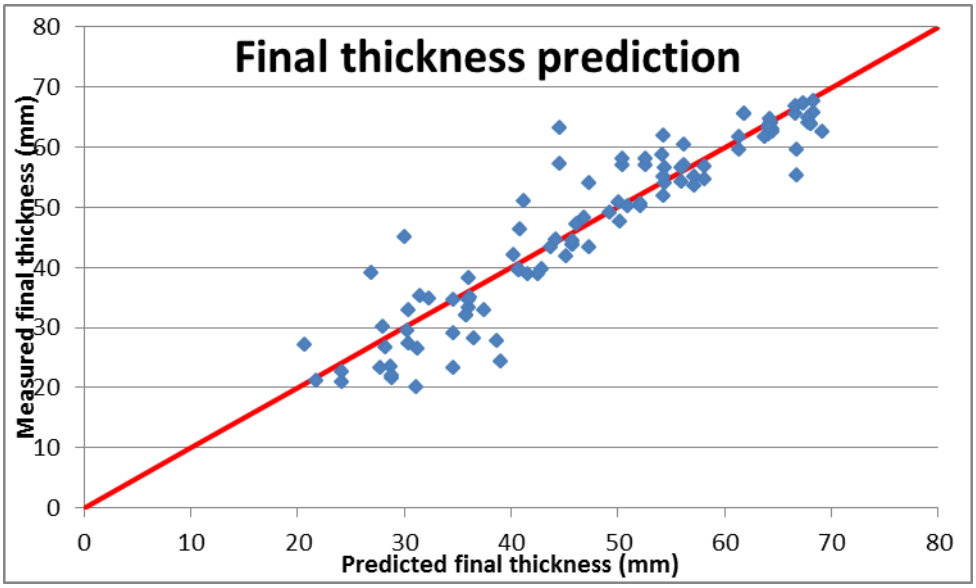

Figure 63 Model fit for the linear assumption

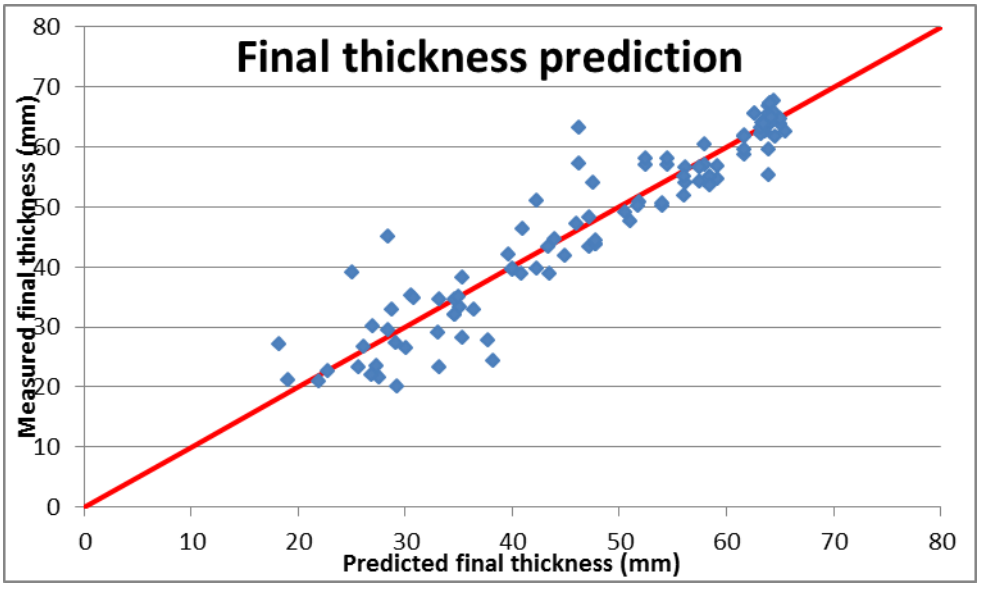

Figure 64 Model fit for the non-linear assumption

The data does not provide a significant reason to reject the assumption that the relationship between coals' Abrasiveness Index and liner wear rate is linear. Thus the formula for the linear relationship is retained.

5.4.3.2 Mill inner end liner

The mill inner end liner data was analysed using the guess values from the outer end liner and optimising the coefficients by using the Generalized Reduced Gradient algorithm. The optimisation goal was to maximise the coefficient of determination between the measured and predicted values. The resultant formula and coefficient of determination are as follows:

$$W.R = 3\left(t_{eq} + \Delta t\right)^{-0.746693} AI + 0.393$$
$$R^2 = 0.8$$

The linear assumption also produces a favourable coefficient of determination between the predicted and measured final thicknesses. This indicates that the model would be reasonably accurate for determining life cycle thickness curves for the inner end liners.

The only drawback is that the data does not include a lot of instances where the final thickness is below the minimum acceptable thickness as the inner liners tend to wear slower than the outer end liners. This results in the model being extrapolation for time to the minimum thickness.

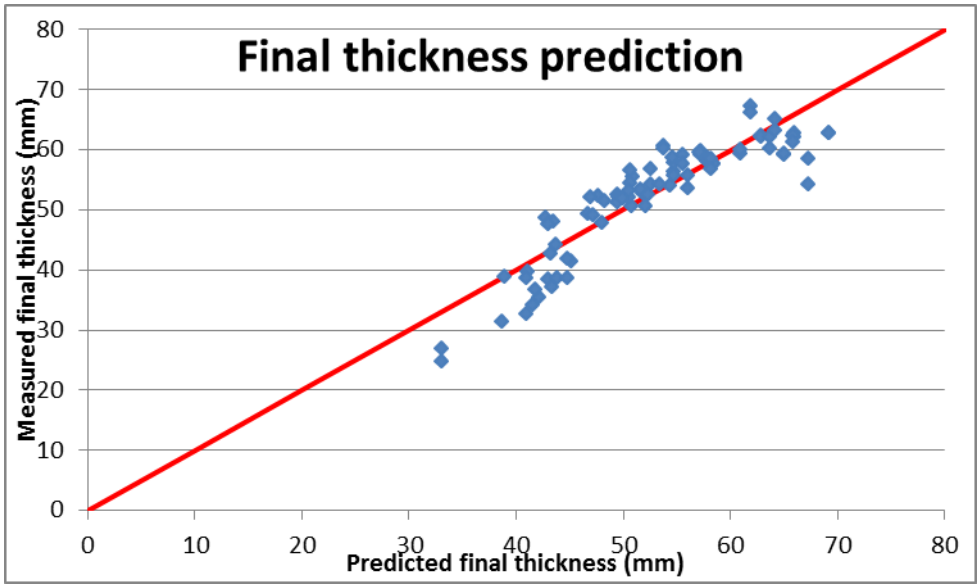

Figure 65 Mill inner end liner model fit

5.5 IMPACT OF COAL ABRASIVENESS INDEX ON LINER WEAR

5.5.1 Mill outer end liner

The formula fitted in 5.4.3 for the mill outer end liner was used, and the abrasiveness index varied between the maximum and minimum average observed during the data-gathering phase. The resulting curves can be seen below:

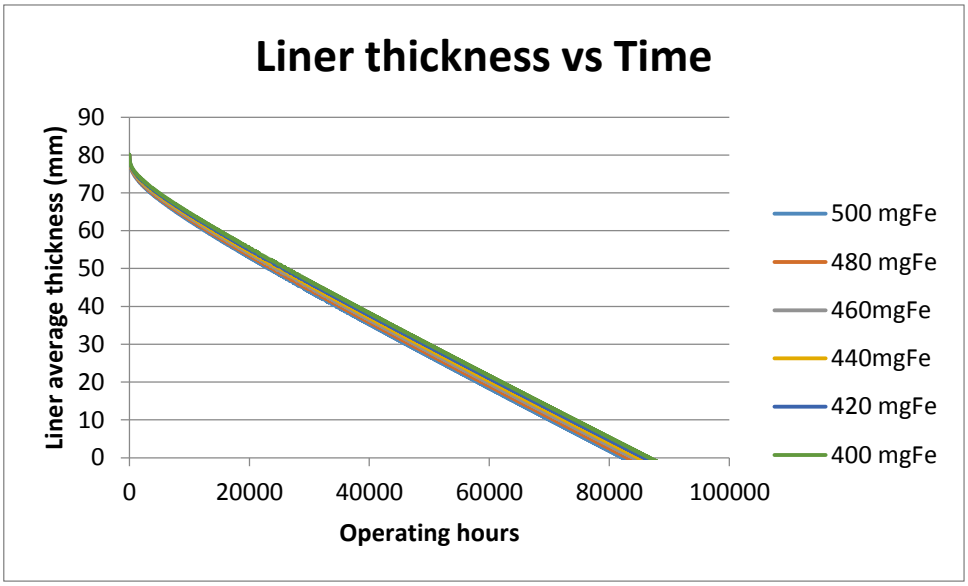

Figure 66 Impact of coal abrasiveness on mill end liner wear

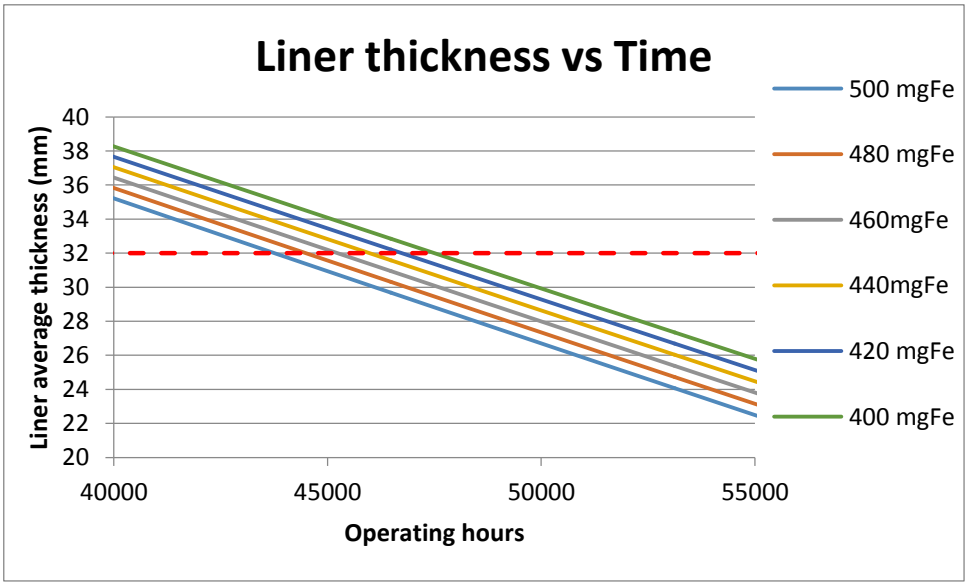

Figure 67 Impact of coal abrasiveness on replacement age of end liners

The age that the mill outer end liner reaches the replacement threshold is given in Table 9 for each coal abrasiveness index evaluated:

Table 9 Replacement age at different abrasiveness indices

Impact on replacement age	
Abrasiveness Index (mgFe)	Age at threshold (hours)
400	47500
420	46737
440	45980
460	45232
480	44490
500	43755

The results indicate that for a 100 mgFe increase in Abrasiveness Index, the operating time to reach the threshold for replacement only differs by 3745 hours. This is a 7.8% reduction in time indicating that Coal Abrasiveness Index does not have a significant impact on liner wear rates for values observed.

5.5.2 Mill inner end liner

The formula fitted in 5.4.3 for the mill inner end liner was used and the abrasiveness index varied between the maximum and minimum average observed during the data-gathering phase. The resulting curves can be seen in Figure 68:

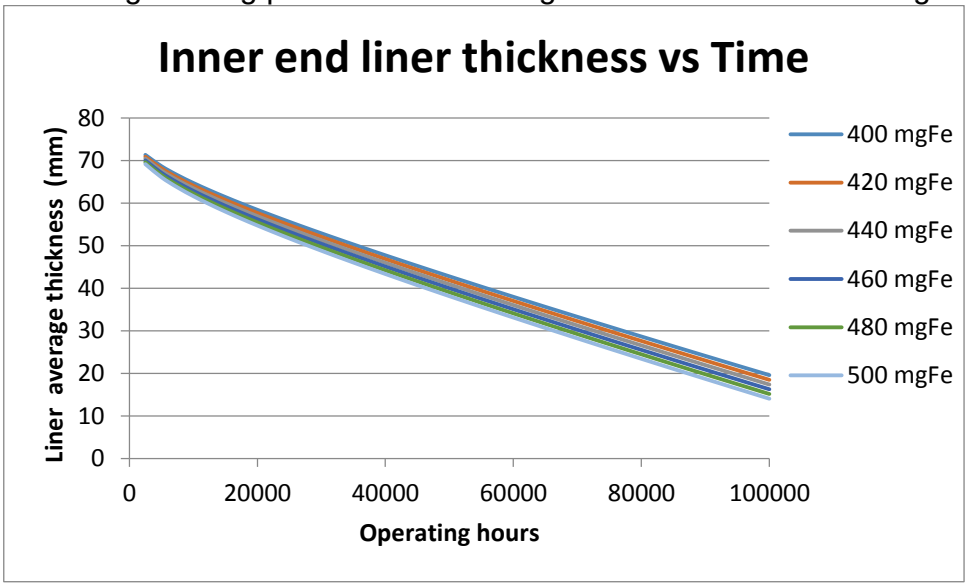

Figure 68 Impact of coal abrasiveness on mill liner wear

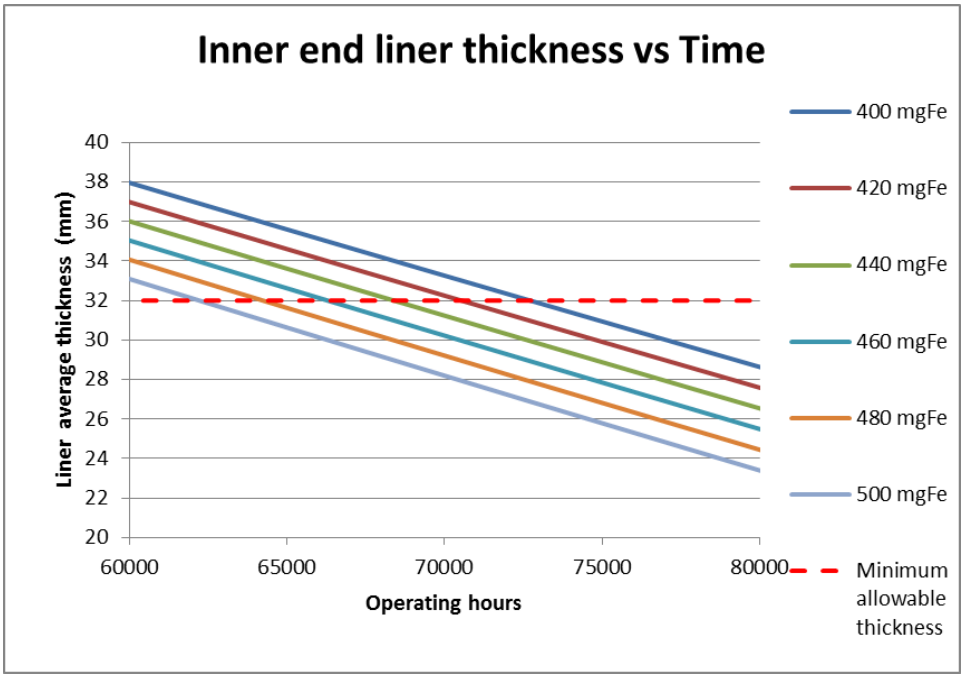

Figure 69 Impact of coal abrasiveness on mill inner end liner replacement age

Table 10 Coal Abrasiveness impact on replacement age of inner end liners

Impact on replacement age	
Abrasiveness Index (mgFe)	Age at threshold (hours)
400	72714.32228
420	70533.57266
440	68392.60225
460	66293.50913
480	64235.9706
500	62220.6933

DISCUSSION

The results of this case study indicate that coal abrasiveness index does have a direct impact on the mill liner lifetime, The impact this variation in AI of the feedstock has on liner wear is not expected to impact the current strategy of 6 yearly liner replacements as 6 years corresponds to 52560 hours. The six yearly replacement strategy is based on availability of the plant and is driven by the boiler

outage strategy. This can, however, influence the decision when outage deferment is contemplated due to demand constraints.

The case study could not quantify the impact grindability of coal has on liner wear, and it is expected that it would have a greater impact as grindability of coal directly correlates with the energy needed to mill coal to a desired fineness.

The study was also carried out on mills with the same classifier vane setting meaning that they all mill to the same fineness. It would be beneficial for future studies to evaluate the impact that the required fineness has on the mill wear rate. The reason this is suggested is that when finer pulverised coal is required, more particles are rejected through the classifier resulting in more re-milling and larger coal residence time in the mill.

6 COMBUSTION CASE STUDY

The energy produced by a coal-powered thermal power station is directly derived from the combustion of coal in a large steam generator. The combustion of the coal occurs in the furnace of the steam generator where after the energy is transferred to the water or steam through a series of heat exchangers.

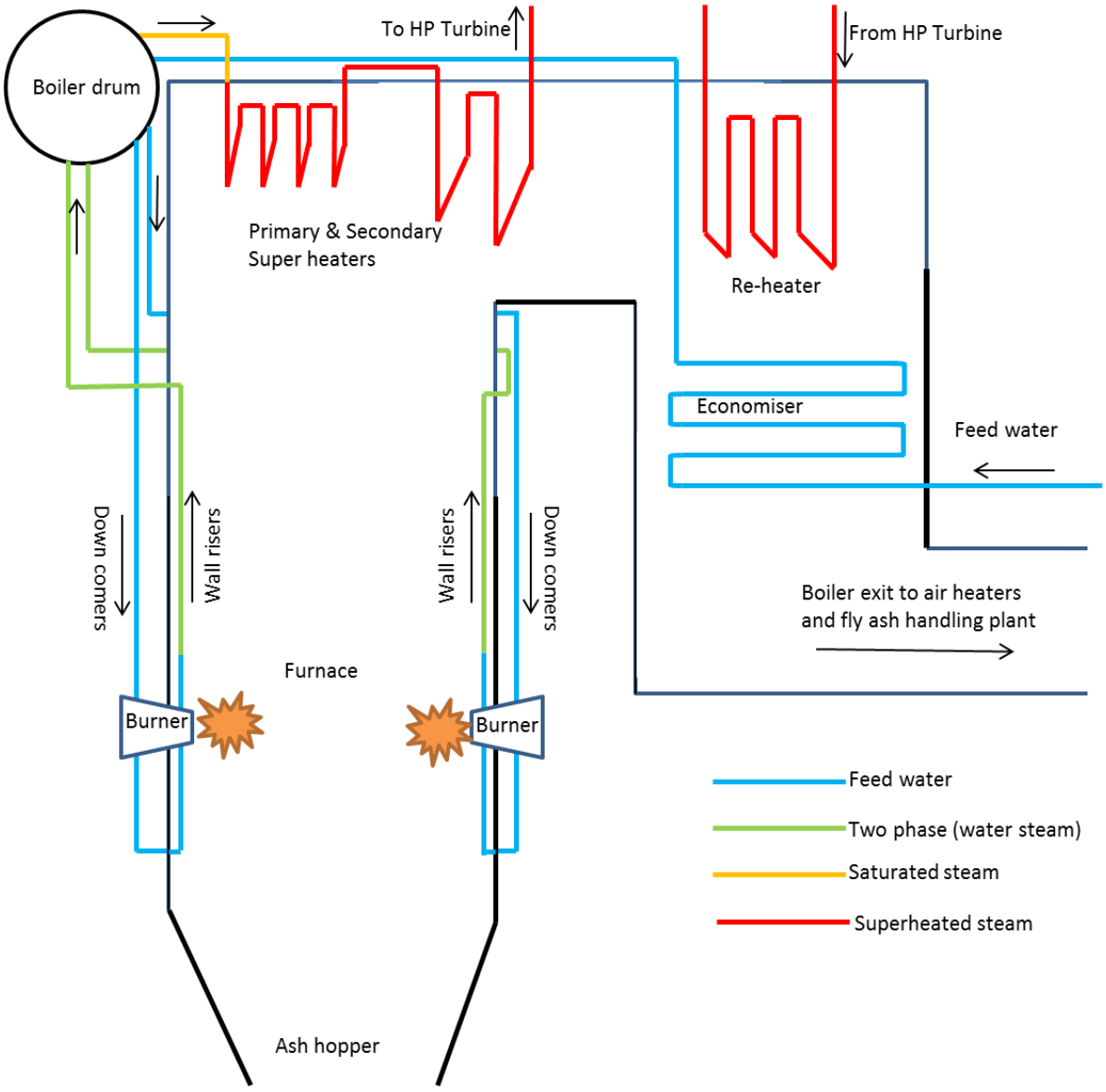

Figure 70 Drum type natural circulation boiler

As can be seen in Figure 70 the flue gas is generated in the furnace by the combustion of coal where after the flue gas travels up through the front gas pass and over the primary and secondary superheaters. After the superheaters, the flue gas travels over the re-heater and the economiser before exiting the boiler. From the boiler, the flue gas travels through the air heaters and into the fly ash handling plant which generally includes an electrostatic precipitator or a bag filter plant.

The feedwater enters the boiler from the deaerator storage tank to the economiser. The economiser heats the feed water before it travels to the boiler drum. From the boiler drum, the feed water travels down the downcomers and up through the wall risers; this flow occurs due to natural circulation. The natural circulation occurs because of a difference in densities between the fluid in the downcomers and the two-phase steam/water mixture in the wall risers. The purpose of the wall risers is to effect a phase change from liquid to saturated steam for the given flow rate. After the wall risers, the two-phase steam/water mixture travels back to the drum where the saturated steam is separated from the water. The saturated steam then moves to the superheaters where it is heated into superheated steam. The super-heated steam is then sent to the high-pressure turbine. From the high-pressure turbine exhaust steam is sent back to the re-heater before flowing to the intermediate pressure turbine.

To adequately understand the effect the coal quality has on the individual components, a mathematical model of a steam generator needed to be set up. This was done by making use of heat transfer, combustion, and hydraulic calculation. The boiler simulated was a utility size boiler without a reheat path after the HP turbine. The boiler was set to produce 520 kg/s steam at 550 ^{o}C.

The model was altered by changing the coal quality to estimate the effect coal calorific value has on the Furnace Exit Gas Temperature (FEGT) as well as temperatures further downstream. This indicated the effects coal quality would have on damage mechanisms such as creep-fatigue as well as erosion due to soot blowing of boiler heat exchange surfaces.

6.1 BOILER MODEL TO DETERMINE EFFECT OF CALORIFIC VALUE ON BOILER DAMAGE

The boiler mathematical model was created with the following assumptions and requirements.

- Full load steam requirement to turbine: 520 kg/s steam at 550 °C
- No reheat cycle, meaning only superheaters before
-
- Furnace Exit Gas Temperature (FEGT): FEGT= 1100°C-1200°C at full load with the specified calorific value of coal
- Water temperature into economiser: 150°C
- The view factor of the furnace walls is 0.9
- Furnace dimensions 24m wide and 13.72m deep (based on actual furnace dimensions).

6.1.1 Furnace model

The function of the furnace is to evaporate the amount of feed water needed for the cycle in this case 520 kg/s. The furnace is therefore optimised to provide the required energy to effect this conversion as well as to suit the FEGT specification. The water to the drum that forms part of the furnace cycle is fed from the economiser, and thus the energy requirement is calculated using the economiser outlet temperature at the drum pressure as the input temperature and pressure.

The main method of heat exchange at the furnace is radiative heat transfer. The model for the furnace (gas side) is taken from Verbanck 1997 where the following equations are given:

$$H_{in} = heat\ in\ fuel\ burnt + heat\ in\ hot\ combustion\ air$$
$$H_{in} = NCV + \dot{m}_{ha}(c_{ha}t_{ha} - c_a t_a)$$

Equation 37

Where:

H_{in}= Nett input into furnace (kJ/kg coal)

NCV= Nett calorific value of the coal (kJ/kg)

$\dot{m}_{ha}$= Hot combustion air mass flow (kg/kg fuel)

c_{ha}= Specific heat of air (KJ/kg°C)

t_{ha}= Temperature of the hot air (°C)

c_a= Specific heat of ambient air (KJ/kg°C)

t_a= Ambient temperature of air (°C)

And

$$H_{out} = Heat\ absorbed\ by\ the\ furnace\ walls + \text{Heat carried by the exit gasses}$$

$$H_{out} = \frac{20{,}53 \times Fr \times BBSA}{m_f}\left[\left(\frac{Te}{100}\right)^4 - \left(\frac{Tw}{100}\right)^4\right] + \dot{m}_g(c_e t_e - c_a t_a)$$

Equation 38

Where:

$20{,}53$= Stefan-Boltzmann constant

Fr= Correction factor for geometry and emissivity

Te=Absolute exit gas temperature (°K)

Tw=Absolute temperature of furnace walls (°K)

$\dot{m}_g$= Mass of flue gas produced per kg fuel (kg/kg)

c_e= Specific heat of exit gas (KJ/kg°K)

t_e= Temperature of the exit gas (°K)

The water energy requirement was calculated by the following equation:

$$Q = \dot{m}(h_{ss} - h_{fw})$$

Equation 39

Where:

Q= Energy absorbed by the feed water

$\dot{m}$= Mass flow of water/steam (kg/s)

h_{ss}= Enthalpy of saturated steam at drum pressure (kJ/kg°K)

h_{fw}= Enthalpy of water at drum pressure and inlet temperature (kJ/kg°K)

6.1.2 Amount of air per kg of coal

The assumption is that the coal used is from the same mine as the coal from the case study on air heater erosion as a function of calorific value. In that case study, a formula was fitted for the mass of combustion air (including excess air) and calorific value.

$$\dot{m}_{ha} = 0.3634(CV) + 0.8553$$

Equation 40

6.1.3 Heat exchange in heat exchangers (Super-heater and economiser)

The overall heat exchange in the heat exchangers is done by determining the heat transfer coefficient for each method of heat transfer applicable. This is then used to calculate an overall heat transfer coefficient. The overall heat transfer coefficient is then used in the Logarithmic Mean Temperature Difference (LMTD) method to calculate the inlet and outlet temperatures of both fluids.

$$Q = U \times A \times \frac{\Delta T(B) - \Delta T(A)}{\ln[\Delta T(B)/\Delta T(A)]}$$

The orientation of the heat exchanger flow is assumed as counter-flow; thus the terms are :

Q=Overall heat transfer (W) U= Overall heat transfer coefficient (W/m^{2}K)

A= Heat transfer surface area (m^2) $\Delta T(A)$=$T_{GasOutlet} - T_{Steam\ Inlet}$

$\Delta T(B)$=$\mathrm{T_{Gas\ Inlet}} - \mathrm{T_{Steam\ Outlet}}$

To determine the inlet and outlet temperatures of both fluids as well as the heat transfer an iterative process is used to solve the above equation as well as the following two equations simultaneously with only flow rates and inlet temperatures are given.

$Q = c_{gas}(T_{Gas\ Inlet} - T_{GasOutlet})$ and $Q = c_{steam/water}(T_{Steam\ Outlet} - T_{Steam\ Inlet})$

Where:

Q= Energy required for temperature change (W) c_{gas}= Specific heat of flue gas (kJ/kgK)

$c_{steam/water}$= Specific heat of steam (kJ/kgK) (water for economiser) $T_{Gas\ Inlet}$= Inlet flue gas temperature (^{o}C)

$T_{GasOutlet}$= Outlet flue gas temperature (^{o}C) $T_{Steam\ Outlet}$= Outlet steam temperature (^{o}C)

$T_{Steam\ Inlet}$= Outlet steam temperature (^{o}C)

The energy used to cause the temperature change of the fluids is equal to the total heat transferred.

6.1.4 Balancing the model

To balance the furnace, the following two conditions need to be satisfied:

$$H_{in} = H_{out}$$

And

$$Q = Heat\ absorbed\ by\ furnace$$

$$\dot{m}(h_{ss} - h_{fw}) = \frac{20{,}53 \times Fr \times BBSA}{m_f}\left[\left(\frac{Te}{100}\right)^4 - \left(\frac{Tw}{100}\right)^4\right]$$

Equation 41

6.1.5 Boiler model results

Under the original conditions the model yields the following results for this hypothetical boiler:

Furnace			
T_water in (°C)	288.5904118	T_steam out (°C)	359.618
FEGT (°C)	1137.189822	Drum Pressure (kPa)	18600

Table 11 Furnace values at initial parameters

Super Heater			
T_steam in (°C)	359.618	T_steam out (after attemperation) (°C)	550
Attemperator spray (kg/s)	3.206836784	Delta P (kPa)	372.346516
Flue gas exit temperature (°C)	846.8735865	Inside wall temp (°C)	558.760152
Outside wall temp (°C)	564.4488108		

Table 12 Superheater initial parameters

Economiser			
T_water in (°C)	150	T_water out (°C)	288.5904118
Detla_P kPa	4.40114453	Flue gas exit temperature (°C)	380.2406849
Outside wall temp (°C)	313.2969437	Inside wall temp (°C)	310.6268536

Table 13 Economiser initial parameters

6.1.6 Effect of variation of calorific value on boiler temperatures

The model parameters were changed to determine the effect it would have on the temperature distribution through the boiler.

Coal information		Furnace	Superheater						Economiser	
Calorific value (MJ/kg)	Fuel consumption (kg/s)	FEGT (°C)	Steam in (°C)	Steam out (°C)	Attemperation spray (kg/s)	Temperature after attemperation (°C)	Outside wall temperature (°C)	Inside wall temprature (°C)	Water outlet temperature (°C)	Flue gas boiler exit temperature
14	99.24628701	1133.250136	359.618	559.6147061	3.520318253	550	565.2974666	559.6147321	291.3303103	384.0321262
15	92.29413776	1135.348949	359.618	559.1709145	3.357829568	550	564.8569984	559.1709406	289.819469	381.9448537
16	86.32368614	1137.189822	359.618	558.7601259	3.206836784	550	564.4488108	558.760152	288.5904118	380.2406849
17	81.07836259	1138.800075	359.618	558.3858163	3.06983077	550	564.0765579	558.3858424	287.499751	378.7251201
18	76.42644433	1140.21115	359.618	558.0323282	2.940357667	550	563.724498	558.0323543	286.5116399	377.3504548

Table 14 effects of calorific value variation on temperatures

The results indicate that higher calorific value coal results in higher furnace exit temperatures while lower calorific coal results in higher temperatures after superheaters as well as higher boiler exit temperatures (after economiser). The lower calorific coal also caused increased metal temperatures of the heat exchangers. The results are specific to this hypothetical model, but the trend of the results is expected to be the same for all pulverised fuel boilers.

The reason that lower furnace exit temperature from the lower grade coal creates higher temperatures throughout the boiler is due to a higher mass flow of flue gas. The lower grade coal results in higher fuel consumption as well as a greater total energy input for the same steam output. This means that the boiler is less efficient with the lower grade coal as is implied with the higher temperature of the exhaust gasses.

Calorific value (MJ/kg)	Fuel consumption (kg/s)	Total energy input from coal (MW)
14	99.24628701	1389.448018
15	92.29413776	1384.412066
16	86.32368614	1381.178978
17	81.07836259	1378.332164
18	76.42644433	1375.675998

Table 15 Coal input results

6.2 EFFECT OF CALORIFIC VALUE VARIATION ON DAMAGE MECHANISMS IN BOILER

6.2.1 Fireside corrosion

Fireside corrosion is a damage mechanism that causes the high-temperature tubes in a coal-fired boiler. Fireside corrosion occurs due to fly ash deposition on the relatively cool boiler tube; the deposited fly ash contains harmful elements such as Sulphur, Sodium, Potassium, and Chlorine [52].

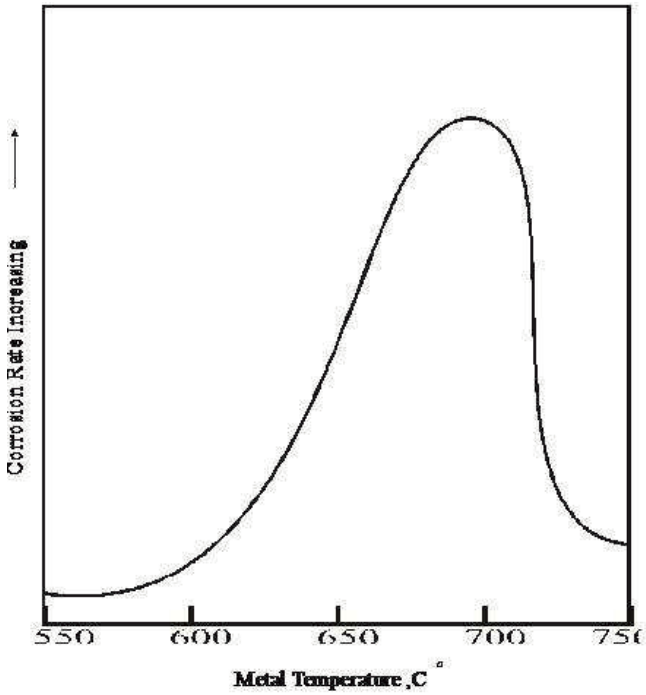

Figure 71 Corrosion vs metal temperature [52]

From Figure 71, the non-linear relationship between metal temperature and fireside erosion is apparent. From the results of the model, it is seen that superheater metal temperatures increase as coal calorific value decreases; this implies that the lower the calorific value is, the higher the corrosion rate will be. It should be noted that calorific value variation is not the only coal property that influences metal temperature.

6.2.2 Creep damage

The influence coal quality has on creep damage is directly linked to the impact coal quality has on the metal temperature of the various components of the boiler. This case study focussed on calorific value variation and has shown that the general trend is that the lower the calorific value, the higher the metal temperature experienced by the super-heaters are.

In Figure 72, the relationship between creep strength at 10^5 hours and temperature is shown for different materials generally used in boilers. In South Africa the grades of steel commonly found are the X20CrMoV12-1 steel for utility boilers built in the 1980s and grade 91 (P91) for newer power plants. The relationship for both these materials and temperature is non-linear.

The increase in metal temperatures caused by lower calorific value coals, therefore, leads to lower creep-rupture strengths. This decreases the life of the components leading to creep failure at an earlier time.

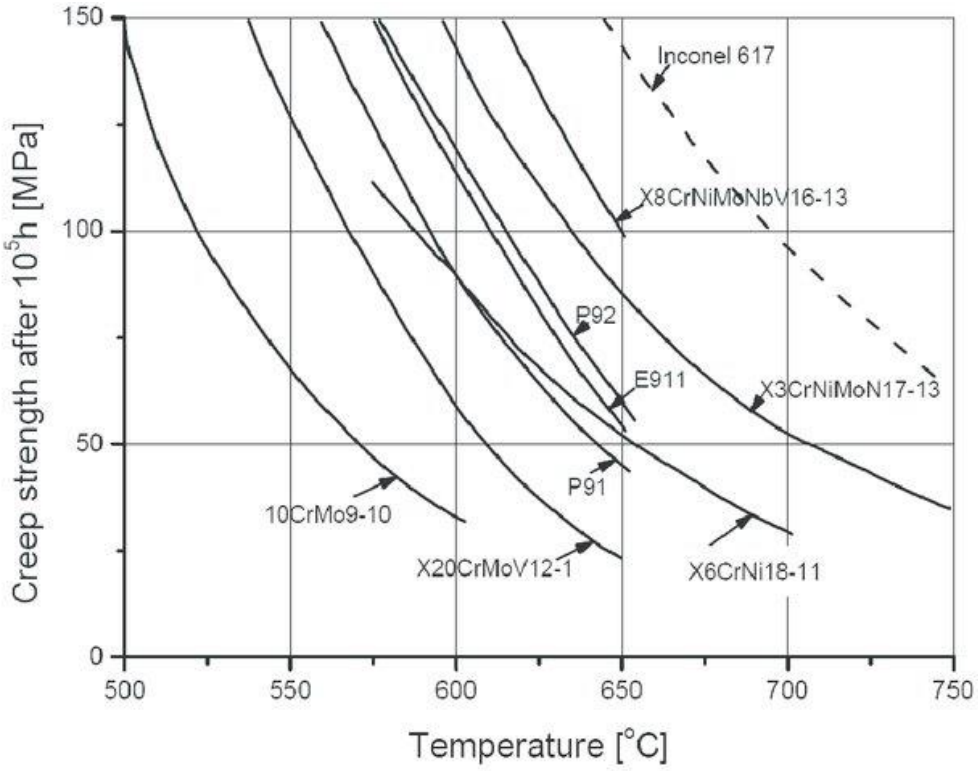

Figure 72 Creep Strength of Exposed Materials as a Function of Temperature [53]

6.2.3 Dew point corrosion

Dew point corrosion in coal-fired boilers occurs when the flue gas temperature decreases below the dew point of acid present in the flue gas. Generally, the acid concerned in coal-fired plants is sulphuric acid. The dew point of sulphuric acid in flue gasses is influenced by both Sulphur-Trioxide (SO_3) and moisture content.

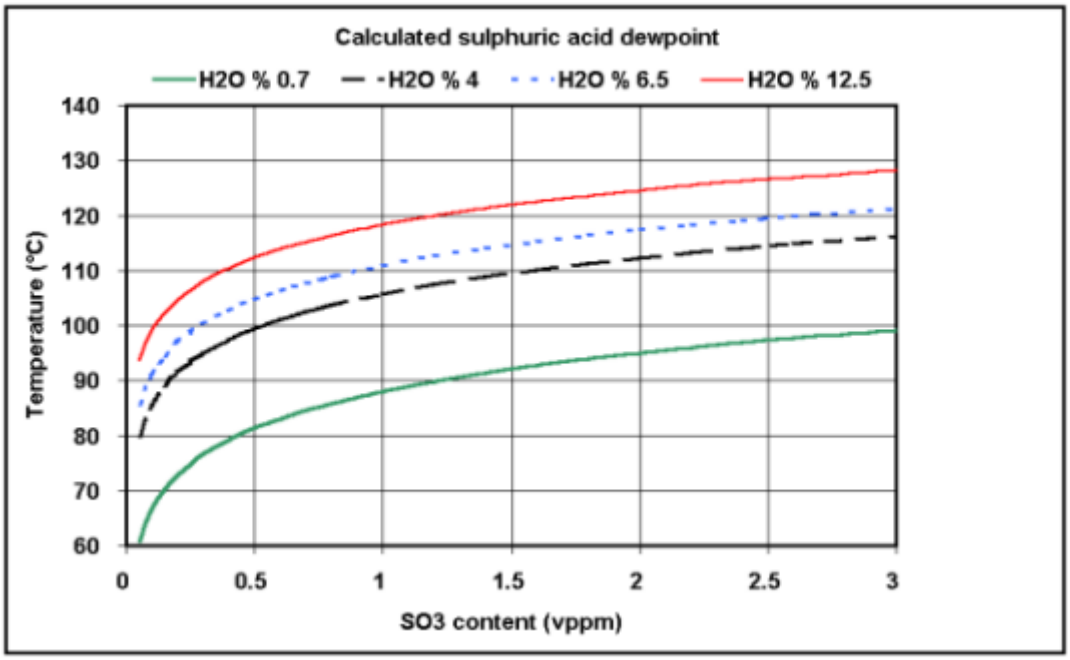

Figure 73 Sulphuric acid dew point at different concentrations [11]

The impact coal quality has on moisture and sulphur-trioxide in flue gas has not been studied; thus, the influence coal quality has on the dew point temperature has not been addressed.

The trend from the model, however, shows that the boiler outlet temperature decreases when higher quality coal is used. The lower outlet temperature gasses then get further cooled in the air-heaters. Thus the indication is that if coal that has a higher calorific value than that for which the boiler is designed for the temperature of the flue gas after the air heater will decrease as with the boiler exit temperature. A model such as the one used in this study can be created to determine if it will result in temperatures below the dew point of sulphuric acid.

6.3 CONCLUSION

The model used indicated that temperature variations occurred for both when coal calorific value increases and decreases. Both could have detrimental effects on the boiler components lifetime as different problems arise for high and low boiler temperatures.

When a power plant operator/owner consider coal calorific value change, it would be necessary to conduct a full study on the effect it would have.

7 DRUM RECLAIMER CASE STUDY

The coal used by power stations is generally sourced from adjacent open-pit mines and delivered directly to the power station using a conveyor belt system. The coal is then stored on a re-claimable stockpile by using a coal stacker, where a drum reclaimer or stacker-reclaimer reclaims the coal and transports the coal to the power station by conveyor belt for grinding in the mills and combustion in the furnace.

Drum reclaimers are critical machines in the bulk material handling process at power stations as the failure of a drum reclaimer causes an entire stockpile area to become unusable. Power stations generally mitigate this risk by making use of at least two drum reclaimers with an associated stockpile slab each. The strategy in place is that one drum reclaimer will be in service and one on standby or unavailable due to preventative maintenance intervention and cleaning. Major equipment failures that have long repair times such as fatigue failure of the reclaiming drum would cause the loss of redundancy as no standby machine will be available during maintenance interventions. The loss of redundancy poses a multiple unit trip risk if the in-service drum reclaimer experiences failure.

On a newly built power station that makes use of a drum reclaimer, there have been concerns about the performance and reliability of the machine. The drum reclaimer in question was designed to achieve a coal reclaiming capacity of 3400 t/h at 95% availability while operating continuously [54, 55]. The actual technical performance of the drum reclaimer was measured at 2400 t/h, and a lowered availability of the machine was observed by. The lowered availability is attributed to excessive coal build-up in the buckets, within the ring chute, on the inside of the drum and along the walkway next to the cross conveyor that runs inside the rotating drum. The coal build-up typically occurs within one week of cleaning and takes approximately three days to clean. [55]. The impact of the coal build-up is not confined only to performance; it also has a physical impact on the machinery. The coal build-up causes unbalance in the rotating drum which translates into drum vibration as well as the brake electronics to overheat when the soiled drum is driven back to the maintenance slab [55].

The focus of this case study was to establish the effect coal quality has on the reliability of a drum reclaimer. The drum reclaimers that were planned to be used for experimental purposes were unfortunately unavailable during the research period due to machinery failures. This chapter focusses on how the research would have been carried out including a laboratory test run of the method.

Figure 74 30 ton rake failure

Figure 75 Rake failure side view

Figure 76 Wire rope failure that lead to rake collapse

The above photos are from one of the incidents that prevented measurements from being taken from the drum reclaimer. Due to the limited duration of the research, this case study could not be completed.

7.1 EXPERIMENTAL PROCEDURE

The procedure that would have been followed would start with strain measurements of the drum reclaimer freely rotating without reclaiming coal and during operation with no coal build up in the buckets; further measurements would then be taken with buckets that have coal “hang-ups” causing an unbalance. The results from the strain gauges would then be used to validate a finite element model (FEM) of the drum reclaimer to establish accuracy as well as loading assumptions.

After the FEM has been validated coal quality in terms of moisture content and fines content would be monitored as well as the frequency of coal “hang-ups” in the drum buckets. An attempt would be made to find a correlation between the frequency of coal “hang-ups” and coal properties/qualities.

If a good correlation exists between coal quality and the frequency of coal hang-ups, a mathematical model would be created to model the magnitude and frequency of strain cycles. This strain cycles would then be used to make a lifetime estimation for different coal qualities by using miners rule.

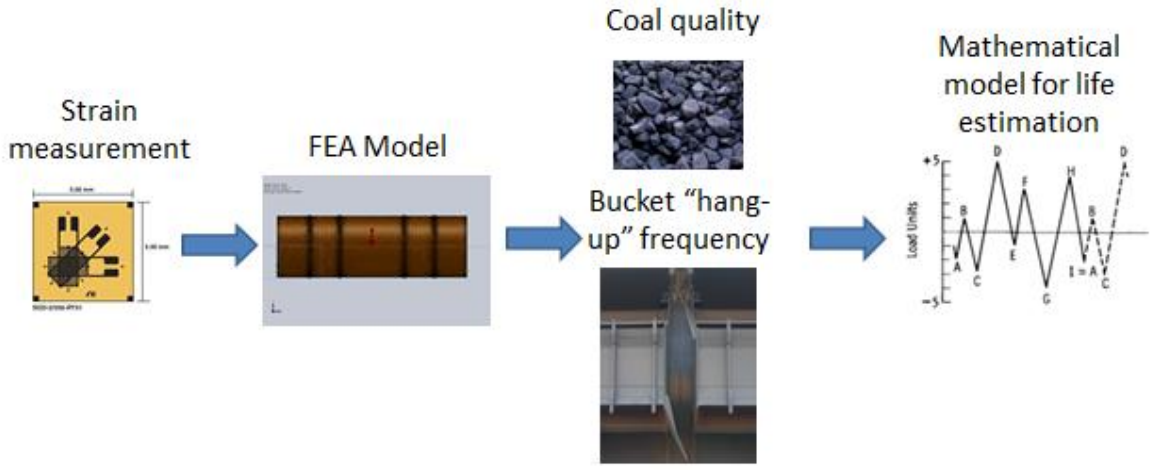

Figure 77 Experimental procedure

7.2 STRAIN MEASUREMENT ON DRUM RECLAIMER

The strain measurement on the reclaimer will be conducted to determine the frequency of loading, and the effect loading has on stress distribution and the general magnitude of stresses experienced by the drum reclaimer during operation.

7.2.1 Measurements to be taken

The measurements that will be taken will consist of measuring bending strain at various points on the drum, drum torque measurements at three progressive points to establish how torque decreases through the drum. As well as quarter bridge strain gauge configurations to measure principle strains that occur due to impact loading by the digging action of the buckets.

7.2.2 Measurement equipment

The equipment that will be used to take the measurements is a Somat eDAQ mobile data acquisition system as can be seen in Figure 78 with a strain gauge bridge layer and rosette strain gauges. The strain gauge bridge unit provides bridge completion automatically eliminating the need for manual completion of the Wheatstone bridge as well as automatic calibration. The bridge layer has the following specifications:

Input range minimum:	±625μV	**Input range maximum:**	±10V
Resolution:	16 bit analog to digital conversion across range	**Sample rates:**	0.1 – 100 kHz
Filtering:	Analogue: 25kHz, 8-pole Butterworth low-pass filter Digital: Software selectable; 8-pole Butterworth and Linear Phase	**Excitation:**	5V or 10V

Internal shunt resistors:	Four per Channel 50k Ω,100k Ω, 200k Ω, 500k Ω	**Amount of strain gauge bridges that can be measured simultaneously:**	16

The mobile data acquisition system will be connected to a 12v external battery to provide power for the acquisition system as well as to supply excitation voltage to the strain gauge bridge through the strain gauge board.

Figure 78 Somat eDAQ unit with various layers

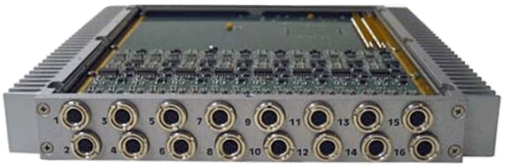

Figure 79 eDAQ strain gauge bridge layer

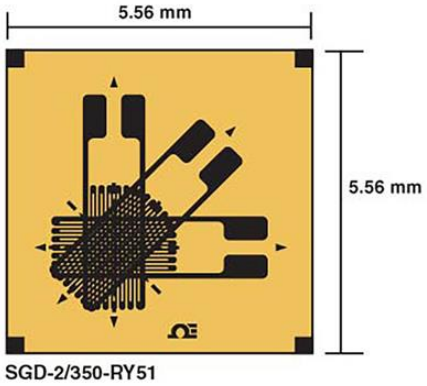

Figure 80 Example of strain rosette

7.2.3 Data logger position and mounting details

The data logger will be positioned behind and between two buckets on the drum reclaimer as can be seen in Figure 81 and Figure 82. It will be fastened by making use of two M16 bolts on the flanges of the bracket.
The cables running from the data logger to the strain gauges will be run inside a galvanised conduit that will be mounted onto the drum to protect the wires from damage.

Figure 81 Bucket location

Figure 82 EDAQ bracket mounting location behind and between two buckets

Figure 83 Manufactured mounting bracket and equipment enclosure

Figure 84 Inside equipment box, manufactured backing plate and battery visible

8 CONCLUSION

The case studies have shown that coal quality does have an impact on equipment lifetimes with different aspects of coal quality, having an effect on different components. Methods were developed that can be used in practice when historic wear and coal quality data is available to estimate the impact a quality change would have on equipment lifetime. The same methods can also be employed to estimate the current condition of equipment if the starting condition, as well as the coal quality information and usage, are available for the period since the previous inspection.

The air heater erosion case study also provided a correlation between coal calorific value and other measures of coal quality, such as ash content. The combustion air requirements, as well as the overall flue gas and ash production, were also determined as a function of the calorific value for the specific source of coal.

The combustion case study provided a general effect that calorific value would have on boiler temperature distribution. Although the possible resultant damage mechanisms are listed the occurrence of these is a function of the design of the individual boiler. This means that such a model would be necessary for each individual boiler to estimate if temperature-dependent damage mechanisms would manifest.

The following table summarises the effect coal quality has on equipment lifetime and damage mechanisms as determined through the case studies performed:

Table 16 Summary of findings

Coal quality metric variation	Impact on equipment
Increased Abrasiveness index	• Mill liner wear increases, the increase is less severe than expected for the ball and tube mills analysed.
Increased calorific value (and the associated change in ash content)	• Possible dew point corrosion due to lower back-end temperatures.
Decreased calorific value (and the associated change in ash content)	• Increase in air heater erosion • Higher metal temperatures of superheaters that might lead to fireside corrosion increased and decreased creep-fatigue life. Due to increase air requirements as well as increased total energy input into the boiler at lower calorific value.

The areas addressed by the case studies are highlighted in Figure 85

Coal Characteristics								
Power Station Equipment		Calorific Value	Ash Content	AI	HGI	Sulphur content	Moisture content	Ash hardness
	Coal reclaimer			Wear			Hang-ups Fatigue Corrosion	
	Coal handling			Chute wear				
	Milling plant			Wear (liners) PF erosion	Wear (liner)			
	Boiler	Erosion Creep Heat damage	Slagging Erosion			Fire side corrosion		
	Air heaters	Erosion	Erosion			Dew point corrosion	Dew point corrosion	Erosion
	Draft group	Erosion	Erosion					
	Ash systems	Wear	Wear					Wear

Figure 85 Areas addressed by case studies

9 FUTURE WORK

The future work to be conducted is aimed at completing the framework of coal quality and damage mechanisms, as seen in Figure 16.

The drum reclaimer case study remains incomplete; this case study is an important piece of the puzzle because coal hang-ups do frequently occur at South African power stations. The hang-ups cause unbalanced loading of the drum and a reduced coal throughput. The outcomes of the case study should address the reason why coal sticks together and also seek to recommend measures to reduce hang-up frequency. The measures should relate to both coal quality control as well as plant design considerations such as bucket geometry.

Older power stations are not fitted with flue gas desulphurisation plants; the flue gas, as a result, does contain sulphur oxides (SO_x). This could potentially cause concrete civil structures to suffer from sulphate attack. The impact of the sulphur content on the possibility of sulphate attack on smokestacks is not known.

The damage caused by flame impingement on boiler water walls and the combustion of coal outside the furnace are common problems faced in power plants. Work could be conducted on determining the effect coal quality could have on flame propagation speeds and damage caused by slow flame propagation. The study should focus the outcomes on how to asses if lower-quality coal is suitable for firing in the furnace without causing damage to plant components.

b

10 BIBLIOGRAPHY

[1] K. Ratshomo and R. Nembahe, “SOUTH AFRICAN COAL SECTOR REPORT,” DEPARTMENT OF ENERGY OF THE REPUBLIC OF SOUTH AFRICA, Pretoria, 2018.

[2] B. G. Miller, “CHAPTER 1 - Introduction to Coal,” in *Coal Energy systems*, B. G. Miller, Ed., Massachusettes, Academic Press, 2005, pp. 1-27.

[3] R. A. Meyers, Coal Handbook, 1st ed., New York: Marcel Dekker inc., 1981.

[4] R. Davis, “Are Richard’s Bay coal exports the cause of SA’s current power crisis?,” *Daily Maverick,* 11 December 2018.

[5] K. Cloete, “Eskom laments poor quality of coal,” *Creamers Engineering News,* 31 January 2019.

[6] A. A. Alekhnovic and N. V. Artem’eva, “EFFECT OF THE ASH CONTENT ON THE SLAGGING PROPERTIES,” *Power Technology and Engineering,* vol. 51, no. 4, pp. 8-15, 2017.

[7] R. Ray, “How to Deal with Ceaseless Slagging,” *Power Engineering,* 25 02 2016.

[8] X. Zhi-Ming, Z. Zhong-Bin and Y. Shan-Rang, “Costs Due to Utility Fouling in China,” *Heat Exchanger Fouling and Cleaning,* vol. RP5, pp. 113-118, 2007.

[9] M. Mengütürk and E. Sverdrup, “Fan erosion control,” *Forschung im Ingenieurwesen A,* vol. 52, no. 1, pp. 9-12, 1986.

[10] J. Oberholzer, “System Status Briefing,” Eskom SOC ltd, Johannesburg, 2019.

[11] W. Huijbregts and R. Leferink, “LATEST ADVANCES IN THE UNDERSTANDING OF ACID DEWPOINT CORROSION:CORROSION AND STRESS CORROSION CRACKING IN COMBUSTION GAS CONDENSATES,” *Anti-Corrosion Methods and Materials,* vol. 51, no. 3, pp. 173-188, 2004.

[12] C. Spero, “Assesment and prediction of coal abrasiveness,” *Fuel,* vol. 69, pp. 1168-1176, 1990.

[13] International Standards Organisation , *BS ISO 12900:2018- Hard coal — Determination of abrasiveness,* Switzerland: ISO, 2018.

[14] India Spectro Analytical Labs Limited, “Coal Testing Definition,” 2017. [Online]. Available: http://www.spectro.in/Coal-definition.html#1. [Accessed 06 09 2019].

[15] J. G. Speight, Handbook of Coal Analysis, 2nd ed., Online: John Wiley & Sons, 2015.

[16] Encyclopedia Britannica, “Coal utilization | Volatile Matter & Chemistry,” Encyclopedia Britannica, London, 2017.

[17] ISO, *ISO 562:2010 Hard coal and coke — Determination of volatile matter,* International Stanadards Organisation, 2010.

[18] J. Theron and E. Roux, “Representation of coal and coal derivatives in process modelling,” *Journal of the Southern African Institute of Mining and Metallurgy,* vol. 115, no. 5, pp. 339-348, 2015.

[19] N. E. Dowling, “Mechanical behavior of materials (4th),” Boston, 2012.

[20] K. G. Budinski and M. K. Budinsky, ENGINEERING MATERIALS : Properties and Selection, 8th ed., Columbus, Ohio: Prentice hall, 2004.

[21] R. Nagarajan, B. Ambedkar and S.Gowrisankar, “Development of predictive model for fly-ash erosion phenomena in coal-burning boilers,” *Wear,* vol. 267, no. 1, pp. 122-128, 2009.

[22] V. T. Sathyanathan, “Fly ash erosion in boilers firing high ash coals,” 2010. [Online]. Available: https://www.brighthubengineering.com/power-plants/32174-fly-ash-erosion-in-boilers-firing-high-ash-coals/. [Accessed 09 10 2019].

[23] J. G. Mbabazi, T. J. Sheer and r. Shandu, “A model to predict erosion on mild steel surfaces impacted,” *Wear,* vol. 1, no. 257, p. 612–624, 2004.

[24] H. Dong, Surface Engineering of Light Alloys, 1st ed., Cambridge: Woodhead Publishing Limited, 2010.

[25] J. F. Archard and W. Hirst, “Wear of metals under unlubricated conditions,” *Proceedings of theRoyal Society of London. Series A, Mathematical and Physical Sciences,* vol. 236, no. 1, pp. 397-410, 1956.

[26] M. R. Shayan, “On the Failure Analysis of an Air Preheater in a Steam Power Plant,” *Journal of Failure Analysis and Prevention,* vol. 15, no. 6, pp. 941-951, 2015.

[27] A. M. Sadegh and W. M. Worek, Marks' Standard Handbook for Mechanical Engineers, 12 ed., Sydney: McGraw-Hill , 2018.

[28] American Society for Testing and Materials, *E 1049 – 85 Standard Practices for Cycle Counting in Fatigue Analysis,* Pennsylvania: ATSM, 2005.

[29] D. F. Socie, “Fatigue-life prediction using local stress-strain concepts,” *Experimental Mechanics,* vol. 17, no. 2, pp. 50-56, 1977.

[30] M. A. Khamsi, “The Bisection method,” [Online]. Available: http://www.sosmath.com/calculus/limcon/limcon07/limcon07.html. [Accessed 23 10 2019].

[31] Frontline Solvers, “EXCEL SOLVER - LINEAR PROGRAMMING,” 2019. [Online]. Available: https://www.solver.com/excel-solver-linear-programming. [Accessed 15 10 2019].

[32] L. Nichols and G. Christofaro, “Explanation of the simplex method,” Iowa State University, Ames, Iowa, 2015.

[33] D. FYLSTRA, L. LASDON, J. WATSON and A. WAREN, “Design and Use

of the Microsoft Excel Solve," *Interfaces,* vol. 28, no. 5, pp. 29-55, 1998.

[34] Frontline Solvers, "EXCEL SOLVER - ALGORITHMS AND METHODS USED," 2008. [Online]. Available: https://www.solver.com/excel-solver-algorithms-and-methods-used. [Accessed 20 10 2019].

[35] F. P. Incropera, D. P. Dewitt, T. L. Bergman and A. S. Lavine, Fundamentals od heat and mass transfer, 6th ed., Hoboken , NJ: John Wiley & Sons, 2007.

[36] R. Nave, "Hyper Physics," [Online]. Available: http://hyperphysics.phy-astr.gsu.edu/hbase/thermo/heatra.html. [Accessed 24 10 2019].

[37] F. Otto, "Rayleigh-Bénard Convection," [Online]. Available: https://www.mis.mpg.de/applan/research/rayleigh.html. [Accessed 24 10 2019].

[38] H. Verbanck, "DEVELOPMENT OF A MATHEMATICAL MODEL FOR WATERTUBE BOILER HEAT TRANSFER CALCULATIONS," *Proc S Afr Sug Technol Ass,* vol. 71, pp. 166-171, 1997.

[39] R. F. Storm, "Typical Causes of Slagging and Fouling Problems in Boilers," 06 January 2015. [Online]. Available: https://www.powermag.com/typical-causes-of-slagging-and-fouling-problems-in-boilers/?pagenum=1. [Accessed 24 November 2019].

[40] M. F. Abbott and L. G. Austin, "Studies on slag deposit formation in pulverized-coal combustors. 4. Comparison of sticking behaviour of minerals and low-temperature and ASTM high-temperature coal ash on medium carbon steel substrates," *Fuel,* vol. 61, no. 8, pp. 765-770, 1982.

[41] A. R. McLennan, W. Bryant, W. Bailey, B. R. Stanmore and T. F. Wall, "Index for Iron-Based Slagging for Pulverized Coal Firing in Oxidizing and Reducing Conditions," *Energy Fuels,* vol. 14, no. 2, pp. 349-354, 2000.

[42] A. Lawrence, R. Kumar, K. Nandakumar and K. Narayanan, "A Novel tool for assessing slagging propensity of coals in PF boilers," *Fuel,* vol. 87, no. 1, p. 946–950, 2008.

[43] A. Kumari, S. K. Das and P. K. Srivastava, "Modeling Fireside Corrosion Rate in a Coal Fired Boiler Using Adaptive Neural Network Formalism," *Port. Electrochim. Acta,* vol. 34, no. 1, pp. 23-38, 2016.

[44] R. Schallert and E. Levy, "Effect of a combination of two elbows on particle roping in pneumatic conveying," *Powder Technology,* vol. 107, no. 3, pp. 226-233, 2000.

[45] A. Y. Edward and K. Levy, "Roping phenomena in pulverized coal conveying lines," *Powder Technology,* vol. 95, no. 1, pp. 43-48, 1998.

[46] S. Guda, S. Rowan and I. Celik, " ROPE FORMATION FOR GAS SOLID FLOW IN A 90 DEGREE BEND WITH VARYING PARTICLE SIZE DISTRIBUTIONS," Florida, 2015.

[47] G. Huang, K. M. Bryden, E. Vasquez and R. Avancha, "Using CFD to

Model Coal Roping Phenomenon in Coal Transport Systems," *Power,* pp. 753-759, 2004.

[48] J. Wellsa, F. Wigleya, D. Foster, W. Livingstonb, H. Gibbc and J. Williamson, "The nature of mineral matter in a coal and the effects on erosive and abrasive behaviour," *Fuel Processing Technology,* vol. 86, no. 5, pp. 535-550, 2005.

[49] U.S Environmental Protection Agency, " Course SI:428A".

[50] Howden Power, "U5 air heater mass loss report," Howden, Vereeniging, 2016.

[51] M. &. S. R. P. &. C. P. &. R. B. &. E. K. &. S. L. Powell, "Selection and design of mill liners. 2006 SME Annual Conference - Advances in Comminution. 2006.," Johannesburg, 2006.

[52] M. Mittal, Tube Failures in Pulverised Coal Fired Boilers : an Investigation, 1st ed., Saarbrucken: Lap Lambert Academic Publishing, 2017.

[53] Z.-F. Hu, "Heat-Resistant Steels, Microstructure Evolution and Life Assessment in Power Plants," in *Thermal Power Plants* , M. Rasul, Ed., Rijeka, Croatia , InTech, 2011, pp. 195-226.

[54] ThyssenKrupp, "Maintenance manual - Drum Reclaimer 02 Bi-directional," ThyssenKrupp, Essen, 2012.

[55] P. Lepota and A. P. Wiid, "Failure of coal stockyard drum reclaimer to meet operational requirements," ESKOM SOC ltd., Midrand, 2018.

[56] Department of Energy of the Republic of South Africa , "INTEGRATED RESOURCE PLAN 2018," Department of Energy of the Republic of South Africa , Pretoria, 2018.

[57] ESKOM SOC LTD, "Peaking power stations: Eskom SOC LTD," [Online]. Available: http://www.eskom.co.za/Whatweredoing/ElectricityGeneration/PowerStations/Peaking/Pages/default.aspx. [Accessed 15 10 2019].

APPENDIX A AIRHEATER CASE STUDY FIGURES AND CALCULATIONS

Table 17 Coal combustion calculations

Coal Characteristics		
Element	Molecular mass	Mass fraction (%)
N2	28	1.86984
O2	32	-34.96365147
C	12	43.312
Ash		42.25
S	32	0.7
H2	2	4.581811474
H2O	18	42.25

Combustion requirements	
Oxygen required per kg of coal (kg/kg)	1.528532
Oxygen already present in 1 kg of coal (kg)	-0.34964
Aditional oxygen needed (kg/kg)	1.878168
Stoichiometric volume of air needed per kg of coal (23% of air is oxygen)	8.165948
% excess air	20
Combustion air required per kg coal (kg)	9.799138

General info and results			
CV (MJ/kg)	14.8	Mass of ash produced per second (kg/s)	17.64223
Unit load (MW) (MJ/s)	618	Mass of Bottom ash produced per second (kg/s)	3.528446
Cycle efficiency (%)	35	Mass of fly ash produced per second (kg/s)	14.11378
Mass of coal per second (kg/s)	41.75676		
Mass of air required per second (kg/s)	409.1802		
Mass of flue gas produced per second	433.2947		

Combustion Calculations

C (12)	+	O2 (32)	=	CO2(44)
0.43312	+	1.154986667	=	1.588107
H2 (2)	+	1/2 O2 (32)	=	H2O (18)
0.045818115	+	0.366544918	=	0.412363
S (32)	+	O2 (32)	=	SO2 (64)
0.007	+	0.007	=	0.014

Table 18 Unit load history

Unit	Date from	Date to	Boiler hours	Average ash Content (%)	Average CV (MJ/kg)	Average Boiler load MW
2	2013/05/01	2016/04/30	21972	40.21474	15.62821	546.335535
5	2013/08/01	2016/12/31	26465	40.33959	15.63531	546.567447

Table 19 Air heater weight measurements

Unit	Start date	End date	Ring	Layer	Type	Original mass	Measured mass	Mass loss	%mass loss	Aproximate ash through air heater	kg metal loss per kg ash through air heater (10^-9)	% metal loss per kg ash (10^-9)
2	2013/05/01	2016/04/30	3	HE	Und	1.47	1.3	0.17	11.56463	988733263.4	0.171937	11.69641
2	2013/05/01	2016/04/30	3	HE	Corig	2.59	1.9	0.69	26.64093	988733263.4	0.697863	26.9445
2	2013/05/01	2016/04/30	3	INT	Und	1.31	1.2	0.11	8.396947	988733263.4	0.111253	8.492631
2	2013/05/01	2016/04/30	3	INT	Corig	2.32	1.7	0.62	26.72414	988733263.4	0.627065	27.02866
2	2013/05/01	2016/04/30	3	CE	Und	1.54	1.5	0.04	2.597403	988733263.4	0.040456	2.627
2	2013/05/01	2016/04/30	3	CE	Corig	2.71	2.5	0.21	7.749077	988733263.4	0.212393	7.837379
2	2013/05/01	2016/04/30	5	HE	Und	2.2	1.8	0.4	18.18182	988733263.4	0.404558	18.389
2	2013/05/01	2016/04/30	5	HE	Corig	3.89	2.75	1.14	29.30591	988733263.4	1.15299	29.63986
2	2013/05/01	2016/04/30	5	INT	Und	1.99	1.8	0.19	9.547739	988733263.4	0.192165	9.656536
2	2013/05/01	2016/04/30	5	INT	Corig	3.81	2.5	1.31	34.3832	988733263.4	1.324928	34.775
2	2013/05/01	2016/04/30	5	CE	Und	1.93	1.9	0.03	1.554404	988733263.4	0.030342	1.572117
2	2013/05/01	2016/04/30	5	CE	Corig	3.42	2.65	0.77	22.51462	988733263.4	0.778774	22.77118
5	2013/08/01	2016/12/31	3	HE	Und	1.5	1.25	0.25	16.66667	1161395562	0.215258	14.35055
5	2013/08/01	2016/12/31	3	HE	Corig	2.65	2	0.65	24.5283	1161395562	0.559672	21.11968
5	2013/08/01	2016/12/31	3	INT	Und	1.59	1.3	0.29	18.23899	1161395562	0.2497	15.70438
5	2013/08/01	2016/12/31	3	INT	Corig	2.81	2.05	0.76	27.04626	1161395562	0.654385	23.28773
5	2013/08/01	2016/12/31	3	CE	Und	1.37	1.2	0.17	12.40876	1161395562	0.146376	10.68435
5	2013/08/01	2016/12/31	3	CE	Corig	2.43	1.75	0.68	27.98354	1161395562	0.585502	24.09475
5	2013/08/01	2016/12/31	5	HE	Und	2.2	1.8	0.4	18.18182	1161395562	0.344413	15.65515
5	2013/08/01	2016/12/31	5	HE	Corig	3.89	2.9	0.99	25.44987	1161395562	0.852423	21.91318
5	2013/08/01	2016/12/31	5	INT	Und	2.32	1.85	0.47	20.25862	1161395562	0.404686	17.44334
5	2013/08/01	2016/12/31	5	INT	Corig	4.1	2.95	1.15	28.04878	1161395562	0.990188	24.15093
5	2013/08/01	2016/12/31	5	CE	Und	2.16	2.1	0.06	2.777778	1161395562	0.051662	2.391759
5	2013/08/01	2016/12/31	5	CE	Corig	3.81	3.05	0.76	19.94751	1161395562	0.654385	17.17546

Error! Not a valid link.

Table 20 Model output

	Monthly average				
Date	CV (MJ/kg)	U2 hours	u 5 hours	U2 erosion	U5 erosion
May-13	15.79400511	0	0	0	0
Jun-13	15.74411724	414.16	0	0.306572	0
Jul-13	15.7014966	595.87	0	0.444284	0
Aug-13	15.77128826	744	306.68	0.548182	0.225963
Sep-13	15.613224	720	720	0.544881	0.544881
Oct-13	16.04731078	744	744	0.522497	0.522497
Nov-13	15.95826096	720	720	0.513626	0.513626
Dec-13	15.33544829	742.87	625.81	0.588538	0.495798
Jan-14	15.62415793	637.81	744	0.481797	0.562012
Feb-14	15.25069907	672	614.91	0.539727	0.493874
Mar-14	15.33961289	744	744	0.589035	0.589035
Apr-14	15.70784787	720	720	0.536258	0.536258
May-14	15.85322162	740.67	685.48	0.538103	0.498007
Jun-14	15.93851245	720	720	0.515401	0.515401
Jul-14	15.71952656	744	744	0.553036	0.553036
Aug-14	15.86895639	686.83	738.83	0.497633	0.535309
Sep-14	16.18398586	590.9	720	0.404977	0.493457
Oct-14	15.56002317	744	744	0.568071	0.568071
Nov-14	15.41229451	505.02	665.81	0.395122	0.520923
Dec-14	15.21939481	339.3	671	0.273886	0.541637
Jan-15	15.72959639	742.97	710.7	0.551327	0.52738
Feb-15	15.83041269	672	384.17	0.490137	0.280202
Mar-15	16.0141974	740.27	690.05	0.522926	0.487451
Apr-15	15.13803002	720	720	0.588776	0.588776
May-15	15.12237935	714.7	744	0.585894	0.609913
Jun-15	15.41941617	664.37	683.11	0.51919	0.533835
Jul-15	15.35656929	744	711.15	0.587415	0.561479
Aug-15	15.40507776	624	744	0.488788	0.582786
Sep-15	15.35839168	720	720	0.568297	0.568297
Oct-15	15.12117662	744	701.1	0.61003	0.574854
Nov-15	15.14374394	400.65	720	0.327332	0.588242
Dec-15	15.45836373	744	744	0.577713	0.577713
Jan-16	15.75619349	699.41	932.64	0.516657	0.688945
Feb-16	16.01356812	430.15	696	0.303891	0.491708
Mar-16	16.2797963	0	744	0	0.501128
Apr-16	15.82517761	0	603.43	0	0.440521
May-16	16.05737947	0	523.18	0	0.366765
Jun-16	15.50665566	0	720	0	0.554639
Jul-16	15.72463389	0	707.95	0	0.525783
Aug-16	15.69216458	0	744	0	0.555607
Sep-16	15.38818756	0	691.64	0	0.543269
Oct-16	15.50035815	0	673.08	0	0.519035
Nov-16	16.22480524	0	98.07	0	0.066719
Dec-16	15.57775645	0	0	0	0
			Total	16.6	20.44483

APPENDIX B MILL LINER CASE STUDY FIGURES AND CALCULATIONS

UNIT: 2A Mill DATE: 9 / 3 / 2016

Trunnion Shell Liners (End Liners)

End Liner (Inner)		DE	End Liner (Outer)	
			LH	RH
1	85,4	1	44,1	38,1
2	73,2	2	60,2	46,3
3	61,4	3	55,6	55,2
4	39,7	4	58,4	66,3
5	48,5	5	69,8	54,5
6	46,8	6	59,4	68,5
7	55,4	7	42,8	42,7
		8	62,8	46,5
		9	59,5	57,9
		10	62,7	68,1
		11	61,8	58,5
		12	66,0	58,1
		NDE	LH	RH
1	86,4	1	53,5	49,7
2	71,2	2	33,7	65,2
3	47,9	3	59,6	68,4
4	39,9	4	62,9	59,7
5	40,1	5	82,1	61,0
6	31,8	6	60,6	59,5
7	43,4	7	41,1	47,0
		8	48,3	53,2
		9	26,4	30,7
		10	64,9	53,7
		11	57,3	69,2
		12	69,4	55,1

Figure 86 Sample thickness measurement sheet

```
Function timetest(Thickness, AI, c1, c2, c3, c4, c5) As Variant
Application.Volatile

g1 = 0
g2 = 75000
g3 = 150000
test2 = 100
If Thickness = 81 Then
timetest = 0

Else

Do Until test2 < 10
   test = (AI ^ c3) * c1 * (g2 ^ c2) + c4 - (1000 * (81 - Thickness) / g2)
   test2 = g3 - g2

   If test > 0 Then
    g3 = g2
    g2 = (g1 + g3) / 2


End If

   If test < 0 Then
    g1 = g2
    g2 = (g1 + g3) / 2


End If


Loop

timetest = g2
End If
```

Figure 87 Bisection method code for mill liner study

Table 21 End liner inner wear data with predicted results from model

Unit	Mill	Side	DE/NDE	Date from	Date to	Days	Average thickness at start (mm)	Avarage thickness at end of period (mm)	Average wear	Wear rate (mm/year	Mill hours (for time period)	Wear rate per 1000 hours (mm/1000hr)	Average grindability index	Average abrasiveness (mgFe)	Average CV (MJ/kg)	Month start	month end	Measured wear rate	Expected wear rate
6	a	Ave	NDE	2009/04/19	2012/12/15	1336	53.4375	42.550	10.888	2.974504117	19573.7255	0.556230341	62.212	424.8	15.67931	04-2009	12-2012	0.55623	0.509403
6	a	Ave	NDE	2014/06/01	2017/03/14	1017	81.0000	57.500	23.500	8.434119961	14827.9	1.584850181	62.98666018	488.8919601	15.62592	06-2014	03-2017	1.58485	1.256707
6	a	Ave	DE	2009/04/19	2012/12/15	1336	55.5750	41.281	14.294	3.905103855	19573.7255	0.730251888	62.212	424.8	15.67931	04-2009	12-2012	0.730252	0.532347
6	a	Ave	DE	2014/06/01	2017/03/14	1017	81.0000	57.375	23.625	8.478982301	14827.9	1.593280235	62.98666018	488.8919601	15.62592	06-2014	03-2017	1.59328	1.256707
6	b	Ave	DE	2009/04/19	2012/12/15	1336	64.3125	52.444	11.869	3.242585142	25158.5617	0.471757891	62.212	424.8	15.67931	04-2009	12-2012	0.471758	0.472891
6	b	Ave	DE	2016/03/01	2017/03/14	378	81.0000	61.875	19.125	18.4672619	4975.63	3.843734361	62.84741893	503.8712802	15.73165	03-2016	03-2017	3.843734	3.992853
6	b	Ave	NDE	2009/04/19	2012/12/15	1336	66.4750	55.225	11.250	3.073540419	25158.5617	0.447163877	62.212	424.8	15.67931	04-2009	12-2012	0.447164	0.490951
6	b	Ave	NDE	2016/03/01	2017/03/14	378	81.0000	62.625	18.375	17.74305556	4975.63	3.69299968	62.84741893	503.8712802	15.73165	03-2016	03-2017	3.693	3.992853
6	c	Ave	DE	2009/04/19	2012/12/15	1336	45.5250	24.594	20.931	5.718492702	25514.5869	0.820364056	62.212	424.8	15.67931	04-2009	12-2012	0.820364	0.310687
6	c	Ave	DE	2014/06/01	2017/03/14	1017	81.0000	58.625	22.375	8.030358899	15802.33667	1.415929838	62.98666018	488.8919601	15.62592	06-2014	03-2017	1.41593	1.175255
6	c	Ave	NDE	2009/04/19	2012/12/15	1336	45.5000	26.819	18.681	5.103784618	25514.5869	0.732179207	62.212	424.8	15.67931	04-2009	12-2012	0.732179	0.310481
6	c	Ave	NDE	2014/06/01	2017/03/14	1017	81.0000	57.875	23.125	8.29953294	15802.33667	1.463391174	62.98666018	488.8919601	15.62592	06-2014	03-2017	1.463391	1.175255
6	d	Ave	DE	2012/02/13	2012/12/15	306	81.0000	62.488	18.513	22.08190359	3563.576667	5.194921207	61.86636364	438.8181818	15.70856	02-2012	12-2012	5.194921	4.869101
6	d	Ave	NDE	2012/02/13	2012/12/15	306	81.0000	62.494	18.506	22.07444853	3563.576667	5.193167352	61.86636364	438.8181818	15.70856	02-2012	12-2012	5.193167	4.869101
6	e	Ave	DE	2012/08/01	2017/03/14	1686	81.0000	56.500	24.500	5.303973903	28743.41	0.852369291	62.57404368	473.2379758	15.65696	08-2012	03-2017	0.852369	0.5954
6	e	Ave	NDE	2012/08/01	2017/03/14	1686	81.0000	54.250	26.750	5.791073547	28743.41	0.930648103	62.57404368	473.2379758	15.65696	08-2012	03-2017	0.930648	0.5954
6	f	Ave	DE	2009/04/19	2012/12/15	1336	55.7625	49.200	6.563	1.792898578	16890.01744	0.388543116	62.212	424.8	15.67931	04-2009	12-2012	0.388543	0.629467
6	f	Ave	DE	2015/10/01	2017/03/14	530	81.0000	62.125	18.875	12.99882075	5386.246667	3.504295508	62.74758034	491.5181468	15.66692	10-2015	03-2017	3.504296	3.591684
6	f	Ave	NDE	2009/04/19	2012/12/15	1336	56.8750	52.138	4.738	1.294302021	16890.01744	0.280491125	62.212	424.8	15.67931	04-2009	12-2012	0.280491	0.643306
6	f	Ave	NDE	2015/10/01	2017/03/14	530	81.0000	61.125	19.875	13.6875	5386.246667	3.689953548	62.74758034	491.5181468	15.66692	10-2015	03-2017	3.689954	3.591684
5	a	Ave	DE	2010/05/02	2013/07/15	1170	59.7000	51.850	7.850	2.448931624	17946.08667	0.437421269	62.16410256	422.5384615	15.72535	05-2010	07-2013	0.437421	0.631024
5	a	Ave	NDE	2010/05/02	2013/07/15	1170	59.5813	51.150	8.431	2.630261752	17946.08667	0.469809946	62.16410256	422.5384615	15.72535	05-2010	07-2013	0.46981	0.629641
5	b	Ave	DE	2013/05/15	2016/12/02	1297	81.0000	56.250	24.750	6.965111796	21653.98	1.142976949	62.65590909	471.8409091	15.6429	05-2013	12-2016	1.142977	0.808765
5	b	Ave	NDE	2013/05/15	2016/12/02	1297	81.0000	57.750	23.250	6.542983809	21653.98	1.073705619	62.65590909	471.8409091	15.6429	05-2013	12-2016	1.073706	0.808765
5	c	Ave	DE	2015/03/01	2016/12/02	642	81.0000	59.250	21.750	12.36565421	11542.51	1.884338848	62.68454545	485.8181818	15.59473	03-2015	12-2016	1.884339	1.622014
5	c	Ave	NDE	2015/03/01	2016/12/02	642	81.0000	59.750	21.250	12.08138629	11542.51	1.841020714	62.68454545	485.8181818	15.59473	03-2015	12-2016	1.841021	1.622014
5	d	Ave	DE	2010/05/02	2013/07/15	1170	54.3625	38.175	16.188	5.049946581	21834.10667	0.741385954	62.16410256	422.5384615	15.72535	05-2010	07-2013	0.741386	0.456137
5	d	Ave	DE	2014/07/01	2016/12/02	885	81.0000	59.500	21.500	8.867231638	17284.03667	1.243922378	62.90766667	479.0333333	15.62027	07-2014	12-2016	1.243922	1.046149
5	d	Ave	NDE	2010/05/02	2013/07/15	1170	54.8313	36.944	17.888	5.580288462	21834.10667	0.819245792	62.16410256	422.5384615	15.72535	05-2010	07-2013	0.819246	0.460623
5	d	Ave	NDE	2014/07/01	2016/12/02	885	81.0000	58.875	22.125	9.125	17284.03667	1.280082913	62.90766667	479.0333333	15.62027	07-2014	12-2016	1.280083	1.046149
5	e	Ave	NDE	2010/05/02	2013/07/15	1170	55.0438	38.375	16.669	5.200080128	21277.47	0.78339906	62.16410256	422.5384615	15.72535	05-2010	07-2013	0.783399	0.47644
5	e	Ave	NDE	2014/03/01	2016/12/02	1007	81.0000	53.375	27.625	10.01303376	19213.39333	1.437799119	62.935	476.1176471	15.63081	03-2014	12-2016	1.437799	0.928572
5	e	Ave	DE	2010/05/02	2013/07/15	1170	53.1063	35.256	17.850	5.568589744	21277.47	0.838915529	62.16410256	422.5384615	15.72535	05-2010	07-2013	0.838916	0.45741
5	e	Ave	DE	2014/03/01	2016/12/02	1007	81.0000	55.500	25.500	9.242800397	19213.39333	1.327199186	62.935	476.1176471	15.63081	03-2014	12-2016	1.327199	0.928572
5	f	Ave	DE	2010/05/02	2013/07/15	1170	58.0938	50.338	7.756	2.419684829	13131.16667	0.590674858	62.16410256	422.5384615	15.72535	05-2010	07-2013	0.590675	0.860384
5	f	Ave	NDE	2010/05/02	2013/07/15	1170	59.2813	52.581	6.700	2.09017094	13131.16667	0.51023646	62.16410256	422.5384615	15.72535	05-2010	07-2013	0.510236	0.879284
4	a	Ave	DE	2009/12/20	2012/04/26	858	62.8563	58.444	4.412	1.877112471	13618.04333	0.324018649	62.37448276	417.5862069	15.70222	12-2009	04-2012	0.324019	0.88911
4	a	Ave	DE	2012/04/26	2013/12/30	613	58.4438	53.819	4.625	2.753874388	6866.093333	0.673599932	61.8547619	444.8571429	15.697	04-2012	12-2013	0.6736	1.80865
4	a	Ave	NDE	2009/12/20	2012/04/26	858	60.3750	56.556	3.819	1.624526515	13618.04333	0.280418406	62.37448276	417.5862069	15.70222	12-2009	04-2012	0.280418	0.851478
4	a	Ave	NDE	2012/04/26	2013/12/30	613	56.5563	54.006	2.550	1.518352365	6866.093333	0.371390233	61.8547619	444.8571429	15.697	04-2012	12-2013	0.37139	1.748165
4	b	Ave	DE	2009/12/29	2011/03/09	435	45.7063	39.619	6.088	5.107902299	9313.38	0.653629509	62.538125	416.25	15.70751	12-2009	03-2011	0.65363	0.946161
4	b	Ave	DE	2012/08/26	2015/11/21	1182	81.0000	60.438	20.563	6.349672166	23564.95667	0.872588068	62.5055	467	15.62626	08-2012	11-2015	0.872588	0.729743
4	b	Ave	NDE	2009/12/29	2011/03/09	435	46.4500	36.500	9.950	8.348850575	9313.38	1.06835542	62.538125	416.25	15.70751	12-2009	03-2011	1.068355	0.962602
4	b	Ave	NDE	2012/08/26	2015/11/21	1182	81.0000	60.125	20.875	6.446171743	23564.95667	0.885849284	62.5055	467	15.62626	08-2012	11-2015	0.885849	0.729743
4	c	Ave	DE	2012/04/20	2013/12/30	619	81.0000	67.131	13.869	8.177857431	11972.91333	1.158343806	61.8547619	444.8571429	15.697	04-2012	12-2013	1.158344	1.424338
4	c	Ave	DE	2013/12/30	2015/11/21	691	67.1313	58.375	8.756	4.625226122	11613.91	0.753945054	62.925	483.25	15.52719	12-2013	11-2015	0.753945	1.317368
4	c	Ave	NDE	2012/04/20	2013/12/30	619	81.0000	65.981	15.019	8.855967286	11972.91333	1.254393946	61.8547619	444.8571429	15.697	04-2012	12-2013	1.254394	1.424338
4	c	Ave	NDE	2013/12/30	2015/11/21	691	65.9813	**59.375**	6.606	3.489553184	11613.91	0.568822214	62.925	483.25	15.52719	12-2013	11-2015	0.568822	1.293701
4	d	Ave	DE	2009/12/20	2012/04/26	858	53.7938	38.500	15.294	6.506082459	17253.403	0.886419334	62.37448276	417.5862069	15.70222	12-2009	04-2012	0.886419	0.579758
4	d	Ave	DE	2014/09/01	2015/11/21	446	81.0000	58.875	22.125	18.10678251	6233.49	3.549376032	63.19933333	494.5333333	15.46765	09-2014	11-2015	3.549376	3.114163
4	d	Ave	NDE	2009/12/20	2012/04/26	858	52.4000	47.844	4.556	1.93826486	17253.403	0.264078339	62.37448276	417.5862069	15.70222	12-2009	04-2012	0.264078	0.563073
4	d	Ave	NDE	2014/09/01	2015/11/21	446	81.0000	59.250	21.750	17.79988789	6233.49	3.489217116	63.19933333	494.5333333	15.46765	09-2014	11-2015	3.489217	3.114163
4	e	Ave	DE	2014/05/01	2015/11/21	569	81.0000	62.188	18.813	12.06777241	8880.15	2.118488989	63.19947368	487.0526316	15.5471	05-2014	11-2015	2.118489	2.133127
4	e	Ave	NDE	2014/05/01	2015/11/21	569	81.0000	62.000	19.000	12.18804921	8880.15	2.139603498	63.19947368	487.0526316	15.5471	05-2014	11-2015	2.139603	2.133127
4	f	Ave	DE	2009/12/20	2012/04/27	859	81.0000	60.131	20.869	8.867396682	10607.65333	1.967329563	62.37448276	417.5862069	15.70222	12-2009	04-2012	1.96733	1.512924
4	f	Ave	DE	2012/04/27	2015/11/21	1303	60.1313	51.850	8.281	2.319766884	22508.9	0.367910027	62.44363636	464.3863636	15.61259	04-2012	11-2015	0.36791	0.549392
4	f	Ave	NDE	2009/12/20	2012/04/27	859	81.0000	61.850	19.150	8.137077998	10607.65333	1.805300324	62.37448276	417.5862069	15.70222	12-2009	04-2012	1.8053	1.512924
4	f	Ave	NDE	2012/04/27	2015/11/21	1303	61.8500	51.294	10.556	2.957046239	22508.9	0.468981159	62.44363636	464.3863636	15.61259	04-2012	11-2015	0.468981	0.56693
1	a	Ave	DE	2010/11/28	2015/04/20	1604	57.6813	48.500	9.181	2.089249532	27499.23	0.333872985	62.32185185	441.7777778	15.68742	11-2010	04-2015	0.333873	0.394123
1	a	Ave	NDE	2010/11/28	2015/04/20	1604	57.9563	47.375	10.581	2.407828086	27499.23	0.384783501	62.32185185	441.7777778	15.68742	11-2010	04-2015	0.384784	0.396309
1	b	Ave	DE	2011/02/23	2013/08/08	897	81.0000	**58.281**	22.719	9.244530379	18374.55	1.236424838	61.99903226	430.6129032	15.68331	02-2011	08-2013	1.236425	0.874679
1	b	Ave	DE	2013/08/08	2015/04/21	621	58.2813	53.188	5.094	2.993911031	11217.81	0.454077044	62.80285714	462.9047619	15.67219	08-2013	04-2015	0.454077	1.125306
1	b	Ave	NDE	2011/02/23	2013/08/08	897	81.0000	56.569	24.431	9.941367057	18374.55	1.329624399	61.99903226	430.6129032	15.68331	02-2011	08-2013	1.329624	0.874679
1	b	Ave	NDE	2013/08/08	2015/04/21	621	56.5688	52.000	4.569	2.685336151	11217.81	0.407276465	62.80285714	462.9047619	15.67219	08-2013	04-2015	0.407276	1.090354
1	c	Ave	DE	2011/11/16	2015/04/21	1252	81	58.875	22.125	6.450179712	21809.65	1.014459196	62.34	447.9285714	15.66349	11-2011	04-2015	1.014459	0.758609
1	c	Ave	NDE	2011/11/16	2015/04/21	1252	81.0000	57.438	23.563	6.869259185	21809.65	1.080370387	62.34	447.9285714	15.66349	11-2011	04-2015	1.08037	0.758609
1	e	Ave	DE	2010/09/29	2015/04/21	1665	81.0000	51.813	29.188	6.398460961	31224.97	0.934748696	62.35285714	440.1785714	15.69384	09-2010	04-2015	0.934749	0.500563
1	e	Ave	NDE	2010/09/29	2015/04/21	1665	81.0000	53.000	28.000	6.138138138	31224.97	0.896718235	62.35285714	440.1785714	15.69384	09-2010	04-2015	0.896718	0.500563
1	d	Ave	DE	2014/05/01	2015/04/21	355	81.0000	58.250	22.750	23.39084507	4696.643333	4.843884959	63.44083333	465.25	15.70568	05-2014	04-2015	4.843885	3.904406
1	d	Ave	NDE	2014/05/01	2015/04/21	355	81.0000	54.063	26.938	27.69630282	4696.643333	5.735479168	63.44083333	465.25	15.70568	05-2014	04-2015	5.735479	3.904406
3	a	Ave	DE	2011/09/11	2014/03/10	911	47.5250	32.575	14.950	5.989846323	12932.28667	1.156021389	61.88419355	438.7419355	15.65371	09-2011	03-2014	1.156021	0.733262
3	a	Ave	NDE	2011/09/11	2014/03/10	911	45.1625	31.175	13.988	5.604212404	12932.28667	1.081595263	61.88419355	438.7419355	15.65371	09-2011	03-2014	1.081595	0.69362
3	d	Ave	DE	2010/03/05	2011/09/11	555	81.0000	63.106	17.894	11.76796171	10309.22003	1.735703568	62.46421053	410.2631579	15.82619	03-2010	09-2011	1.735704	1.530121
3	d	Ave	DE	2011/09/11	2014/03/10	911	63.1063	54.125	8.981	3.598415203	15724.16667	0.571174943	61.88419355	438.7419355	15.65371	09-2011	03-2014	0.571175	0.806699
3	d	Ave	NDE	2010/03/05	2011/09/11	555	81.0000	65.013	15.988	10.5143018	10309.22003	1.550796272	62.46421053	410.2631579	15.82619	03-2010	09-2011	1.550796	1.530121
3	d	Ave	NDE	2011/09/11	2014/03/10	911	65.0125	55.556	9.456	3.788728046	15724.16667	0.601383221	61.88419355	438.7419355	15.65371	09-2011	03-2014	0.601383	0.833007
3	e	Ave	DE	2011/09/11	2014/03/10	911	59.7625	52.300	7.463	2.989914929	12700.59333	0.587570974	61.88419355	438.7419355	15.65371	09-2011	03-2014	0.587571	0.956899
3	e	Ave	NDE	2011/09/11	2014/03/10	911	59.5750	50.331	9.244	3.70358809	12700.59333	0.727820328	61.88419355	438.7419355	15.65371	09-2011	03-2014	0.72782	0.953696
3	f	Ave	DE	2011/09/11	2014/03/10	911	50.0000	44.094	5.906	2.366389956	12177.25	0.485023302	61.88419355	438.7419355	15.65371	09-2011	03-2014	0.485023	0.826813
3	f	Ave	NDE	2011/09/11	2014/03/10	911	53.7750	48.875	4.900	1.963227223	12177.25	0.402389702	61.88419355	438.7419355	15.65371	09-2011	03-2014	0.40239	0.894084
2	a	Ave	NDE	2010/03/09	2010/11/03	239	49.8750	47.613	2.263	3.455282427	3730.626667	0.606466474	62.7	393.3333333	15.92274	03-2010	11-2010	0.606466	2.536654
2	a	Ave	NDE	2010/11/03	2013/04/20	899	47.6125	38.469	9.144	3.712423526	13305.24667	0.687228898	62.04933333	426.8333333	15.69216	11-2010	04-2013	0.687229	0.691258
2	a	Ave	DE	2010/03/09	2010/11/03	239	51.8250	51.694	0.131	0.200444561	3730.626667	0.035181757	62.7	393.3333333	15.92274	03-2010	11-2010	0.035182	2.638342
2	a	Ave	DE	2010/11/03	2013/04/20	899	51.6938	41.575	10.119	4.108280033	13305.24667	0.760508261	62.04933333	426.8333333	15.69216	11-2010	04-2013	0.760508	0.756015
2	b	Ave	DE	2010/03/09	2013/04/20	1138	49.5125	38.650	10.863	3.484018014	21114.60667	0.514454291	62.20078947	420.3157895	15.74067	03-2010	04-2013	0.514454	0.423285
2	b	Ave	NDE	2010/03/09	2013/04/20	1138	52.3813	33.888	18.494	5.931650923	21114.60667	0.87587471	62.20078947	420.3157895	15.74067	03-2010	04-2013	0.875875	0.45153

Table 22 End liner outer wear data and model prediction

Unit	End	Mill	Date from	Date to	Days	Average thickness at start (mm)	Avarage thickness at end of period (mm)	Average wear	Wear rate (mm/year)	Mill hours (for time period)	Wear rate per 1000 hours (mm/1000hr)	Mill balls added (tons)	Mill balls aded per 1000 mill hours	Average grindability index	Average abrasiveness (mgFe)	Average CV (MJ/kg)	Measured wear rate	Predicted wear rate	Predicted hours on curve for e	Predicted final thickness (new method) (mm)
1	DE	a	2010/11/28	2015/04/20	1604	53.78333333	45	8.783333333	1.998701164	27499.23	0.319402883	184	6.691096442	62.3556	441.5	15.68741629	0.319403	0.738837049	52746.88044	35.84252901
1	DE	b	2011/02/23	2013/08/08	897	81	60.5	20.5	8.341694537	18374.55	1.115673581	109.6	5.964771926	62.0137037	428.4444444	15.68330739	1.115674	1.269936553	18374.55	56.25618762
1	DE	b	2013/08/08	2015/04/21	621	60.5	47.66666667	12.83333333	7.542941492	11217.81	1.144014147	72	6.418365082	62.80285714	462.9047619	15.67219057	1.144014	1.380010012	22029.86168	50.26248007
1	DE	c	2011/11/16	2015/04/21	1252	81	57	24	6.996805112	21809.65	1.100439314	144.8	6.639262895	62.38631579	448.2105263	15.66348643	1.10043	1.202181166	21809.65	51.82559547
1	DE	e	2010/09/29	2015/04/21	1665	81	63.16666667	17.83333333	3.909409409	31224.97	0.571124114	193.6	6.200166085	62.38769231	439.7884615	15.69383588	0.571124	0.972428287	31224.97	46.5563291
1	DE	d	2014/05/01	2015/04/21	355	81	62.5	18.5	19.02112676	4696.643333	3.938983373	36.8	7.835383142	63.44083333	465.25	15.70567932	3.938983	3.015620998	4696.643333	69.66743786
1	NDE	b	2011/02/23	2013/08/08	897	81	57.01666667	23.98333333	9.759104422	18374.55	1.305247385	109.6	5.964771926	62.0137037	428.4444444	15.68330739	1.305247	1.269936553	18374.55	56.25618762
1	NDE	b	2013/08/08	2015/04/21	621	57.01666667	48.33333333	8.683333333	5.103730542	11217.81	0.774066715	72	6.418365082	62.80285714	462.9047619	15.67219057	0.774067	1.308270042	27386.18126	46.47772089
1	NDE	c	2011/11/16	2015/04/21	1252	81	58	23	6.705271565	21809.65	1.054579051	144.8	6.639262895	62.38631579	448.2105263	15.66348643	1.054579	1.202181166	21809.65	51.82559547
1	NDE	e	2010/09/29	2015/04/21	1665	81	57.33333333	23.66666667	5.188188188	31224.97	0.757940413	193.6	6.200166085	62.38769231	439.7884615	15.69383588	0.75794	0.972428287	31224.97	46.5563291
2	DE	a	2010/11/03	2013/04/20	899	47.45	33.26666667	14.18333333	5.758527994	13305.24667	1.06599552	78.4	5.892412367	62.07230769	424	15.69216195	1.065996	0.938965274	61193.30503	6.912354319
2	DE	a	2015/03/01	2016/03/17	382	81	65.56666667	15.43333333	14.7465096	6415.903333	2.405480964	41.6	6.483888213	62.65692308	492.7692308	15.50668491	2.405481	2.647804947	6415.903333	64.9260725
2	DE	b	2010/03/09	2013/04/20	1138	41.83333333	20.93333333	20.9	6.703427065	21114.60667	0.989836104	126.4	5.986377203	62.23617647	417.3823529	15.74067089	0.989836	0.658183403	95265.10119	25.17963379
2	DE	b	2013/04/20	2016/03/17	1062	81	54.1	26.9	9.245291902	19181.65667	1.402381477	124	6.464509409	62.61555556	470	15.62663241	1.402381	1.347235331	19181.65667	51.87090738
2	DE	b	2008/09/07	2010/03/09	548	53.73333333	41.83333333	11.9	7.926094891	9739.4	1.221841181	64	6.571246689	62.16468354	441.046371	15.44866911	1.221841	1.285273055	35173.10375	44.2106715
2	DE	c	2010/01/13	2011/04/12	454	48.51666667	39.46666667	9.05	7.275881057	9165.203333	0.987430357	52	5.673632991	62.519375	406.375	15.75123996	0.98743	1.12867885	58315.60492	38.41723107
2	DE	c	2011/04/12	2013/04/20	739	39.46666667	23.48333333	15.98333333	7.894339197	12857.93333	1.243071722	70.4	5.475218931	62.04380952	423.7142857	15.69121745	1.243072	0.817465224	95782.09856	23.98558753
2	DE	c	2014/08/01	2016/03/17	594	81	62.5	18.5	11.36784512	8602.686667	2.150490971	75.2	8.741455189	63.005	481.95	15.56957838	2.150491	2.182622437	8602.686667	62.19328705
2	DE	d	2010/03/09	2013/04/20	1138	55.56666667	32.83333333	22.73333333	7.291446983	20844.95667	1.090591537	114.4	5.488138058	62.23617647	417.3823529	15.74067089	1.090592	0.838545488	45353.11317	42.1132625
2	DE	d	2014/10/01	2016/03/17	533	81	64.1	16.9	11.57317073	8637.383333	1.956611088	62.4	7.224410171	62.96055556	485.6666667	15.51881252	1.956611	2.193258777	8637.383333	61.89548684
2	DE	e	2010/03/09	2013/04/20	1138	53.41666667	34.51666667	18.9	6.061950791	20252.08667	0.933237168	123.2	6.08332376	62.23617647	417.3823529	15.74067089	0.933237	0.820916581	50429.2562	39.97373588
2	DE	e	2015/06/01	2016/03/17	290	81	67.63333333	13.36666667	16.82356322	5047.536667	2.648156427	33.6	6.656712416	62.591	485.8	15.53122971	2.648156	3.011030235	5047.536667	67.86187417
2	DE	f	2010/03/09	2013/04/20	1138	47.96666667	31.95	16.01666667	5.137155829	14241.80667	1.124623234	76	5.336401608	62.23617647	417.3823529	15.74067089	1.124623	0.901844846	62155.7843	35.49781691
2	DE	f	2015/04/01	2016/03/17	351	81	67.26666667	13.73333333	14.28110161	5847.733333	2.348488303	36.8	6.293036618	62.60083333	492	15.46439221	2.348488	2.792895042	5847.733333	65.98572318
2	NDE	a	2010/11/03	2013/04/20	899	41.61666667	27.38333333	14.23333333	5.778828328	13305.24667	1.069753436	78.4	5.892412367	62.07230769	424	15.69216195	1.069753	0.840005722	85538.95525	26.8871526
2	NDE	a	2015/03/01	2016/03/17	382	81	66.9	14.1	13.47251309	6415.903333	2.197664034	41.6	6.483888213	62.65692308	492.7692308	15.50668491	2.197664	2.647804947	6415.903333	64.9260725
2	NDE	b	2010/03/09	2013/04/20	1138	38.23333333	27.03333333	11.2	3.592267135	21114.60667	0.530438486	126.4	5.986377203	62.23617647	417.3823529	15.74067089	0.530438	0.613074393	114018.5238	20.31433441
2	NDE	b	2013/04/20	2016/03/17	1062	81	56.63333333	24.36666667	8.374607659	19181.65667	1.270310854	124	6.464509409	62.61555556	470	15.62663241	1.270311	1.347235331	19181.65667	51.87090738
2	NDE	b	2008/09/07	2010/03/09	548	44.35	38.23333333	6.116666667	4.074057178	9739.4	0.628033212	64	6.571246689	62.16468354	441.046371	15.44866911	0.628033	1.084228784	64032.90642	31.4542209
2	NDE	c	2010/01/13	2011/04/12	454	50.78333333	39.63333333	11.15	8.964207048	9165.203333	1.216557843	52	5.673632991	62.519375	406.375	15.75123996	1.216558	1.175149589	49995.09831	41.58203763
2	NDE	c	2011/04/12	2013/04/20	739	39.63333333	21.68333333	17.95	8.865696888	12857.93333	1.396025281	70.4	5.475218931	62.04380952	423.7142857	15.69121745	1.396025	0.820351479	94931.53959	24.22260787
2	NDE	c	2014/08/01	2016/03/17	594	81	62.96666667	18.03333333	11.08108866	8602.686667	2.096244352	75.2	8.741455189	63.005	481.95	15.56957838	2.096244	2.182622437	8602.686667	62.19328705
2	NDE	d	2010/03/09	2013/04/20	1138	52.41666667	28.96666667	23.45	7.521309315	20844.95667	1.124972355	114.4	5.488138058	62.23617647	417.3823529	15.74067089	1.124972	0.79606739	53907.4222	38.58409744
2	NDE	d	2014/10/01	2016/03/17	533	81	62.56666667	18.43333333	12.623202	8637.383333	2.134133987	62.4	7.224410171	62.96055556	485.6666667	15.51881252	2.134134	2.193258777	8637.383333	61.89548684
2	NDE	e	2010/03/09	2013/04/20	1138	47.4	29.48333333	17.91666667	5.746558289	20252.08667	0.8846825	123.2	6.08332376	62.23617647	417.3823529	15.74067089	0.884683	0.743544698	70301.95481	32.69085741
2	NDE	e	2015/06/01	2016/03/17	290	81	65.68333333	15.31666667	19.27787356	5047.536667	3.034483487	33.6	6.656712416	62.591	485.8	15.53122971	3.034483	3.011030235	5047.536667	67.86187417
2	NDE	f	2010/03/09	2013/04/20	1138	47.96666667	31.95	16.01666667	5.137155829	14241.80667	1.124623234	76	5.336401608	62.23617647	417.3823529	15.74067089	1.124623	0.901844846	62155.7843	35.49781691
2	NDE	f	2015/04/01	2016/03/17	351	81	67.26666667	13.73333333	14.28110161	5847.733333	2.348488303	36.8	6.293036618	62.60083333	492	15.46439221	2.348488	2.792895042	5847.733333	65.98572318
3	DE	a	2011/09/11	2014/03/10	911	42.23333333	26.5	15.73333333	6.303695573	12932.28667	1.216593302	86.4	6.680953046	61.88185185	437.7777778	15.65371453	1.216593	0.886946912	76840.34726	27.46257585
3	DE	d	2010/03/05	2011/09/11	555	81	63.76666667	17.23333333	11.33363363	10309.22003	1.671642789	57.6	5.587231606	62.46421053	410.2631579	15.82618944	1.671643	1.692254605	10309.22003	65.04292595
3	DE	d	2011/09/11	2014/03/10	911	63.76666667	49.01666667	14.75	5.909714599	15724.16667	0.938046531	96	6.105252001	61.88185185	437.7777778	15.65371453	0.938047	1.140699125	23718.1436	51.47684326
3	DE	e	2011/09/11	2014/03/10	911	57.38333333	47.16666667	10.21666667	4.093395536	12700.59333	0.80442436	83.2	6.550875051	61.88185185	437.7777778	15.65371453	0.804424	1.168613843	30633.82509	47.11792561
3	DE	f	2011/09/11	2014/03/10	911	58.28333333	53.96666667	4.316666667	1.729509696	12177.25	0.354486166	87.2	7.160894291	61.88185185	437.7777778	15.65371453	0.354486	1.212707784	28409.99284	48.44590994
3	NDE	a	2011/09/11	2014/03/10	911	34.98333333	22.6	12.38333333	4.961489206	12932.28667	0.957551719	86.4	6.680953046	61.88185185	437.7777778	15.65371453	0.957552	0.757692016	112122.8243	17.18498052
3	NDE	d	2010/03/05	2011/09/11	555	81	64.75	16.25	10.68693694	10309.22003	1.576258917	57.6	5.587231606	62.46421053	410.2631579	15.82618944	1.576259	1.692254605	10309.22003	65.04292595
3	NDE	d	2011/09/11	2014/03/10	911	64.75	50.73333333	14.01666667	5.61589828	15724.16667	0.89140919	96	6.105252001	61.88185185	437.7777778	15.65371453	0.891409	1.156223236	22600.19166	52.25313529
3	NDE	e	2011/09/11	2014/03/10	911	54.9	43.43333333	11.46666667	4.594218807	12700.59333	0.902844959	83.2	6.550875051	61.88185185	437.7777778	15.65371453	0.902845	1.123839675	35874.3683	44.20948476
4	DE	a	2009/12/20	2013/12/30	1471	58.21666667	42.15	16.06666667	3.98663041	20484.13667	0.784346782	116.8	5.701973283	62.18577778	426.4222222	15.70542355	0.784347	0.893456165	37979.44109	44.44618958
4	DE	b	2009/12/29	2011/03/09	435	35.8	30.05	5.75	4.824712644	9313.38	0.617391323	56.8	6.098752547	62.538125	416.25	15.7075104	0.617391	0.87833742	117129.1799	19.75974512
4	DE	b	2012/08/26	2015/11/21	1182	81	57	24	7.411167513	23564.95667	1.018461453	158.4	6.721845588	62.57277778	469.4166667	15.62626006	1.018461	1.200132065	23564.95667	48.4872127
4	DE	c	2012/04/20	2013/12/30	619	81	65.61666667	15.38333333	9.070947765	11972.91333	1.284844624	80	6.681748859	61.84411765	444.7647059	15.69699541	1.284845	1.673190487	11972.91333	60.72222379
4	DE	c	2013/12/30	2015/11/21	691	65.61666667	58.83333333	6.783333333	3.583092137	11613.91	0.584069735	83.2	7.163823381	62.925	483.25	15.5271947	0.58407	1.514660061	16251.13099	53.32830172
4	DE	d	2009/12/20	2012/04/26	858	49.26666667	34.55	14.71666667	6.260586636	17253.403	0.852971826	100	5.79595805	62.37448276	417.5862069	15.70221698	0.852972	0.83429424	60426.0795	36.09441575
4	DE	d	2014/09/01	2015/11/21	446	81	55.33333333	25.66666667	21.00523169	6233.49	4.1754357	44.8	7.18698514	63.19933333	494.5333333	15.46764598	4.117544	2.702473418	6233.49	65.14131434
4	DE	e	2009/12/20	2012/04/15	847	41.88333333	39.16666667	2.716666667	1.170700512	17869.21667	0.15203054	98.4	5.506676752	62.37448276	417.5862069	15.70221698	0.152031	0.716498871	91684.75789	26.14143371
4	DE	e	2014/05/01	2015/11/21	569	81	62.16666667	18.83333333	12.0811365	8880.15	2.120835046	57.6	6.486376919	63.19947368	487.0526316	15.54710035	2.120835	2.16383539	8880.15	61.45936892
4	NDE	a	2009/12/20	2012/04/26	858	63.41666667	50.21666667	13.2	5.615384615	13618.04333	0.969302247	77.6	5.698322299	62.37448276	417.5862069	15.70221698	0.969302	1.178353532	23118.31308	53.8511841
4	NDE	a	2012/04/26	2013/12/30	613	50.21666667	44.61666667	5.6	3.334420881	6866.093333	0.815602079	39.2	5.709214556	61.84411765	444.7647059	15.69699541	0.815602	1.482534612	40840.10808	40.84729538
4	NDE	b	2009/12/29	2011/03/09	435	39.31666667	35.2	4.116666667	3.454214559	9313.38	0.442016396	56.8	6.098752547	62.538125	416.25	15.7075104	0.442016	0.951454364	96910.04143	24.91924985
4	NDE	b	2012/08/26	2015/11/21	1182	81	58	23	7.102368866	23564.95667	0.976025559	158.4	6.721845588	62.57277778	469.4166667	15.62626006	0.976026	1.200132065	23564.95667	48.4872127
4	NDE	c	2012/04/20	2013/12/30	619	81	65.65	15.35	9.051292407	11972.91333	1.282060562	80	6.681748859	61.84411765	444.7647059	15.69699541	1.282061	1.673190487	11972.91333	60.72222379
4	NDE	c	2013/12/30	2015/11/21	691	65.65	61.83333333	3.816666667	2.016039556	11613.91	0.328628917	83.2	7.163823381	62.925	483.25	15.5271947	0.328629	1.515361438	16225.41015	53.35288641
4	NDE	d	2009/12/20	2012/04/26	858	44.98333333	32.85	12.13333333	5.161616162	17253.403	0.70324291	100	5.79595805	62.37448276	417.5862069	15.70221698	0.703243	0.773409389	76984.89889	30.50460939
4	NDE	d	2014/09/01	2015/11/21	446	81	59.5	21.5	17.59529148	6233.49	3.449111172	44.8	7.18698514	63.19933333	494.5333333	15.46764598	3.449111	2.702473418	6233.49	65.14131434
4	NDE	e	2009/12/20	2012/04/15	847	47.46666667	34.86666667	12.6	5.429752066	17869.21667	0.705123243	98.4	5.506676752	62.37448276	417.5862069	15.70221698	0.705123	0.794149934	67602.54424	33.5677634
4	NDE	e	2014/05/01	2015/11/21	569	81	63.16666667	17.83333333	11.43966022	8880.15	2.008224336	57.6	6.486376919	63.19947368	487.0526316	15.54710035	2.008224	2.16383539	8880.15	61.45936892
4	NDE	f	2009/12/20	2012/04/27	859	81	61.63333333	19.36666667	8.229142414	10607.65333	1.825725828	72	6.787552132	62.37448276	417.5862069	15.70221698	1.825726	1.692164419	10607.65333	64.1947995
4	NDE	f	2012/04/27	2015/11/21	1303	61.63333333	51.11666667	10.51666667	2.945958046	22508.9	0.467222595	147.2	6.539635433	62.498	466.3	15.61259382	0.467223	0.963151803	31680.38208	43.39369366
5	DE	a	2010/05/02	2013/07/15	1170	56.43333333	39.75	16.68333333	5.20462963	17946.08667	0.929636285	101.6	5.66140139	62.19428571	419.9428571	15.72535116	0.929636	0.92117999	40020.65761	44.22202608
5	DE	b	2013/05/15	2016/02/02	1297	81	50.16666667	30.83333333	8.677075302	21653.98	1.423910678	143.2	6.613102995	62.65590909	471.8409091	15.64289582	1.423911	1.263518833	21653.98	49.7021271
5	DE	c	2015/03/01	2016/02/02	642	81	61.66666667	19.33333333	10.99169263	11542.51	1.674967865	72.8	6.307120375	62.68454545	485.8181818	15.59472829	1.674968	1.853987761	11542.51	58.11909526
5	DE	d	2010/05/02	2013/07/15	1170	47.26666667	21.98333333	25.28333333	7.887535613	21834.10667	1.157974252	120	5.495988539	62.19428571	419.9428571	15.72535116	1.157974	0.717606706	71608.11209	31.87872891
5	DE	d	2014/07/01	2016/02/02	885	81	54.16666667	26.83333333	11.06685499	17284.03667	1.552492271	108	6.24854032	62.90766667	479.0333333	15.62027376	1.552492	1.453328023	17284.03667	52.72720528
5	DE	e	2010/05/02	2013/07/15	1170	52.9	23.25	29.65	9.249786325	21277.47	1.393492741	124	5.827760537	62.19428571	419.9428571	15.72535116	1.393493	0.797738445	52432.88347	38.82735384
5	DE	e	2014/03/01	2016/02/02	1007	81	52	29	10.51142006	19213.39333	1.509363781	124.8	6.495468959	62.935	476.1176471	15.63080611	1.509364	1.36176401	19213.39333	51.29038749
5	DE	f	2010/05/02	2013/07/15	1170	58.98333333	43.31666667	15.66666667	4.887464387	13131.16667	1.193090231	78.4	5.970528133	62.19428571	419.9428571	15.72535116	1.19309	1.133199446	29798.0604	49.51602421
5	NDE	a	2010/05/02	2013/07/15	1170	57.23333333	38.95	18.28333333	5.703774929	17946.08667	1.018792212	101.6	5.66140139	62.19428571	419.9428571	15.72535116	1.018792	0.932339068	38224.11438	45.08568293
5	NDE	b	2013/05/15	2016/02/02	1297	81	50.66666667	30.33333333	8.536365973	21653.98	1.400820234	143.2	6.613102995	62.65590909	471.8409091	15.64289582	1.40082	1.263518833	21653.98	49.7021271
5	NDE	c	2015/03/01	2016/02/02	642	81	59.66666667	21.33333333	12.12876428	11542.51	1.848240403	72.8	6.307120375	62.68454545	485.8181818	15.59472829	1.84824	1.853987761	11542.51	58.11909526
5	NDE	d	2010/05/02	2013/07/15	1170	46.65	26.71666667	19.93333333	6.218518519	21834.10667	0.912944763	120	5.495988539	62.19428571	419.9428571	15.72535116	0.912945	0.709992655	73974.65879	31.10556027
5	NDE	d	2014/07/01	2016/02/02	885	81	56.5	24.5	10.10451977	17284.03667	1.417492943	108	6.24854032	62.90766667	479.0333333	15.62027376	1.417493	1.453328023	17284.03667	52.72720528
5	NDE	e	2010/05/02	2013/07/15	1170	45.68333333	23.36666667	22.31666667	6.962037037	21277.47	1.048840236	124	5.827760537	62.19428571	419.9428571	15.72535116	1.04884	0.707190636	77263.62781	30.0561653
5	NDE	e	2014/03/01	2016/02/02	1007	81	55	26	9.424031778	19213.39333	1.3532227	124.8	6.495468959	62.935	476.1176471	15.63080611	1.353223	1.36176401	19213.39333	51.29038749
6	DE	f	2009/04/19	2012/12/15	1336	53.3	27.85	25.45	6.953031437	16890.01744	1.506807207	105.6	6.252213793	62.24243902	422.804878	15.67930934	1.506807	0.911317799	46402.41134	40.97401461
6	DE	f	2015/10/01	2017/03/14	530	81	64.16666667	16.83333333	11.5927673	5386.246667	3.125243676	46.4	8.614533064	62.74758034	491.5181468	15.6669162	3.125244	2.929644018	5386.246667	66.8821015
6	DE	e	2012/08/01	2017/03/14	1686	81	43.83333333	37.16666667	8.046164492	28743.41	1.293050013	180.8	6.290137461	62.62589319	475.390897	15.6569642	1.29305	1.088206562	28743.41	44.27691319
6	DE	a	2009/04/19	2012/12/15	1336	53.4	28.21666667	25.18333333	6.880177146	19573.7255	1.2865886664	124	6.335022937	62.24243902	422.804878	15.67930934	1.286589	0.844522227	48813.70314	39.94105638
6	DE	a	2014/06/01	2017/03/14	1017	81	54.66666667	26.33333333	9.450999672	14827.9	1.775931409	105.6	7.12170975	62.98666018	488.8919601	15.6259193	1.775931	1.615165909	14827.9	54.26368853
6	DE	b	2009/04/19	2012/12/15	1336	63.23333333	46.26666667	16.96666667	4.635354291	25158.5617	0.674389374	156.8	6.232470754	62.24243902	422.804878	15.67930934	0.674389	0.853741968	34609.09237	46.57964689
6	DE	b	2016/03/01	2017/03/14	378	81	63.83333333	17.16666667	16.57627866	4975.63	3.450149361	36.8	7.39604834	62.84741893	503.8712802	15.73164967	3.450149	3.144803792	4975.63	67.02352207
6	DE	c	2009/04/19	2012/12/15	1336	43.11666667	21.15	21.96666667	6.001372255	25514.5869	0.860945417	155.2	6.082794936	62.24243902	422.804878	15.67930934	0.860945	0.620496847	91377.57098	25.37599461
6	DE	c	2014/06/01	2017/03/14	1017	81	55.16666667	25.83333333	9.271550311	15802.33667	1.634779329	117.6	7.441937384	62.98666018	488.8919601	15.6259193	1.634779	1.557674132	15802.33667	53.28631856
6	DE	e	2012/08/01	2017/03/14	1686	81	43.83333333	37.16666667	8.046164492	28743.41	1.293050013	180.8	6.290137461	62.62589319	475.390897	15.6569642	1.29305	1.088206562	28743.41	44.27691319
6	NDE	f	2009/04/19	2012/12/15	1336	50.66666667	34.98333333	15.68333333	4.284743014	16890.01744	0.928556373	105.6	6.252213793	62.24243902	422.804878	15.67930934	0.928556	0.87291373	54140.64458	37.76659009
6	NDE	f	2015/10/01	2017/03/14	530	81	64.83333333	16.16666667	11.1336478	5386.246667	3.001471649	46.4	8.614533064	62.74758034	491.5181468	15.6669162	3.001472	2.929644018	5386.246667	66.8821015
6	NDE	a	2009/04/19	2012/12/15	1336	56.11666667	24.3	31.81666667	8.692427645	19573.7255	1.625478332	124	6.335022937	62.24243902	422.804878	15.67930934	1.625478	0.880669269	41991.42665	42.95365882
6	NDE	a	2014/06/01	2017/03/14	1017	81	56.83333333	24.16666667	8.673385775	14827.9	1.629810447	105.6	7.12170975	62.98666018	488.8919601	15.6259193	1.629811	1.615165909	14827.9	54.26368853
6	NDE	b	2009/04/19	2012/12/15	1336	65.18333333	38.81666667	26.36666667	7.203468064	25158.5617	1.048019636	156.8	6.232470754	62.24243902	422.804878	15.67930934	1.04802	0.87593749	32172.9873	47.88101095
6	NDE	b	2016/03/01	2017/03/14	378	81	63.83333333	17.16666667	16.57627866	4975.63	3.450149361	36.8	7.39604834	62.84741893	503.8712802	15.73164967	3.450149	3.144803792	4975.63	67.02352207
6	NDE	c	2009/04/19	2012/12/15	1336	52.93333333	20.18333333	32.75	8.947417665	25514.5869	1.283579473	155.2	6.082794936	62.24243902	422.804878	15.67930934	1.283579	0.731260914	56039.06183	37.02396401
6	NDE	c	2014/06/01	2017/03/14	1017	81	53.5	27.5	9.869714848	15802.33667	1.740248963	117.6	7.441937384	62.98666018	488.8919601	15.6259193	1.740249	1.557674132	15802.33667	53.28631856
6	NDE	e	2012/08/01	2017/03/14	1686	81	44.33333333	36.66666667	7.937920127	28743.41	1.275654721	180.8	6.290137461	62.62589319	475.390897	15.6569642	1.275655	1.088206562	28743.41	44.27691319

APPENDIX C BOILER MODEL SPREAD SHEETS

Elevation above sea level (m)	1500	Ambient pressure (kPa)	84.55599								
Drum pressure (Kpa)	18600	Boiler vacuum due to Id fans (Atm-boiler pressure) (kPa)	5								
	T_sat	vf	vg	uf	ug	hf	hfg	hg	sf	sfg	sg
Saturated conditions	359.618	0.00189986	0.007011	1725.22	2350.86	1760.63	719.92	2484.636	3.91494	1.13875	5.05369
	Side walls	Front and rear walls	Furnace cross		Side walls	Front and rear walls	circumference				
BBSA area factors	0.9	0.9	section		13.72	24	75.44				
GCV of Fuel (MJ/kg)	17	NCV of fuel	16		12.348	21.6	67.896				
combustion air per kilogram fuel (10% excess air included)	6.6697	Flue gas produced per kg fuel (kg/kgf)	7.303322								
ambient temperature	25	Combustion air temp C	220								
Cp of air at ambient Temperature (kJ/kgk)	1.003611	Cp of air at combustion temperature Temperature (kJ/kgk)	1.01425								
Correction factor Fr	0.81										

Figure 88 Furnace common details

Furnace height (m)	53.3106521	BBSA (m2)	3619.58	3619.58003	
Fuel consumption rate (kg/h)	194400	FEGT (K)	1303.15		
Mass of air consumed	1296589.68	Te (C)	1030		
Flow rate (kg/s)	340	Water Inlet Temp in C	268.753	inlet water enthalpy	1179.03
Heat required for conversion of water to saturated steam (kW)	443906.275	Saturated steam temp C	359.618	Saturated steam enthalpy	2484.636
Metal temp C	409.618	Metal temp (K)	682.768		
Hin (kJ/kg fuel burnt)	17320.8984	H_out (kJ/kg fuel burnt)	17263.1		1.003346
heat absorbed by the furnace (kW)	445843.123	heat absorbed by the furnace (kJ/kg)	8256.35		0.003346

Figure 89 Furnace calculation

Wall thickness calculation according to BS1113				Wall thickness calculation according to BS1113			
Material	BS3059 grade 91	Minimum thickness (mm)	3.468273	Material	BS3059-243	Minimum thickness (mm)	2.291308
Outer diameter (mm)	50.8	Corosion allowance mm	0.7	Outer diameter (mm)	38	Corosion allowance mm	0.7
Internal pressure (Mpa)	17	Mill tolerance %	0.1	Internal pressure (Mpa)	15.4	Mill tolerance %	0.1
Metal temperature (T_out +35C)	550	Expected tube wall thickness (mm)	4.5851	Metal temperature (T_out +35C)	350	Expected tube wall thickness (mm)	3.290439
design stress f (n/mm^2)	116	ID (mm)	41.6298	design stress f (n/mm^2)	120	ID (mm)	31.41912
Minimum thickness (mm)	3.468273092			Minimum thickness (mm)	2.291307753		
Corosion allowance mm	0.7			Corosion allowance mm	0.7		
Mill tolerance %	10%			Mill tolerance %	10%		
Expected tube wall thickness (mm)	4.585100402			Expected tube wall thickness (mm)	3.290438528		
ID (mm)	41.6297992			ID (mm)	31.41912294		

Figure 90 Tube thickness calculations

Super heater layout details			
Number of elements	75.00004	Number of tubes per flow path	5
Number of flow paths	6	Transverse pitch	0.260656
Maximum velocity (m/s)	6.12003		

Figure 91 Super heater layout details

Tube OD (mm)	50.8	Geometric beam length	0.765681		
Grid length (m)	18.6	C	3.6		
grid width (m)	19.6	Number of tubes per flow path	5	Number of flow paths	6
Grid cross - sectional area (m^2)	364.56	Bend radius	0.138		
Maximum gasflow speed (m/s)	12	Equivalent pipe length (heating only)	0.43354		
		Pipe length (18.6 -bend)	18.14106		
Gas mass flow @100% (kg/s)	394.3794	Total area (m2)	6638.711		
Flue gas density (kg/m^3)	0.21729	Total internal area	5440.319		
Flue gas flow rate m^3/s	1814.991	Tube Id	0.04163		
Horizontal tube pitch (m)	0.260656	total tube length	92.70353		
Number of elements	75.00004		7500.004		
Total area between elements m^2	288.8458	Total gas flow area (including gaps between tubes and furnace walls)	296.5658		
Flue gass velocity @100% MCR m/s	6.12003				
Vertical tube pitch	0.138				

Figure 92 Super heater common data

Convective heat transfer coefficient			
hc	33.14986	K	0.287
D (m)	0.0508	G gas mass flux (kg/m^2s)	1.329820952
c (flue gas)	1177.56	u (kg/ms)	4.07657E-05
k (w/mK)	0.081935		

Figure 93 Super heater convective heat transfer coefficient

Internal heat transfer coeffiecient			
hi	2844.463178	D_i (m)	0.04163
k (W/mk)	0.059407405	steam flow rate (kg/s)	600
G gas mass flux (kg/m^2s)	979.5801335	c (steam)	2095.06
u (kg/ms)	2.65249E-05		

Figure 94 Super heater internal convective heat transfer coefficient

Radiative heat transfer coefficient			
hr	28.99837	hr_300	104.3932207
tg	872.2602	x	0.117850202
MBL	0.765681	Ph	0.103
Pc	0.127	Px	34.42848848
Kt	1.000009		

Figure 95 Super heater non-luminous radiative heat transfer coefficient

Conductive heat transfer			
k (W/mK)	35	wall thickness	0.0045851
DI	0.0416298		

Figure 96 Super heater heat transfer coefficient

Over all heat transfer			
fo	0.82	fi	1
ho	62.1482274	**U**	49.51447232

Figure 97 Super heater overall heat transfer coefficient

Flow calcs			
Mass flow per flow path (kg/s)	1.333332552	Cross sectional area	0.001361127
Density (kg/m^3)	59.05977062	Velocity (m/s)	16.58625022
u	2.65249E-05	Re	1537412.341
Hydraulic Diameter	0.041629799	epsilom	0.00005
f	0.020582454	delta_p (kPa)	372.3465174
L (m)	92.70353143		

Figure 98 Super heater flow calculation

Gas side calculations			
tgas in (°C)	1030	tgas_out (°C)	731.511232
cp	1.17756	Mass flow	394.379361
		Q	138619.7855

Figure 99 gas side temperature calculations

Steam side calculations			
T_steam in	359.618	Tsteam_out (°C)	554.2211384
cp	2.09506	Mass flow	340
		Q	138619.7855

Figure 100 Steam side calculations

Heat Transfer calculation			
A	6638.71086	U	49.51447232
Delta TB	475.778862	Delta TA	371.893232
Q (kW)	138619.785		

Figure 101 Heat transfer calculations (super heater)

Tube OD (mm)	38	Geometric beam length	0.250027						Economiser layout details			
Grid length (m)	18.6	C	3.6									
grid width (m)	19.6	Number of tubes per element	5	Number of flow paths	9				Number of elements	220	Number of tubes per element	5
Grid cross - sectional area (m^2)	364.56	Bend radius	0.106						Number of flow paths	9	Transverse pitch	0.0889
Maximum gasflow speed (m/s)	12	Equivalent pipe length (heating only)	0.333009						Maximum velocity (m/s)	4.941612		
		Pipe length (18.6 -bend)	18.24799									
Gas mass flow @100% (kg/s)	394.3794	Total area (m2)	21881.56									
Flue gas density (kg/m^3)	0.370975	Total internal area	18092.09									
Flue gas flow rate m^3/s	1063.09	Tube Id	0.031419									
Horizontal tube pitch (m)	0.088918	Flow path length	92.74807									
Number of elements	220		22000									
Total area between elements m^2	207.4101	Total gas flow area (including gaps between tubes and furnace walls)	215.1301									
Flue gass velocity @100% MCR m/s	4.941612											
Vertical tube pitch	0.106											

Figure 102 Economiser common data

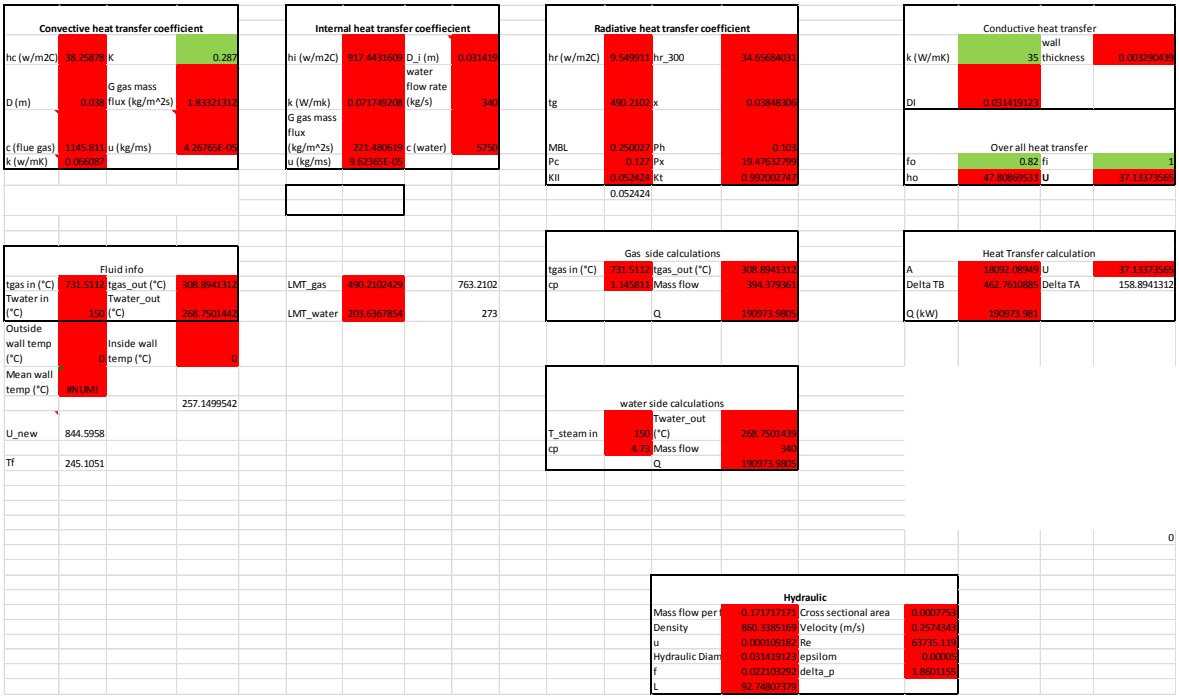

Convective heat transfer coefficient			
hc (w/m2C)	38.25878	K	0.287
D (m)	0.038	G gas mass flux (kg/m^2s)	1.83321312
c (flue gas)	1145.811	u (kg/ms)	4.26765E-05
k (w/mK)	0.066087		

Internal heat transfer coeffiecient			
hi (w/m2C)	917.4431609	D_i (m)	0.031419
k (W/mk)	0.071749208	water flow rate (kg/s)	340
G gas mass flux (kg/m^2s)	221.480619	c (water)	5750
u (kg/ms)	9.62365E-05		

Radiative heat transfer coefficient			
hr (w/m2C)	9.549911	hr_300	34.65684031
tg	490.2102	x	0.03848306
MBL	0.250027	Ph	0.103
Pc	0.127	Px	19.47632799
KII	0.052424	Kt	0.992002747
	0.052424		

Conductive heat transfer			
k (W/mK)	35	wall thickness	0.003290439
DI	0.031419123		

Over all heat transfer			
fo	0.82	fi	1
ho	47.80869533	U	37.13373565

Fluid info			
tgas in (°C)	731.5112	tgas_out (°C)	308.8941312
Twater in (°C)	150	Twater_out (°C)	268.7501442
Outside wall temp (°C)	0	Inside wall temp (°C)	0
Mean wall temp (°C)	#NUM!		
			257.1499542
U_new	844.5958		
Tf	245.1051		

LMT_gas	490.2102429		763.2102
LMT_water	203.6367854		273

Gas side calculations			
tgas in (°C)	731.5112	tgas_out (°C)	308.8941312
cp	1.145811	Mass flow	394.379361
		Q	190973.9805

water side calculations			
		Twater_out	
T_steam in	150	(°C)	268.7501439
cp	4.73	Mass flow	340
		Q	190973.9805

Heat Transfer calculation			
A	18092.08949	U	37.13373565
Delta TB	462.7610885	Delta TA	158.8941312
Q (kW)	190973.981		

0

Hydraulic			
Mass flow per t	0.171717171	Cross sectional area	0.0007753
Density	860.3385169	Velocity (m/s)	0.2574343
u	0.000109182	Re	63735.119
Hydraulic Diam	0.031419123	epsilom	0.00005
f	0.022103292	delta_p	1.8601155
L	92.74807379		

Figure 103 Economiser heat transfer calculation